Physical model testing of piles in thawing soils subjected to single and combined loadings

By

Harshdeep Singh

Supervisor: Dr. M. Fall

Thesis submitted to the University of Ottawa
in partial Fulfillment of the requirements for the master's degree in civil engineering

Department of Civil Engineering
Faculty of Engineering
University of Ottawa

ABSTRACT

The primary purpose of pile foundations is to transfer vertical loads due to the transfer of the weight of the superstructure to the deeper ground. However, many civil engineering structures, such as bridges, transmission towers, tall chimneys, and solar panels, are subjected to significant lateral loads and overturning moments in addition to axial loads. Potential sources of lateral loads (not due to earthquakes) include wind, waves, ice forces, passive earth pressure, etc. On the other hand, axial loadings can be live loads from a structure, forces developed due to ground freezing, etc. Consequently, pile foundations for these structures should be adequately designed to resist compressive loads combined with lateral and uplift loads and moments. In most cases, these forces (compressive, lateral, and uplift) and moments are often simultaneously applied on the piles. One of the key objectives for the engineer and designer is to determine the deflections and stresses in a pile in order to keep them within tolerable limits. Passive soil resistance can be very effective in proving lateral support for the pile. However, passive soil resistance is a function of the soil thermal regime (freezing, thawing, and temperature). Due to global warming, the thermal regimes of the soils in Canada and other cold regions in the world have changed in the past decades. The change in the thermal regimes of the soil may affect the geotechnical response or performance of the pile foundations. This thesis presents and discusses the results of physical model testing on model piles in unfrozen, frozen, and thawing fine sand, which are subjected to individual and combined axial (uplift) and lateral loads. The dimensions of the pile model are established by using physical scaling laws. The physical model is also equipped with various sensors and instruments (e.g., linear variable differential transformer (LVDT), and temperature sensors) to monitor the pile and soil response during and after loading. The results of the study show that the thermal regime in the soil significantly affects the performance of the pile under combined loadings (lateral and uplift). The lateral capacity of the pile under combined loads in frozen soil is increased by 648% compared to that in unfrozen ground whereas the uplift capacity under combined loadings in frozen soil is increased by 29%. Due to the effects of the freezing

and thawing (F-T) cycles of the soil, a steady increase in the lateral capacity of the pile under the combined loadings is observed. On the other hand, the uplift capacity under the combined loadings in soil subjected to F-T cycles remains constant. The results will be useful in the geotechnical design of pile foundations for bridges and other structures in Canada and other cold regions in the world. The findings of this research will contribute to efficient design practices for pile foundations in cold regions with rapid changing climatic conditions.

Acknowledgements

I would like to thank my supervisor and a great mentor, Dr. Mamadou Fall, for his continuous guidance, support and motivation throughout my research at the University of Ottawa. His expertise and profound knowledge have helped to make this thesis a success.

Special thanks to Mr. Jean Claude Celestin for his continual help, useful information, and technical assistance.

I would also like to thank my seniors and friends Imad, Sada and Kunal who have always been very supportive and helpful in every possible way at times when I needed them.

Last but not the least, I would like to take this opportunity to express my gratitude from the deepest part of my heart to my beloved parents, Mr Karamjeet Singh and Mrs. Satnam Kaur, my brother Harpreet Singh, his wife Komal Kaur, my sister Manpreet Kaur and my little niece Seerat. Nothing would have been possible without them.

Table of Contents

List of Figures

List of Tables

Chapter 1- Introduction

1.1 Background and Problem Statement

With increases in the global population, infrastructure growth is considered to be a necessity. Over the past few decades, there has been a tremendous growth in infrastructures worldwide. With rapid modernization and infrastructure development, numerous advanced techniques and construction procedures have been developed and adopted for the construction of modern structures. Many of these structures, such as bridges, transmission towers, tall chimneys, and solar panels, are built on pile foundations. Pile foundations are used due to their high performance and stability characteristics where shallow foundations are not feasible solutions (Fall and Sarr 2017).

Pile foundations are used for onshore and offshore structures. Depending on the type of structure, pile foundations can be subjected to axial and lateral loads, and overturning moments, or a combination of such loads. The sources of lateral loads (not considering earthquakes) comprise wind, waves, ice movement, vehicle acceleration and braking, debris flow, and docking of ships. On the other hand, axial loads can be caused by the weight and live loads of the superstructure (compressive loads), the heaving, freezing and thawing (F-T; uplift loads) of soils in cold regions, etc. Therefore, pile foundations for these civil engineering structures must be properly designed to resist axial loads well as lateral forces along with overturning moments. In most cases, these loads (compressive, lateral, and uplift) and moments are often applied to the piles simultaneously. There have been studies in the past (for e.g. Das and Rozendal 1983, Darr et al. 1990, Rahman and Achmus 2006, Karthigeyan et al. 2006, Shanker et al. 2007, Basu et al. 2008, Gaaver 2013, Chatterjee and Choudhury 2016) to analyze the performance of piles under single and combined loadings.

The geotechnical stability of pile foundations is a function of the geotechnical properties and behavior of the soils beneath and/or adjacent to the piles. However, soil properties and soil behavior are significantly dependent on the thermal regime (e.g., freeze-thaw cycles, freezing, thawing, etc.) of the material. The F-T of soils induced by temperature changes significantly affect the strength and passive resistance of soils under and/or adjacent to the foundation of the structures. When water in the soil freezes and the soil expands, melting and subsequent refreezing of the water cause significant damage to the soil structure and the infrastructure that the soil supports (Climate Atlas 2019). However, other studies (Badeli et al. 2018) have shown that there has been an increase in the number of freeze-thaw cycles of soils in the northern regions of Canada, with or without permafrost, over the past few decades due to climate warming. This climate-induced change in the freeze-thaw cycles of soils have a negative impact on the performance of many civil engineering structures (supported on piles or shallow foundation) with an increase in the maintenance cost and decrease in service life which can jeopardize the safety of people and the economic activities in these regions. For example, many roads, buildings, bridges, towers, tall chimneys, solar panels, etc., have experienced differential movements due to ground freezing or thawing. Figure 1.1 shows an example of a building in Dawson City, Canada, which shows differential settlement of the house due to thawing of the frozen ground. In addition, a growing volume of scientific work has made it clearer that climate change will continue for many decades, if not for centuries, regardless of the outcome of global initiatives to reduce greenhouse gas emissions. This will have an impact on pile foundations which in turn has socio-economic consequences.

Figure 1.1: Building damage due to freezing and thawing of foundation soils (Shetler 2021)

Thus, under this climate warming scenario, changes in the thermal regimes of the soils are expected to intensify which can lead to adverse consequences on the foundations of structures in permafrost or permafrost-free regions in Canada. Therefore, in order to ensure the structural integrity of the infrastructure, such as bridges, transmission towers, tall chimneys, or solar panels, the design of the pile foundation must be updated in response to climate change. The objective of this study is to examine the impact of the thermal regimes of soil on the behavior or geotechnical response of piles subjected to combined loads to address the knowledge gap in this area.

1.2 Objectives

The experimental program is intended to investigate the behavior of piles subjected to single and combined loadings in F-T soils. The key objective is to develop a better understanding of the behavior of piles in F-T soils. The specific objectives of this research work are:

a) To develop a physical model to experimentally determine the deformation behavior of piles in sand subjected to individual/single and combined loads under different temperatures.

b) To measure and compare the horizontal and vertical pile load capacities under only horizontal or only uplift forces in sand with a frozen layer during thawing.

c) To measure and compare the horizontal and vertical pile load capacities under combined horizontal and uplift loads in sand with a frozen layer during thawing.

d) To measure and compare the horizontal and vertical pile load capacities under only horizontal or only uplift forces in sand subjected to F-T cycles.

e) To measure and compare the horizontal and vertical pile load capacities under combined horizontal and uplift loads in sand subjected to F-T cycles.

1.3 Research Statement

To the best of the author's knowledge, there are no published studies that provide comprehensive analyses of piles in F-T saturated sand under individual and combined (lateral and uplift) loadings. The current study is focused on bridging the knowledge gap between theoretical/numerical studies and the actual behavior of piles by testing a prototype pile in the laboratory.

A physical model has been developed to determine the pile behavior in soil subjected to different thermal regimes. The pile is embedded in a sand bed with different sensors (5TE soil moisture sensor, MPS-6 water potential sensor, and strain gauges). The homogeneous sand bed has a relative density of 65%. Static weights are used to load the pile laterally and axially (uplift). The loading increments on the pile are applied at a deflection rate of 0.1 mm/30 min. The pile deflections are recorded by using linear variable differential transformer (LVDT) sensors. The pile is loaded until a predetermined deflection criterion is reached.

This study has two phases. In Phase 1, the pile is subjected to individual/single and combined loads (lateral and uplift) in unfrozen sand and in sand with a frozen layer. The depth of the frozen layer is 5 cm which has been scaled down based on the depth of frost penetration in the Ottawa region. A significant improvement in the pile capacities is observed in the soil with a frozen layer.

In the second phase of the study, the effects of F-T (0, 1, 3, and 5 cycles) of the soil on piles subjected to individual and combined loads are investigated. The sand bed is initially frozen to a depth of 5 cm which is then allowed to thaw at room temperature. The pile deflections and maximum loads are measured under 0, 1, 3, and 5 F-T cycles. Loads are applied on the pile with the use of static weights. For the piles loaded laterally, a constant uplift force is applied which takes into consideration a factor of safety (FOS) of 2 of the maximum force. Similarly, for the axially (uplift) loaded pile, a constant lateral load is applied by using an FOS of 2.

1.4 Thesis Outline

This thesis is organized based on two technical papers. There are five chapters (see Figure 1.2).

Chapter 1 provides a brief background of piles in frozen soils, the problem statement, objectives, and research statement.

Chapter 2 is the literature review and a technical review of pile foundations in frozen and unfrozen grounds under individual and combined axial and lateral loads.

Chapter 3 discusses the response of a pile in unfrozen and freezing soils subjected to individual and combined loads (Technical Paper I).

Chapter 4 discusses the response of a pile in sand under F-T cycles subjected to individual and combined loads (Technical Paper II).

Chapter 5 provides the conclusions and recommendations for further studies.

Note that this thesis is presented in a paper-based format, so there will be unavoidable repetition of the technical contents in each paper since each paper is written independently according to the requirements for journal submission.

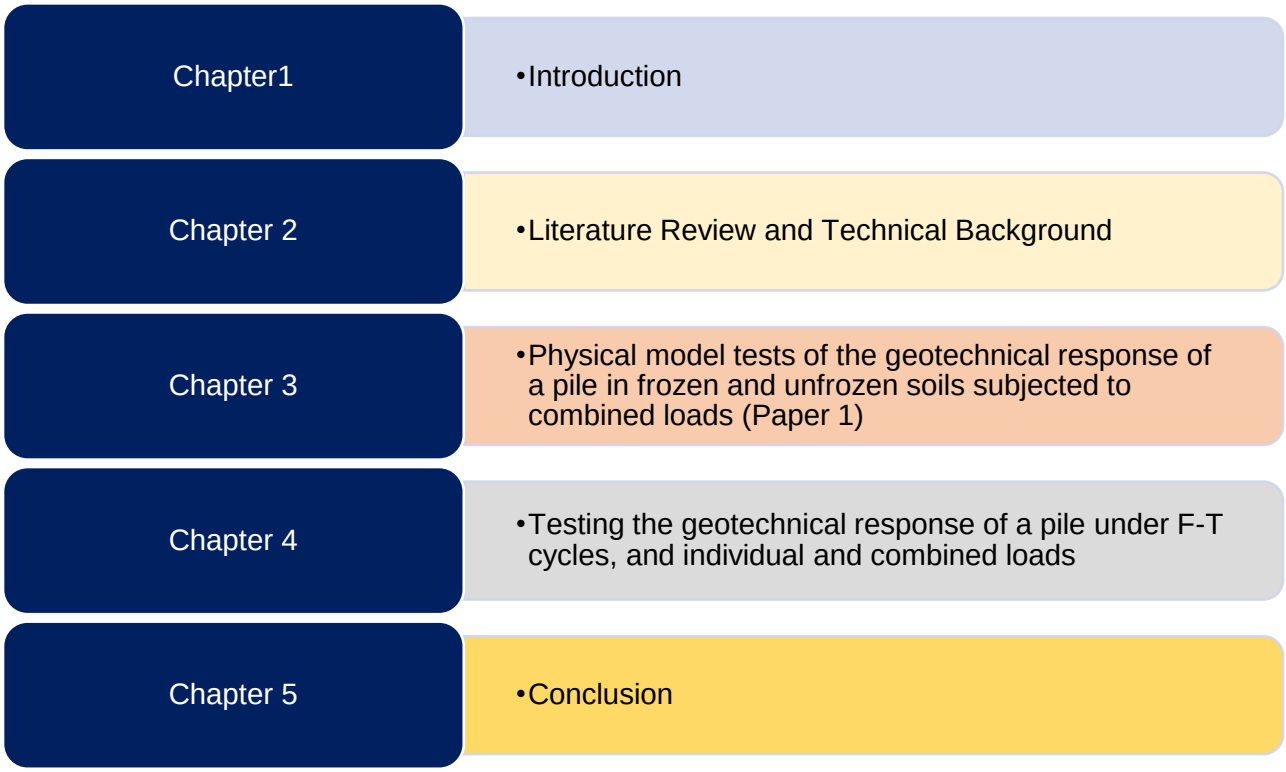

Figure 1.2 Thesis outline

1.5 References

Badeli, S., Solatiyan, E., Carter, A., and Dore, G. (2018). *Evaluation of the asphalt mix performance under repeated freeze-thaw cycles and application of Geosynthetics in cold region*. Presented at the Transportation Association of Canada, Saskatoon.

Basu, D., Salgado, R., and Prezzi, M. (2008). *Analysis of laterally loaded piles in Multilayered soil deposits* (Publication No. FHWA/IN/JTRP-2007/23, SPR-2630). Indiana, US: School of Civil Engineering Purdue University.

Chatterjee, K., and Choudhury, D. (2016). Analytical and numerical approaches to compute the influence of vertical load on lateral response of single pile. *Japanese Geotechnical Society Special Publication*, *2*(36), 1319–1322.

Climate Atlas. (2019). Freeze-Thaw Cycles. Retrieved August 19, 2020, from Climate Atlas website: https://climateatlas.ca/map/canada/freezethaw_2060_85#

Darr, K. A., Reese, L. C., and Wang, S., T. (1990, May). *Coupling Effects of Uplift Loading and Lateral Loading on Capacity of Piles*. Presented at the 22nd Annual Offshore Technology Conference, Huston, Texas.

Das, B. M., and Rozendal, D. B. (1983). *Ultimate Uplift Capacity of Piles in Sand*. Transportation Research Record 945.

Fall, M., and Sarr A. M. (2007). *Geotechnical characterization of expansive soils and their implications in ground movement in Dakar*. Bulletin of Engineering Geology and Environment 66 (3): 279-288.

Gaaver, K. E. (2013). Uplift capacity of single piles and pile groups embedded in cohesionless soil. *AEJ - Alexandria Engineering Journal*, *52*(3), 365–372.

Karthigeyan, S., Ramakrishna, V. V. G. S. T., and Rajagopal, K. (2006). Influence of vertical load on the lateral response of piles in sand. *Computers and Geotechnics, Indian Institute of Technology Madras, Chennai 600 036*, *33*(2), 121–131.

Rahman, K. A., and Achmus, M. (2006). *Numerical modelling of the combined axial and lateral loading of vertical piles*. 575–581. Graz, Austria.

Shanker, K., Basudhar, P., and Patra, N. (2007). Uplift capacity of single piles: Predictions and performance. *Geotech Geol. Eng*, *25*(2), 151–161.

Shetler, S. (2021, April). The Kissing Buildings in Dawson City, Yukon. Retrieved from https://quirkytravelguy.com/kissing-buildings-dawson-city-yukon/

Chapter 2- Literature Review and Technical Background

2.1 Permafrost

Permafrost is defined as a type of soil or rock that stays frozen (i.e., with a ground temperature below 0ºC) continuously for two years. It is found in the high latitude and altitude regions with long winters. The depth of the permafrost can vary from a few meters in warmer areas to hundreds of meters in cold arctic regions. An article by Schoeneich and Fabre, (2019), reported that depending on the distribution of permafrost, it can be categorized as continuous permafrost (>80% region covered with permafrost), discontinuous permafrost (30%–80% region covered with permafrost), and sporadic permafrost (<30% of the total area covered with permafrost).

Permafrost is an important part of the northern Canadian landscape. Figure 2.1 shows the distribution of permafrost in Canada. Almost 50% of the total Canadian landscape (9,984,670 km^2) is covered by permafrost (Government of Canada 2021). The remainder, or the non-permafrost zone, lies in the southern part of Canada which is affected by seasonal F-T of the ground. A main concern for engineers/researchers is the increase in global temperature, which forces the permafrost to thaw and subjects it to thermal cycles. Figure 2.2 shows an example of the damages on a road due to thawing of the permafrost in the Yellowknife region, Canada. A Government of Canada (2019) report compared the temperature change in Canada with the rest of the world and showed that the temperature increase in Canada is twice as much as the other countries. This change in the climate has caused serious problems in many Canadian territories

and other parts of the world at a different scale. The thawing of permafrost has resulted in serious damages to infrastructure in these regions.

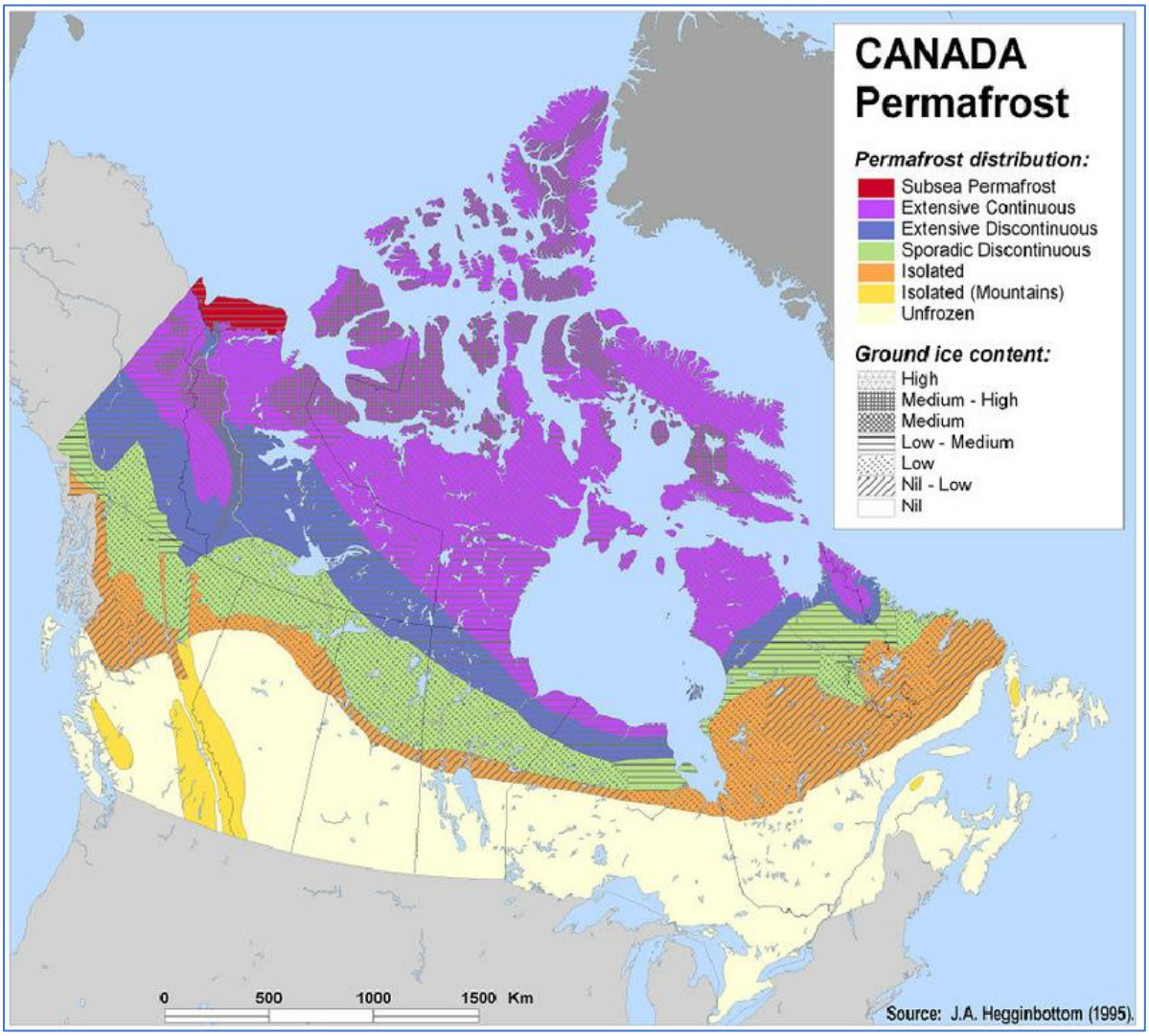

Figure 2.1 Permafrost distribution in Canada (Cruden 2010)

Denchak (2018) stated that scientists estimate that almost 10% of all of the permafrost has melted since the 1900s with an increase in temperature by 1°C and approximately 1.5 million sq. miles of permafrost turf could be exposed to the risk of melting down.

Thawing of permafrost due to climate change makes the ground unstable for development (Streletskiy et al. 2012). In addition to being an engineering challenge, the thawing of permafrost

is a danger to humans since it may lead to the spreading of bacteria and viruses, which have been embedded in the permafrost for thousands of years (Childress 2020).

Figure 2.2 Permafrost damaged roads (Neill, 2011)

2.2 Soil Freezing

2.2.1 Introduction

Soil freezing is a process in which water in the pores of soil freezes when the temperature in the soil falls below its freezing point (<0°C). It is evident from different studies in the literature (Pewe and Paige, 1963; Kozlowski, 2003; Fall et al., 2009; Briaud, 2013; Chang and Fall, 2022) that water present in the soil does not freeze at 0°C, mainly because of the presence of dissolved salts and minerals in the water that reduce the freezing point of water. Therefore, temperature alone is insufficient to define the frozen state of the soil. To do so, it is important to consider the phase change from water to ice. Frozen soil can be defined as seasonally frozen (frost soil) or permanently frozen (permafrost), depending on the duration of the frozen state. The mechanical and the physical properties of the soil change markedly because of soil freezing (Lai et al., 2009; Fall et al. 2010; Briaud, 2013; He et al., 2014; Loria et al., 2017; Tang et al., 2018). As stated earlier, ground that stays frozen for over two years is defined as permafrost. On the one hand, the frozen ground offers certain advantages; for example, frozen ground instantaneously

increases the stiffness and shear strength of the soil (Aldaeef and Rayhani, 2019). The bonding of the ice between the soil particles acts like a cementing agent among the aggregates which increases the stiffness of the soil structure against deformation.

On the other hand, there are a few disadvantages associated with ground freezing. First, ground freezing leads to frost heaving (see Section 1.2.2.) thus causing damage to infrastructures due to differential movement, which is a serious problem in the northern territories. Second, the frozen ground loses its strength when it thaws. In severe conditions, surface runoff from meltwater can cause soil erosion. Third, the resistance provided by the soil is decreased under long-term sustained loading due to creep. However, the frozen soils may still provide higher strength compared to their unfrozen state.

Frozen ground may be classified as massive, layered, or honeycombed ice on the basis of the ice structure (Tsytovich 1960). These three classes are illustrated in Figure 2.3.

A massive frozen soil structure develops because of quick freezing of the pore water in the soil. The massive frozen soil has a considerable high strength. Even after thawing of the ice, the measured strength is still higher than that before freezing.

A layered structure is seen in dispersed soils, and the freezing process is one-dimensional with a continuous supply of water. This structure can also be found in soil with a high moisture content. The formation of ice layers occurs because of the redistribution of water in the soil. The strength of the layered frozen soil varies depending on the ice layer and the mineral composition of the soil. Still, the frozen strength is much higher than the unfrozen soil strength. After thawing, the bearing capacity of the soil is considerably reduced compared to that under unfrozen conditions.

A honeycombed structure of frozen soils is formed when the water supply during freezing of the soil comes from more than one direction. The frozen soil properties are similar to those of layered

frozen soil, and after the thawing process, the soil-bearing strength is not much reduced compared to the unfrozen soil.

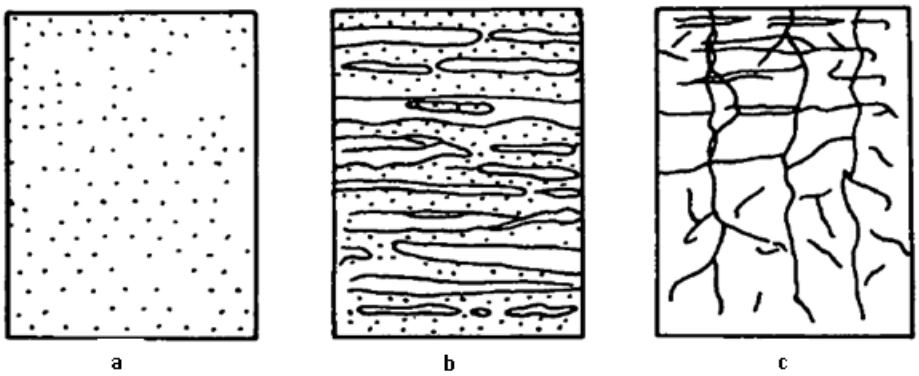

Figure 2.3 Frozen soil structures: (a) massive, (b) layered, and (c) honeycombed ice (Tsytovich 1960)

2.2.2 Frost Heaving

Figure 2.4 illustrates the frost heaving process when the ground freezes. Ground freezing is a top-to-bottom phenomenon due to a drop in the atmospheric temperature. Frost heaving is defined as the swelling of the ground due to ground freezing. It is a well-established fact that the molar volume expansion of water is 9% when the temperature drops below the freezing point and water changes its phase. Due to freezing, the pore water in the soil either freezes or develops negative pore water pressure. Unfrozen water migrates toward the freezing front to form ice lenses. Depending on the rate of freezing, water may freeze in place or flow to the freezing front. The formation of ice lenses pushes the soil matrix apart thus forcing the ground to heave.

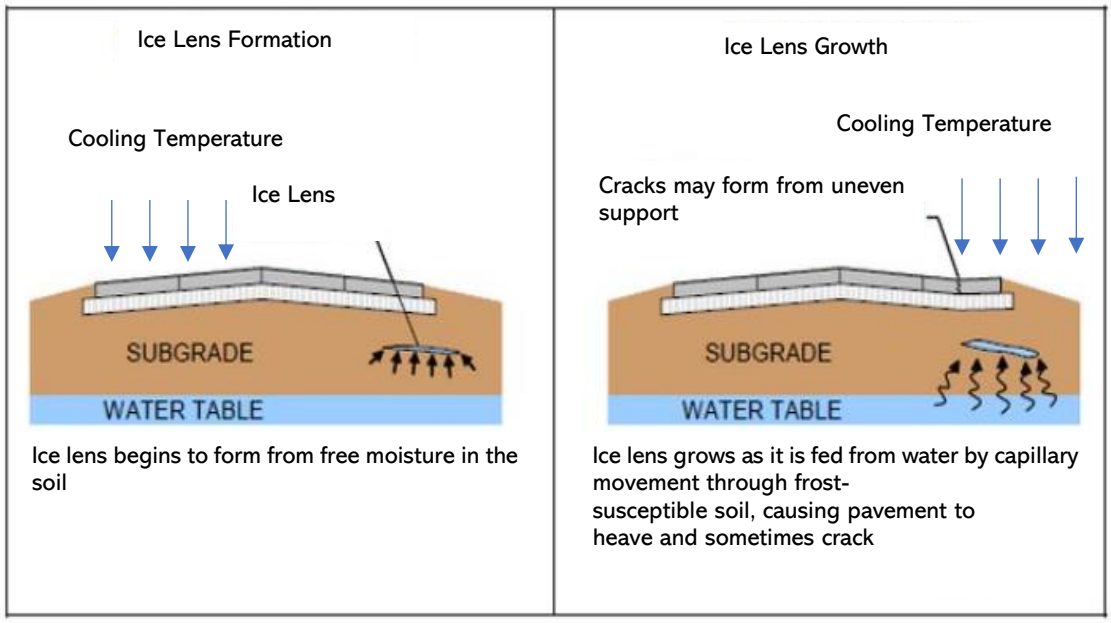

Figure 2.4 Physical process of soil freezing (Ahmad and Khawaja, 2018)

Frost heave is developed when the heaving pressure surpasses the overburden pressure (Semnani, 2018). Frost heave primarily depends on the supply of water to the freezing front and ice accumulation (Taber 1930). These factors in turn depend on the following:

1. The rate of freezing: If water in the soil freezes rapidly, it is more difficult for water to reach the freezing front. Due to rapid freezing, the water supply to the freezing front may be stopped which limits the amount of frost heave.

2. Unsaturated hydraulic conductivity: A higher unsaturated hydraulic conductivity results in a larger frost heave. It has been experimentally observed in Li et al. (2018) that fine-textured soil has more potential to heave than coarse grained soil since the latter has a lower unsaturated hydraulic conductivity compared to the former.

Some examples of the damage caused by frost heave are shown in Figure 2.5. The rate of frost heave for different types of soils is shown in Figure 2.6. Upward water movement from the

groundwater table due to capillary action has a limitation. Water can flow upward to the freezing front if the height of the flow is less than the maximum height of the capillary action. Peck et al. (1974) presented the following relationship to calculate the maximum height of the capillary action:

$$hc = {C}/{eD10} \quad (2.1)$$

where hc is the maximum height of the capillary action, C is a constant that ranges from 10 and 50 mm^2 depending on the surface impurities, e is the void ratio, and D10 is the effective grain size of the soil.

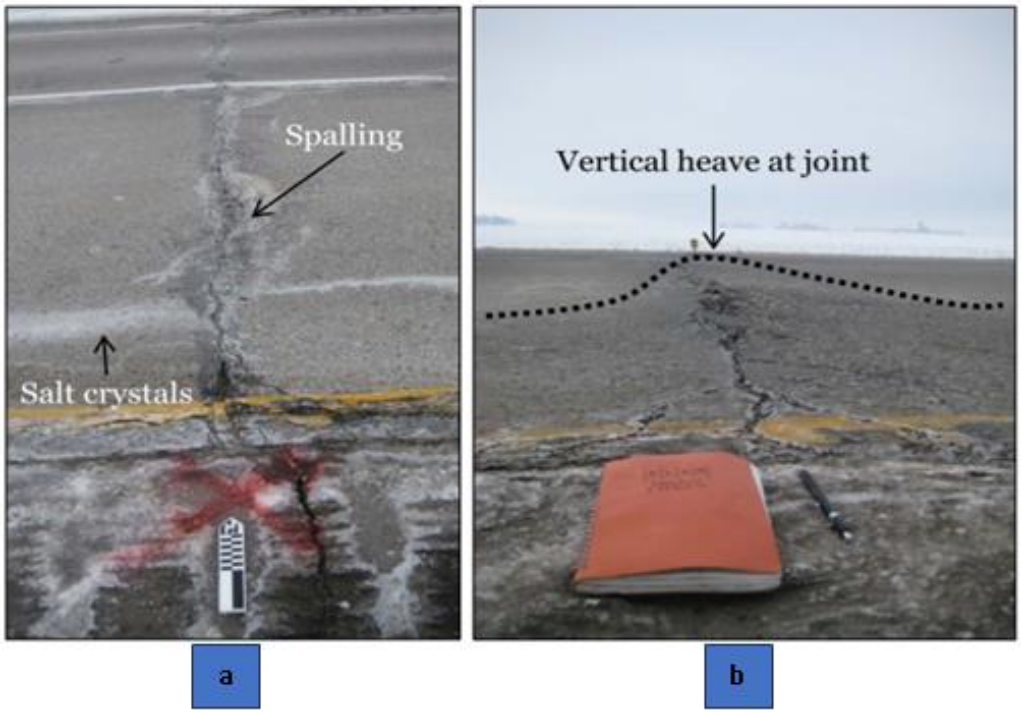

Figure 2.5 Damage due to frost (a) joint deterioration with spalling; (b) vertical heave at joint location of road (Zhang et al. 2018)

If there is an abundant water supply during freezing, frost heave could be very serious and large enough to push piles out of the ground for bridges. Since frost action can develop in any direction except straight up, foreign objects (like a pile) can be pushed out of the ground.

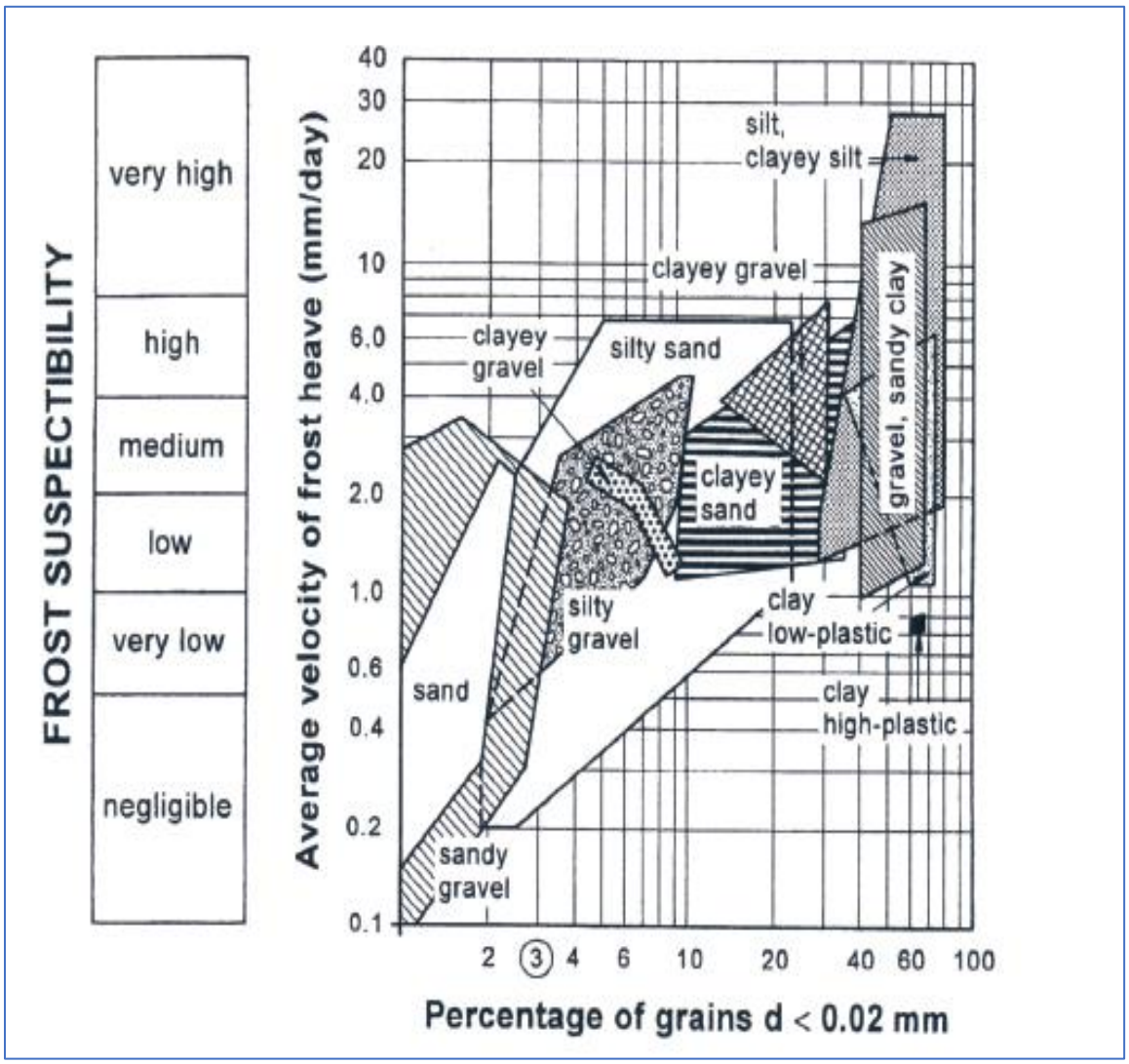

Figure 2.6 Frost heaving in different types of soils (Tiedje 2015)

2.3 Thaw Behavior

2.3.1 Introduction

The thawing of frozen soil is initiated when the ground temperature is higher than the freezing temperature. During the thawing of frozen soil, ice in the pores of the soil melts, which causes

water to drain to the surface. Due to the reduction of hydraulic conductivity of the frozen soil with only one dimensional drainage to the ground surface, excess water cannot flow through the pores since it is blocked by the ice. This supersaturated soil condition causes the soil to be more easily eroded. The shear strength of the soil consists of the cohesive bonds between the soil particles, and frictional resistance at particle contact and/or particle interlocking. In essence, the shear strength provides the resistance of the soil against erosion. In general, there are two forms of cohesion: true cohesion and apparent cohesion. True cohesion is the chemical bonding between particles which depends on the type of soil. On the other hand, apparent cohesion is due to water tension in the soil matrix and governed by the water content in the soil. When the soil thaws, the generation of excess water reduces the apparent cohesion to zero. The shear stress, τ, caused by water flowing over the soil surface, is given by (Flerchinger et al. 2005):

$$\boldsymbol{\tau = \gamma RS} \qquad 2.2$$

where *R* is the hydraulic radius of the flow, γ is the unit weight of water, and *S* is the slope of the soil surface.

The gradual draining of water causes soil to consolidate. As the ice lenses melt the layers below, the pores begin to open. Since the pores are saturated with water, water penetrates the ground only to the unfrozen and unsaturated layers. For Instance, continuous thawing of the permafrost was the main cause of embankment settlements in the Qinghai-Tibet highway and railway (Yu et al. 2002). The damaged section of the embankment was underlain by permafrost with a high ice content. Thaw consolidation is also one of the main factors that cause damage to oil pipelines across permafrost regions (Oswell 2011). This study report on the Trans-Alaska Pipeline System shows that large thaw consolidation usually occurs at locations with ice-rich frozen soil. Another example is the oil pipeline in Siberia, Russia. One of the case studies conducted by Greenpeace

states that “Up to 55 billion roubles (1.9 billion dollars) a year is spent on repairs to infrastructure and pipelines damaged by changes in the permafrost in western Siberia” (Independent 2009). Figure 2.7 shows the oil pipeline in Siberia affected by the thawing of the ground. Hanna et al. (1990) explained the factors that affect thaw settlement, including the thaw depth and potential difficulties in determining the water content in soil.

Figure 2.7 Thawing of permafrost threatens Russia’s oil and gas pipelines (Independent 2009)

2.4 Seasonal Freeze–Thaw Process

The engineering properties of soils, such as the permeability, bearing capacity, hydraulic and electrical conductivities etc., change considerably due to changes in their physical state (frozen, thawing or unfrozen). Permafrost can provide a very high bearing capacity to support building loads. However, seasonal F-T cycles that result in the redistribution of pore water lead to

differential ground settlements which cause permanent distortion that significantly damages the overlying structures.

Seasonal F-T, due to fluctuations of the temperature of the ground surface and the atmosphere, occur in the topmost layer of the ground. This topmost layer is known as the frost penetration layer, and influenced by variations in the atmospheric temperature.

Figure 2.8 shows the annual temperature profile of frozen ground. The annual mean permafrost surface temperature is obtained by extrapolating from the common linear portion of the temperature profile with depth. The effects of the soil particle, solutes, and hydrostatic pressure decrease the phase equilibrium temperature so that the layer just above the base of the permafrost does not contain ice. The change in the slope of the temperature profile at the base of the ice-bearing permafrost is caused by the difference in thermal conductivities between the frozen and unfrozen ground.

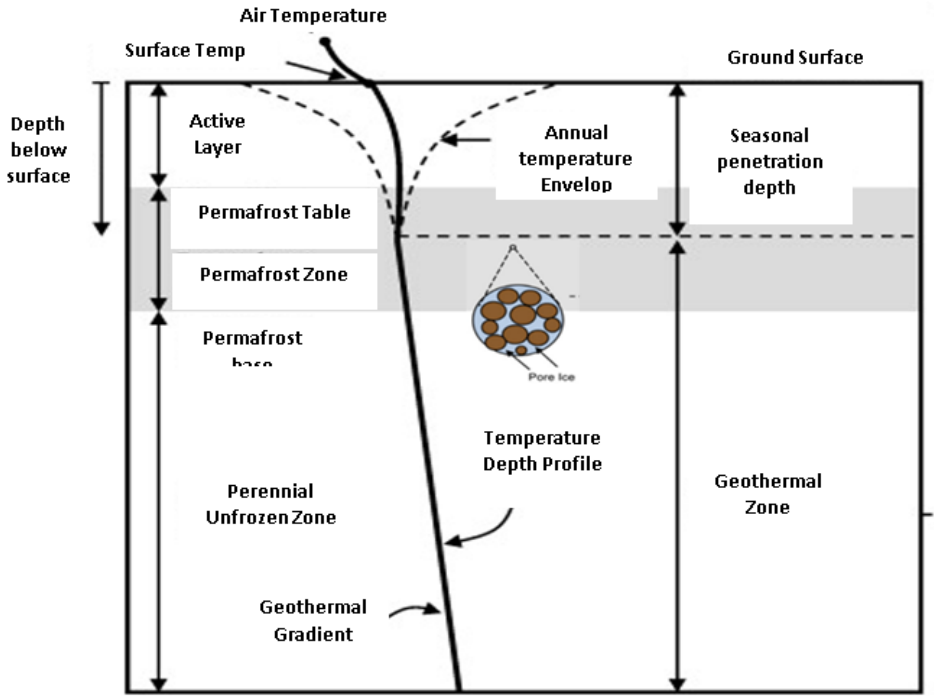

Figure 2.8 Schematic temperature profiles in permafrost (Luthi 2010)

In other parts of Canada with no permafrost, the seasonal and long-term changes in freezing of the ground play an important role in the environment and construction of infrastructure. When the ground freezes, the mechanical strength of the frozen ground increases, thus providing a strong foundation for buildings and infrastructures. However, the seasonal F-T cycle leads to an increase in the depth of thawing of the frozen layer which may severely affect building foundations and cause deterioration of the ground conditions.

During the winter season, suspended water in the ground freezes which increases the mechanical strength of the soil. However, this causes frost heaves and additional stress on buried structures. On the other hand, during the summer season, frozen water in the ground melts down which leads to the loss of the mechanical strength of the soil, which may eventually cause ground subsidence and ground settlements, and even foundation failure. The thawing of frozen soil drastically changes the properties of the soil. Brandl (2008) explained the F-T behavior of soils and suggested that the following factors affect the F-T of soils:

- grain size distribution, mineral composition
- organic components
- soil chemistry
- water content and degree of saturation
- density and degree of compaction
- hydraulic permeability
- capillarity
- groundwater levels
- availability and supply of water (precipitation, seepage water, groundwater)
- temperature, hydraulic gradient, and chemistry of the groundwater
- temperature conditions (magnitude and period of freezing temperature, temperature gradient)

- the local climate, especially F-T cycles
- overburden
- composite behavior of the soil structure (multiple layer road systems).

2.5 Pile Foundation

2.5.1 Introduction

The use of piles in civil engineering construction dates back to ancient times. In medieval times, wooden piles were used as foundations to support large structures and timber piles were driven into the ground by hammers. Wooden piles were best suited for the foundation because of their strength, weight, and durability. However, in modern days, wooden piles have been largely replaced by concrete and steel because of their ease of fabrication, durability, and strength. The first ever pile driving equipment was invented by a Swedish inventor by the name of Christoffer Polhem in 1740 (Adejumo and Boiko 2012).

Pile foundation is a substructure for the transfer of loads from the superstructure to the deeper underlying stratum located at a certain depth. Drive pile foundation is used in places with poor ground conditions where shallow foundations cannot provide a viable solution economically, or where ground water is difficult to control during construction. Shallow foundations are not suitable for large lateral loads. They are usually not recommended in cold regions where ground heaving is expected because of seasonal freezing since shallow foundations have very low resistance to withstand uplift forces.

Depending on the geology of the site, a pile can transfer the load to the underlying soil through either the base resistance or the shaft friction along the embedded length of the pile.

Figure 2.9 shows the different components of a typical pile foundation. The main components of the pile foundation are the piles and the pile cap. Piles are a long slender member that transfers

the load to the soil beneath the ground surface. The pile cap is a slab provided on top of the piles to distribute the load evenly from the superstructure.

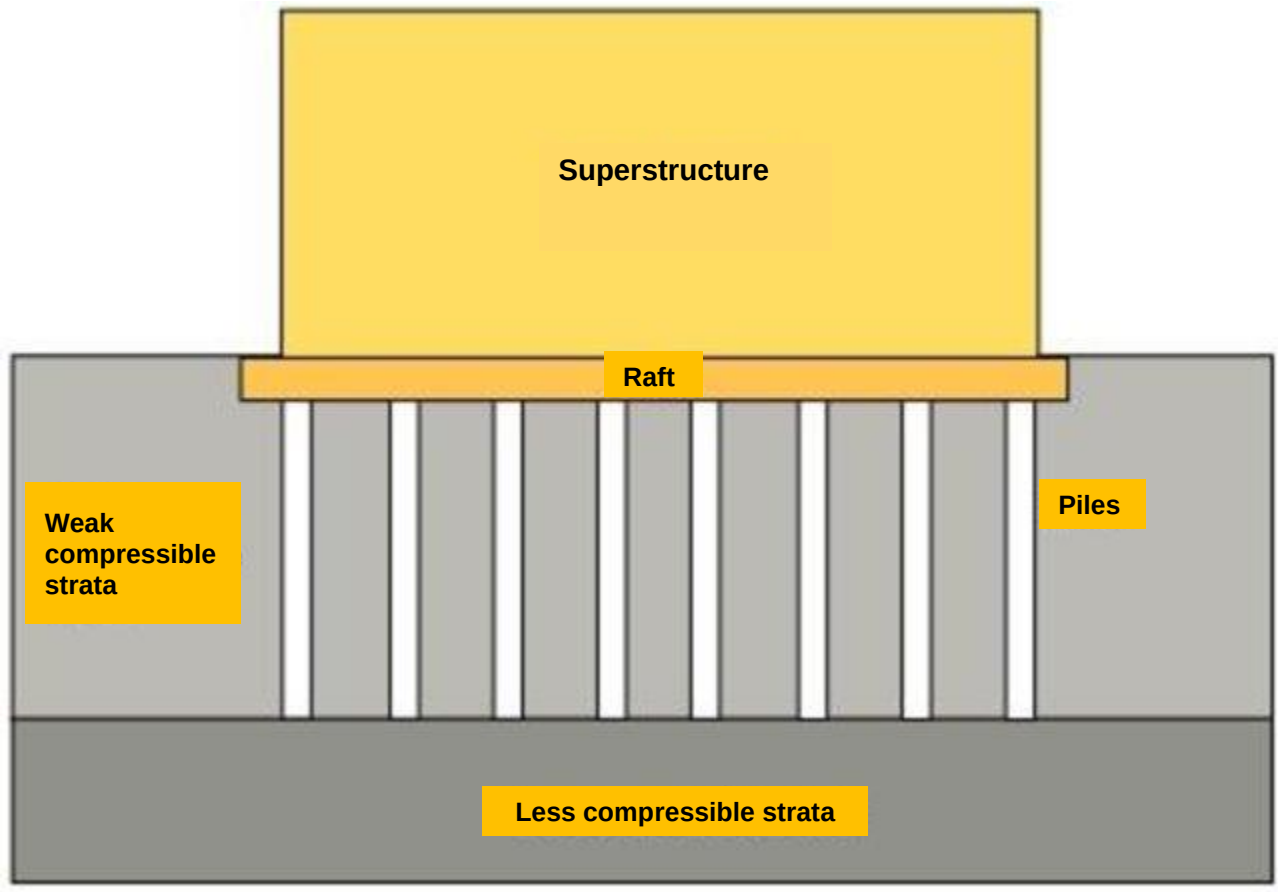

Figure 2.9 A typical pile foundation (Shakir et al., 2020)

2.5.2 Classification of Piles

2.5.2.1 Load Transfer Mechanism

The load from a superstructure is distributed to the soil either through the skin friction of the pile or the end bearing of the pile that rests on a hard stratum. Depending on the load transfer mechanism, piles can be classified as a friction pile or end bearing pile as illustrated in Figure 2.10. In the former, more than 80% of the overall resistance is derived from skin friction. In a friction pile, the pile–soil interaction at the surface of the pile provides most of the resistance against pile movement (Taha and Fall, 2013, 2014). On the other hand, end bearing piles transfer

the load to a firm stratum found at a considerable depth below the ground surface. An end bearing pile provides most of its resistance from the toe of the pile. In summary, friction piles provide the most resistance through their shaft while end bearing piles provide most of the resistance from

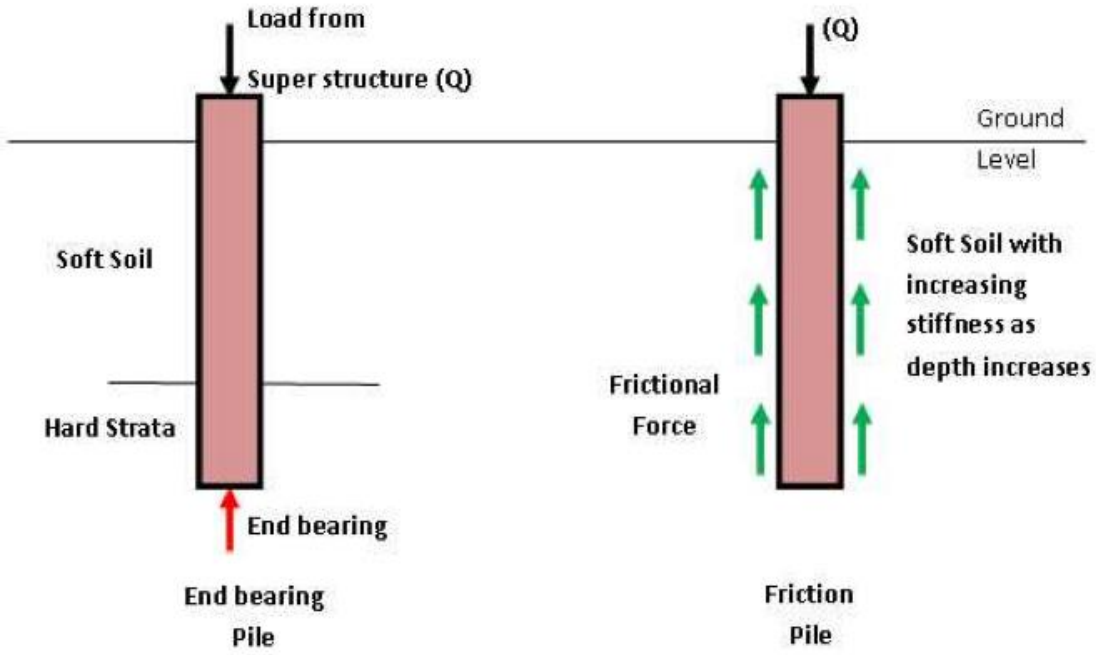

the base (Basu et al. 2008)

Figure 2.10 End-bearing and friction piles (JICA 2019)

2.5.2.2 Pile Material

As stated earlier, modern day civil engineering construction has adopted the use of piles made of different materials. Based on the material, piles can be classified as timber, concrete, steel, or composite piles as shown in Figure 2.11. The selection of pile material depends on the construction requirements.

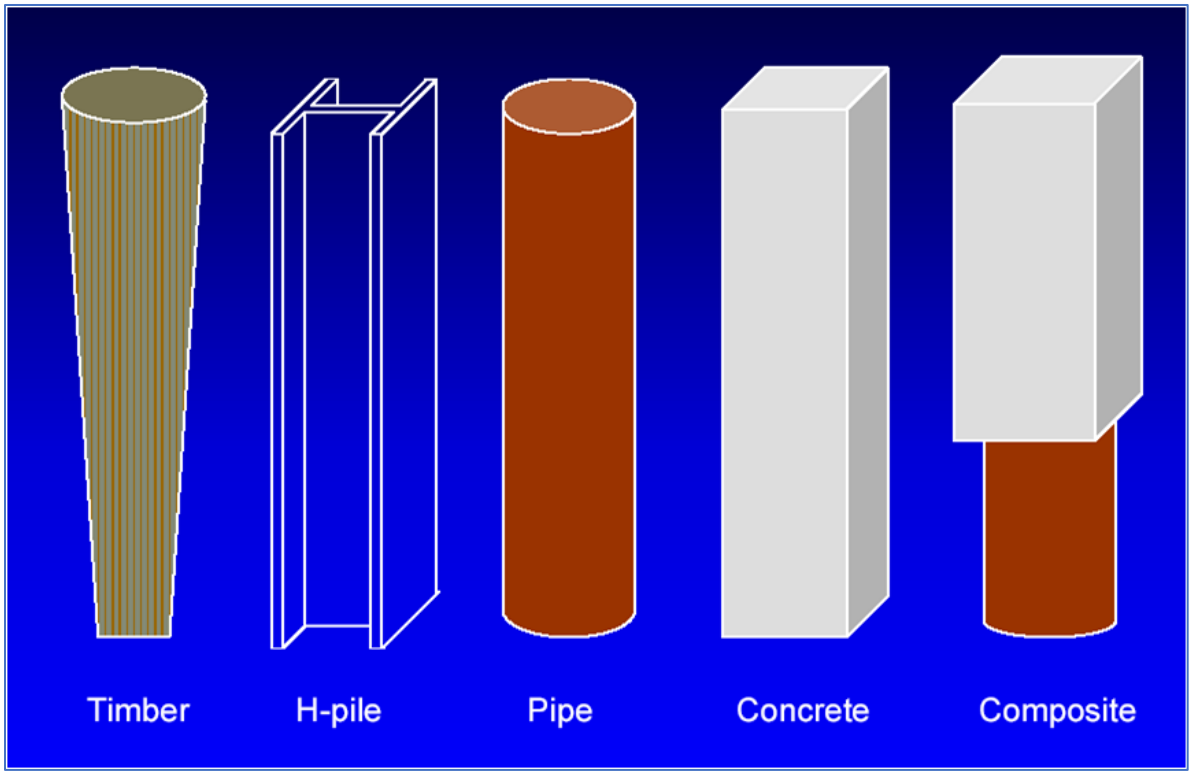

Figure 2.11 Typical Materials used in Piles (Engineering Discoveries, n.d.)

2.5.2.3 Methods of Pile Installation and Ground Disturbance

Piles can be classified as driven or bored piles according to the installation method. These are also called displacement or non-displacement piles (Figure 2.13). The selection of pile installation method (Figure 2.12) depends on a number of factors, such as ground conditions, environmental conditions, hydrological conditions, etc. For example, bored piles are suited for dense ground, whereas driven piles are preferred in loose soils. Since displacing firm soil is difficult, minimal or no support is needed for bored piles. On the other hand, if bored piles are used in loose ground, proper support is required to avoid soil collapsing into the pile cavity during construction.

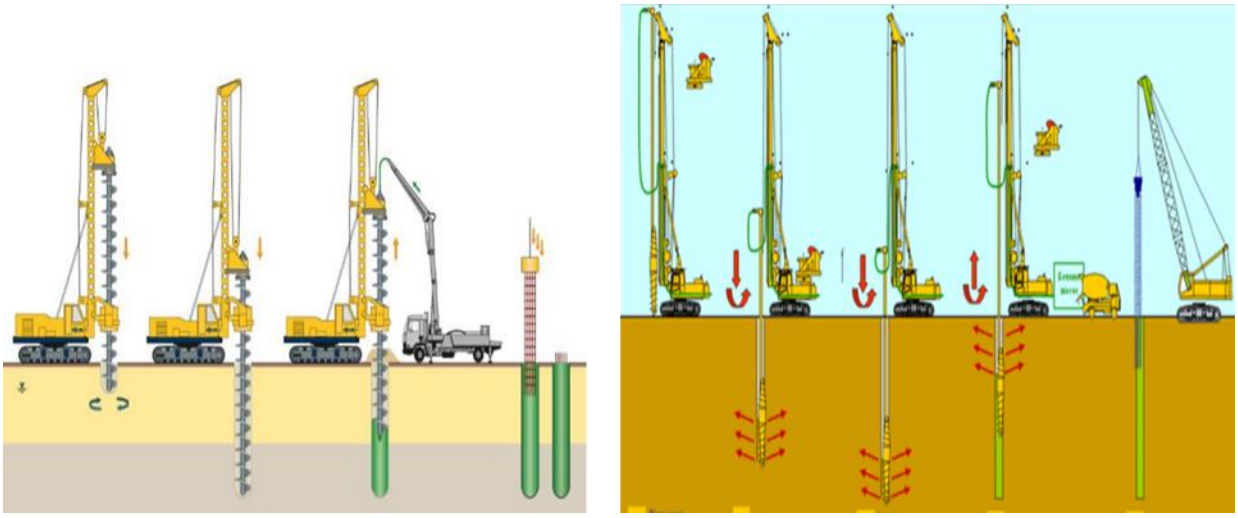

Figure 2.12 Methods of Pile Installation (JICA 2019)

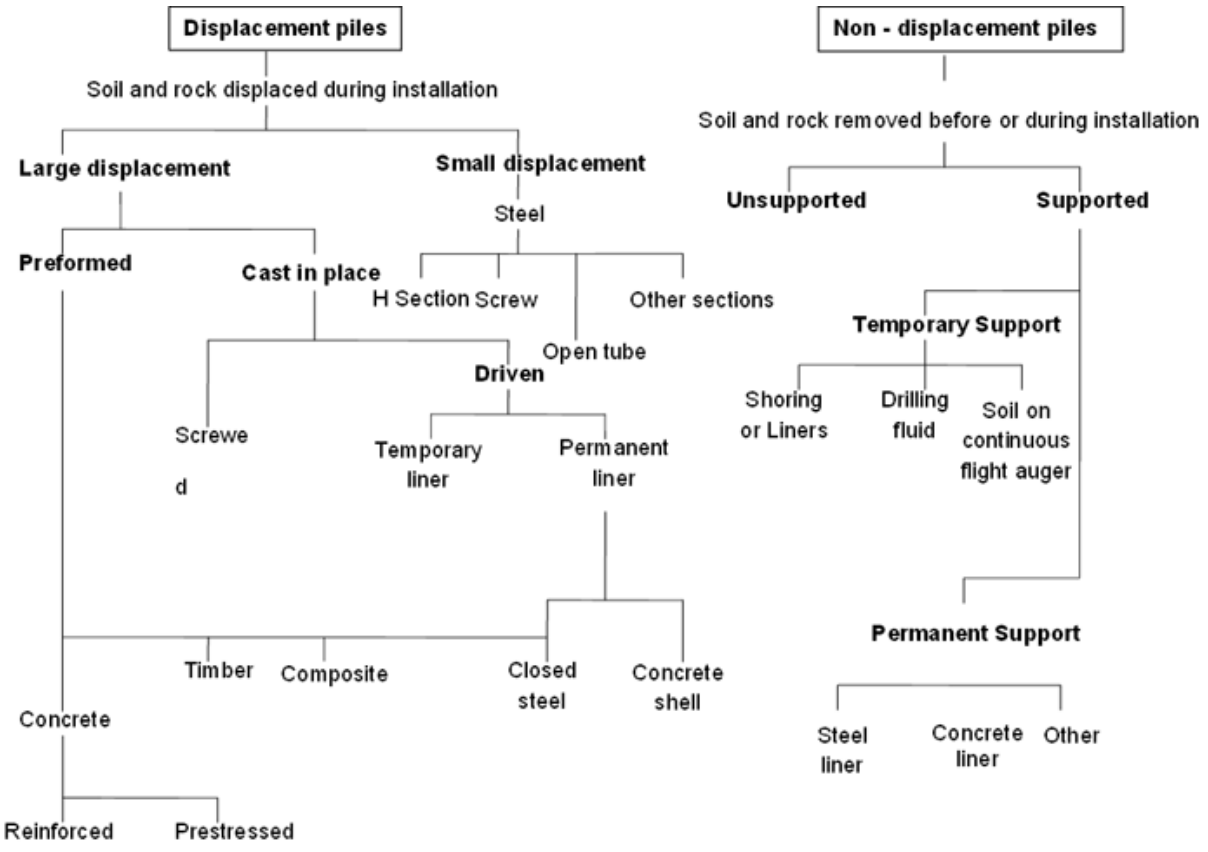

Figure 2.13 Displacement and non-displacement piles (Kouretzis 2018)

2.5.2.4 Pile Loading and Load Transfer Mechanism

Piles can be loaded axially under compression or tension and laterally subjected to horizontal forces as shown in Figure 2.14. The compressive loading is the sum of the self-weight of the pile and the load transferred from the superstructure. The pile can be under tension due to moment, rotation, or frost jacking. At the same time, horizontal forces can include wind, seismic, traffic, and shear loads, etc. Lateral loading on the pile depends on the length of the pipe and head-fixing condition. Free-head short piles tend to rotate at the center, whereas fixed-head piles move laterally.

The load carrying capacity of the pile subjected to a load “P” is the result from a combination of skin friction from the pile shaft and tip resistance from the end-bearing of the pile (Basu et al. 2008).

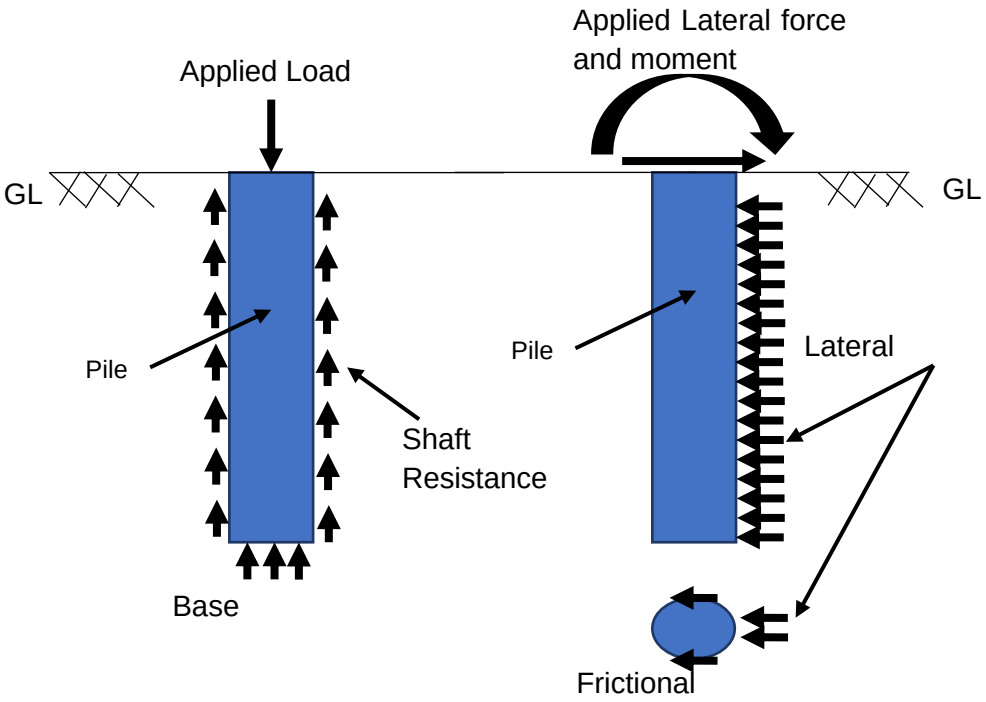

Figure 2.14 Load transfer mechanism in piles (Basu et al. 2008)

2.5.3 Pile Design for Axial Loading

Two types of axial loadings, namely, compression and tension, are likely to act on a pile. Loads on the pile are also dependent on the ground and seasonal conditions, etc. For instance, pile foundations in cold regions such as Canada are subjected to compression during summer and tension during the winter. As discussed in Section 2.5.2.4, two types of resistances are provided by the pile to transfer loads to the ground. The ultimate capacity of the pile is the combination of both resistances provided by the pile. Therefore, the carrying capacity of the pile can written as (Tomlinson and Woodward 2008):

$$\boldsymbol{Q_{ult} = Q_b + Q_s} \qquad 2.3$$

where Q_{ult} is the ultimate resistance of the pile, Q_b is the base resistance and Q_s is the shaft resistance of the pile which are given by:

$$\boldsymbol{Q_s = \int_0^L f_s\, C\, dz} \qquad 2.4$$

$$\boldsymbol{Q_b = f_b\, A_b} \qquad 2.5$$

fs = Ultimate skin friction;

C = Circumference of the pile;

L= Embedded length of the pile;

f_b = Ultimate resistance of the pile base;

A_b = Area of the pile base;

and:

$$\boldsymbol{f_s = C_a + K_s\, \sigma'_v\, tan\delta} \qquad 2.6$$

C_a = Pile adhesion;

δ = angle of friction between the pile and the soil;

σ_v =Vertical effective stress;

K_s = Coefficient of lateral earth pressure;

and:

$$\boldsymbol{f_b = C_h\, N_c + \sigma'_{vb}\, N_q + 0.5\, \Upsilon\, B\, N_\Upsilon} \qquad 2.7$$

where

N_c, N_q, and N_Υ are the bearing capacity factors;

γ = Unit weight of the soil;

B = Pile diameter;

C_h = Cohesion of the soil beneath the base; and

σ'_{vb} = Vertical effective stress at the pile base.

The Vesic bearing capacity factor gives the values of N_q for different soil friction angles (ϕ) and different pile installation methods in cohesionless soil. N_Y can be calculated by using the Vesic bearing capacity equation.

$$N_\gamma = 0.6(N_q - 1)tan\emptyset \qquad 2.8$$

Table 2-1 Vesic bearing capacity factor of N_q for different friction angles and different methods of pile installation (Rayhani, 2018b).

Φ°	**20**	**25**	**28**	**30**	**32**	**34**	**36**	**38**	**40**	**42**	**45**
N_q Driven	**9**	**12**	**20**	**25**	**35**	**45**	**60**	**80**	**120**	**160**	**230**
N_q Drilled	**4**	**5**	**8**	**12**	**17**	**22**	**30**	**40**	**60**	**80**	**115**

Pile Design using α Method

The α method for determining the pile capacity is based on the total stress analysis under undrained conditions $\Phi = 0^0$

$f_s = \alpha \times S_u$, ($C = S_u$)

$\alpha = 1$, for $S_u < 25$ KPa

$\alpha = 1 - 0.5 ((S_u - 25) / 50)$, for 25 KPa $< S_u <$75 KPa

$\alpha = 0.5$, for $S_u >$ 75 KPas

$f_b = S_u \times N_c$

α = reduction coefficient, S_u = undrained cohesion at the pile

$$\boldsymbol{Q_{ult} = \int_0^L \alpha\, s_u\, C\, dz + s_{ub}\, N_c\, A_b} \qquad 2.9$$

S_{ub} = Average value of S_u within a depth of 2-3D beneath the base.

Pile Design using β Method

The β method is based on an effective stress analysis of the pile in cohesive and cohesionless soils.

$f_s = K_s\ \sigma_v\ \tan \delta$

β= Shaft friction coefficient = $K_s \tan \delta$,

K_s = 1- Sin Φ (Normal Consolidation)

K_s = (1- Sin Φ) √ OCR (Over consolidation)

$f_s = \beta\ \sigma_v$

$f_b = S_{ub}\ N_c$

$$\boldsymbol{Q_{ult} = \int_0^{L_e} \beta\, \sigma_v'\, C\, dz + s\, N_c\, A_b} \qquad 2.10$$

σ'_v = vertical effective stress at the point

L_e= effective length

2.5.4 Pile Design for Lateral Loading

Piles subjected to lateral loading is a complex interaction phenomenon that involves a semi-rigid structure and plastic or elastic deforming soils. The lateral loads can be exerted by wind, earthquakes, water currents, the surrounding soil, rotations, etc. When the pile is loaded laterally, the load from the pile cap is initially transferred to the soil closer to the ground surface, which is then transferred to greater depths (Sawant and Kumari 2021).

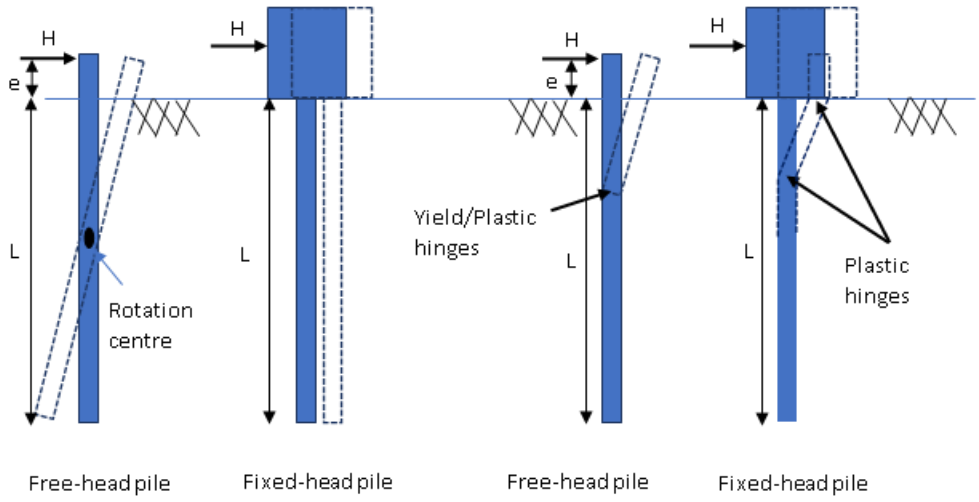

Figure 2.15 Failure modes of long and short piles subjected to lateral loadings (Tomlinson and Woodward 2008)

The design of laterally loaded pile is mainly governed by the length of the pile and the fixity condition of the pile head. Depending on the length of the pile, it can be considered as long or short. The failure modes of piles under lateral loadings are shown in Figure 2.15.

Two types of failure modes exist when a pile is subjected to lateral loading: soil failure and pile failure. The former generally occurs in short piles because of the lower assistance provided to the

pile against rotation and lateral shift, whereas the latter occurs in long piles because of the high passive resistance provided by the soil at the lower part of the pile.

Figure 2.16 shows the stress distribution for both long and short piles subjected to lateral loading.

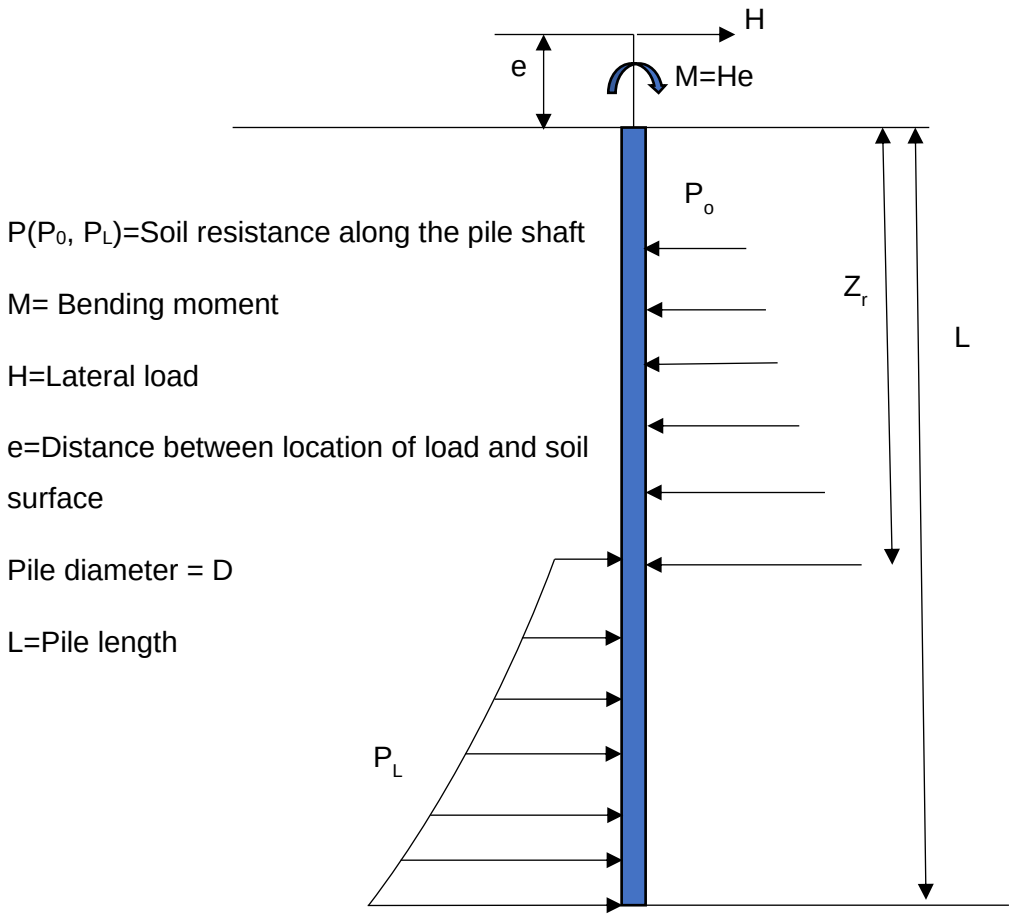

Figure 2.16 Stress distribution on pile subjected to lateral loadings (Rayhani, 2018a)

The lateral capacity of a pile can be calculated by using Brom's method. According to Brom's method, the lateral load capacity of a pile can be determined from:

$$\boldsymbol{H_u = \int_0^{Z_r} P_u D\, dz - \int_{Z_r}^{L} P_u D\, dz} \quad (2.11)$$

P_u= Ultimate soil resistance along the pile shaft;

H_u=Ultimate lateral load;

Z_r= Pile Length subjected to P_0

$$\boldsymbol{M_u = H_u e - \int_0^{Z_r} p_u D\, dz - \int_{Z_r}^{L} p_u D\, dz} \quad (2.12)$$

M_u= Ultimate bending moment;

$$M_{max} = H_u(e + 1.5D + f) - 9c_u D f\frac{f}{2} = H_u\left(e + 1.5D + \frac{f}{2}\right)$$

$$f = \frac{H_u}{9c_u D}$$

M_{max} = Maximum bending moment;

C_u = Soil cohesion (undrained shear strength);

e = Distance between location of load and soil surface;

d = pile diameter;

$$M_{max} = \frac{9c_u D}{4}(L - 1.5D - f)^2$$

$$\boldsymbol{H_u\left(e + 1.5D + \frac{f}{2}\right) = \frac{9c_u D}{4}(L - 1.5D - f)^2} \quad (2.13)$$

$H_u = 9\ C_u\ D\ (L - 1.5D)$, when $M_{max} < M_{yield}$

Short pile failure $M_{yield} > M_{max}$

Long pile failure $M_{yield} < M_{max.}$

2.5.5 Pile in Frozen Soils

When designing piles in freezing or frozen ground, the three following additional factors must be considered:

- Pile capacity based on pile adfreeze;
- Admissible settlement or settlement rate; and
- Uplift forces due to freezing.

When the soil adjacent to the pile freezes around the pile shaft or on the sides of the pile cap, the uplift forces will have a tendency to lift the foundation. Heaving of the ground in a frost-susceptible soil also causes uplift forces that will push on the undersides of the pile cap. These uplift forces acting on the sides of the pile foundation are known as adfreezing forces.

The adfreeze creates a shear force on the pile shaft that supports a significant portion of the load applied on the pile (Ladanyi and Theriault 1990). However, the adfreeze strength is dependent on the temperature, ice content, and strain rate of the frozen ground. Therefore, the worst ground condition is usually considered in the design which is mainly based on summer conditions when the adfreeze strength is the lowest. During winter, the frozen soil increases the adfreeze bonding between the pile and soil at their interface. However, during summer, melting of the ice in the soil causes a drastic reduction in the soil strength (Chang and Liu 2013). Proper foundation design is needed to ensure that there is enough resistance to withstand uplift force due to frost heave during ground freezing (Penner and Burn 1970). Finally, the creep laws for ice and frozen ground can

be used to estimate the rate of settlement of the pile base to determine the settlement of the structure during its lifetime.

The allowable load on the pile is based on the capacity of the pile. The load carrying capacity of a pile in frozen ground can be estimated from the shearing resistance on the pile shaft and the bearing capacity at the tip of the pile. Figure 2.17 shows the forces acting on the pile during summer and early fall, when the strength of the soil is the lowest in terms of its bearing capacity. Downward force is generated during the thawing of the frozen soil due to the consolidation of thawed soil. The excess water is drained out of the voids to the surface, whereas the frozen layer underneath provides an uplift force.

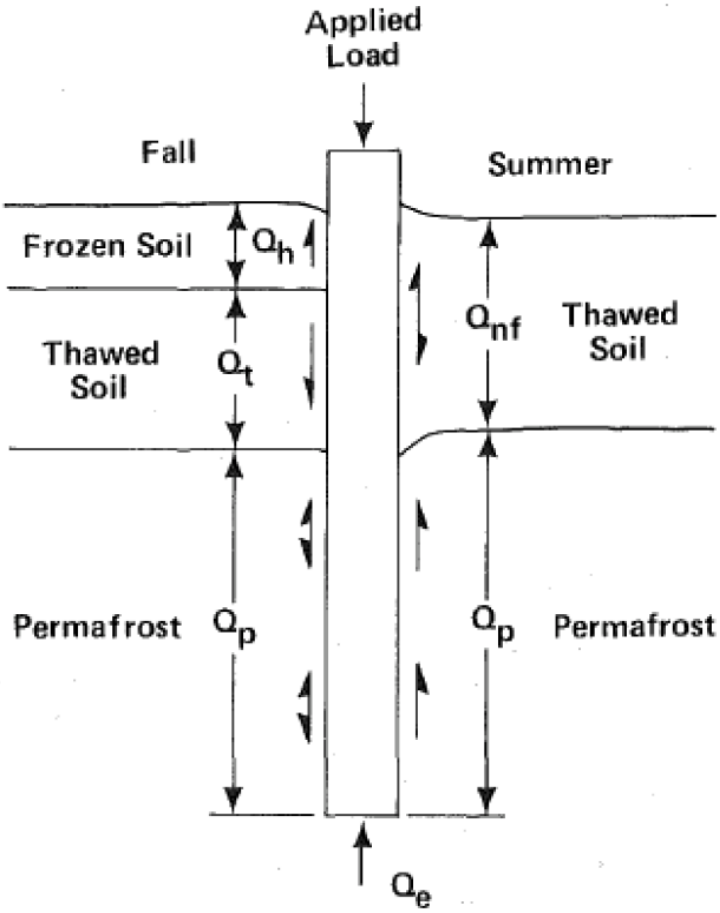

Figure 2.17 Forces acting on a pile in freezing and thawing ground (Heydinger 1987)

Hence, the equation to calculate the pile capacity can be written as:

$$\boldsymbol{Q_n = \frac{1}{FS}\left(Q_p - Q_{nf} + Q_e\right)} \qquad 2.14$$

where Q_p is adfreeze force, Q_{nf} is the negative side friction, and Q_e is the end-bearing resistance.

As discussed earlier, the adfreeze force that acts on the shaft of the pile represents the cohesive force between the pile surface and the soil, and at the same time, provides the adfreeze strength for the pile. The adfreeze force is directly proportional to the roughness of the pile surface, and can be calculated from the following (Aldaeef and Rayhani 2019):

$$\boldsymbol{\tau_a = m * C_{lt}} \qquad 2.15$$

where τ_a is the adfreeze shear strength, m is the roughness coefficient of the pile surface, and C_{lt} is the long-term soil cohesion of the frozen soil, which depends on the ice content of the soil and the permafrost temperature.

It is worth noting that if the soil has low ice content, the adfreeze cohesion will be very small. Therefore, the pile should be designed in consideration of the thawed condition with no adfreeze force of cohesion. Moreover, for cast in place piles, the empty space shall be filled with slurry instead of dry sand/gravel to ensure back freezing. Due to the thawing of frozen soil, the soil undergoes thaw consolidation. The structures built on ground subjected to F-T will settle during this process. The settlements can be calculated by using the following expression (Crory 1973):

$$\frac{\Delta H}{H_f} = 1 - {\rho_{df}}/{\rho_{dth}} \quad (2.16)$$

where ρ_{df} is the density of the frozen soil, $\rho_{d,th}$ is the density of the thawed soil, H_f is the thickness of the frozen soil, and ΔH is the change in thickness before and after thawing.

It has been experimentally determined that the adfreezing forces can be removed by replacing frost-susceptible soil, up to the depth of the frost penetration, with a non-frost-susceptible soil such as sand or crushed well-graded rock. A compressible layer can be used beneath the pile cap between the soil and structure to reduce the effect of the uplift.

2.5.6 Pile Subjected to Frost Heave and Thaw Settlements

It is known that soil displacements around a pile in unfrozen soil are larger than soil movement away from the pile. A similar response is observed for a pile during freezing or thawing of the ground. In a study conducted by Tang et al. (2018), maximum ground heave and thaw settlement are observed at a distance of 2D (D is the pile diameter) from the pile during F-T cycles. Furthermore, soil movements are reduced as the distance from the pile is increased.

In the analysis in Tang et al. (2018) of unfrozen water distribution in soil that surrounds the pile, the unfrozen water migrates to the pile–soil interface. During the freezing process, this water forms a film of ice on the surface of the pile (Tang et al. 2018). This film around the pile creates suction of unfrozen water in the surrounding soil. Since water migrates to the freezing front, more ice lenses are developed which leads to frost heave. The in-situ frost heave is caused by the continuous cooling of unfrozen water in the pores of the soil thus resulting in a volumetric increase of 9%. The migration of unfrozen water to the freezing front causes segregation of the water and soil which results in a volumetric expansion of 109%. Therefore, the volumetric expansion of segregation heave is much larger than in-situ frost heave. Theoretically, soil heave at the pile-soil

interface should be the largest. However, since the pile is much more rigid than the soil, it imposes a constraint on the vertical and lateral movements of the soil. The influence zone of the constraint imposed by the pile ranges from the pile surface up to 7D from the pile surface. The general movement of the soil that surrounds the pile during freezing is shown in Figure 2.18. The effect of soil heave on the pile can be seen in Figure 2.19 where the pile is pushed out of the ground by the frozen ground forces at Clearwater Lake bridge in Alaska, USA.

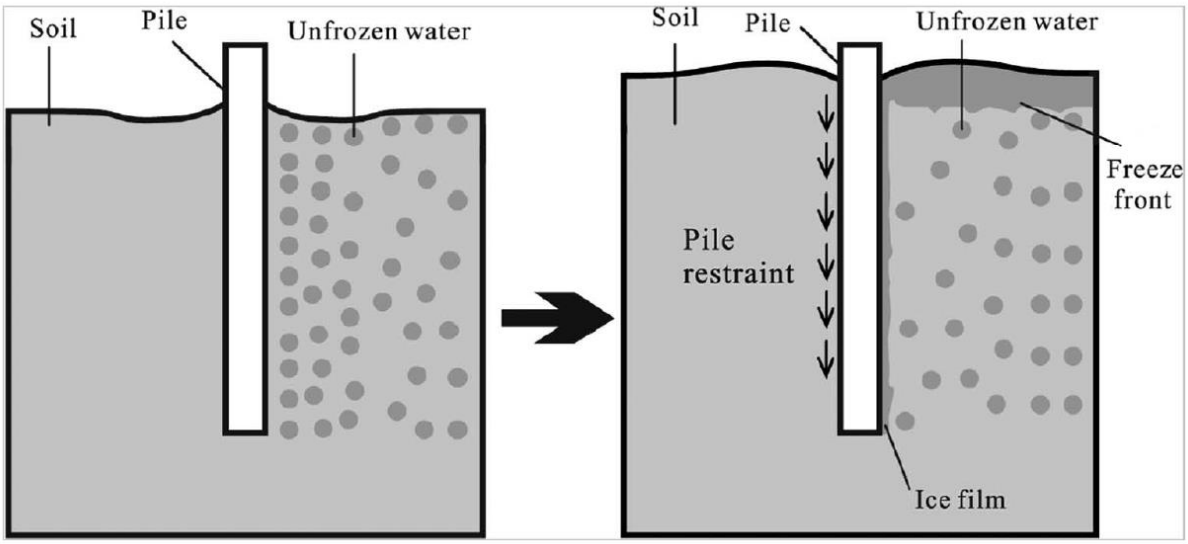

Figure 2.18 Frost heave around pile (Tang et al. 2018)

Figure 2.19 Piles at Clearwater Lake bridge in Alaska being forced out of ground due to frost heave (Pewe and Paige 1963)

Tang et al. (2018) showed that during the thawing of frozen soil, the ice that surrounds the pile and the surrounding soil begins to melt. This results in excess water within the soil due to thawing as illustrated in Figure 2.20. During thawing, the soil loses its frozen strength and the ground begins to settle. The thaw settlement is the difference between free settlement and the settlement due to the constraint imposed by the pile on the vertical and lateral movements of the soil. It is seen that the constraint of the pile affects the settlement of the surrounding soil. The adhesion between the pile and the soil provides vertical resistance on the soil movement, but this effect is reduced as the distance from the pile is increased. Tang et al. (2018) found that maximum thawing settlement occurs at a distance 2D from the pile. According to this study, the settlement patterns are similar for frost action and free thaw settlement. The results may vary if the free movement of the soil is restricted.

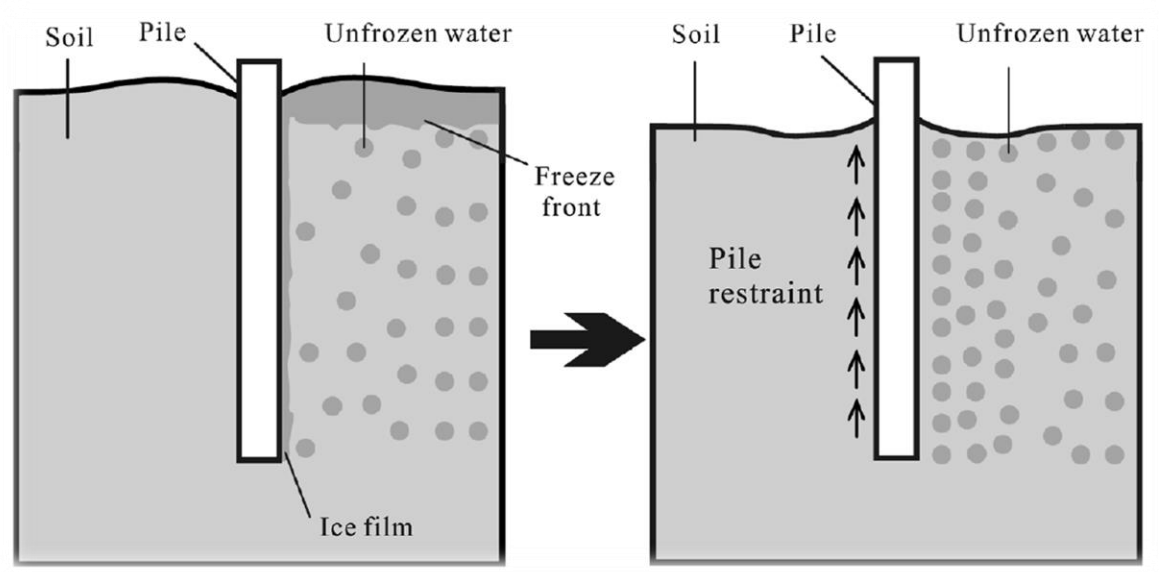

Figure 2.20 Thaw settlement around pile (Tang et al. 2018)

2.6 Literature Review on Physical Testing and Numerical Modelling of Piles Subjected to Lateral and Axial Loadings

In addition to the studies discussed earlier, there are other numerical modeling and physical experiments done on piles subjected to axial and lateral loadings.

A three-dimensional numerical model was developed by Rahman and Achmus (2006) to determine the behavior of a vertical pile under combined (axial and lateral loads) loadings. In this study, steel piles of 20 m in length with a wall thickness of 2 cm was modelled numerically. The angle of the loading varied from 0° (horizontal) to −90° (compressive load) and 90° (tensile load). The vertical and horizontal pile head displacements were plotted against the applied loads. They found that the horizontal pile head displacement is not affected by the compressive loads, but the presence of the lateral load reduces the uplift and vertical displacement under compression which increases the axial load capacity.

Lee et al. (2010) proposed a method to estimate the ultimate lateral load capacity, H_u of piles by using cone penetration test (CPT) results. The correlation between the lateral soil pressure, P_u, and cone tip resistance, q_u, from the CPT was analyzed. Their method is based on the fact that H_u and q_c are dependent on similar parameters such as the relative density of the soil and effective stresses. The values for P_u were calculated from existing methods, and the q_c values were obtained from tests. The correlation was used to determine H_u. To verify the CPT method to determine H_u, three different tests were conducted. The calculated H_u. values were found to be in reasonable agreement with the experimental results.

To determine the uplift capacity of the pile and pile groups embedded in cohesionless soils, Gaaver (2013) conducted tests on model steel piles with an outer diameter of 23 mm and a wall thickness of 3 mm. The length to diameter ratios used were 14, 20, and 26. The pile was attached to a pile cap of 30 mm in thickness. The pile was embedded in a cohesionless soil bed with different relative densities (75%, 85%, and 95%). The soil bed was prepared by filling a steel circular tank of 650 mm in diameter and 900 mm in depth with sand. The increment in uplift load on the pile was measured for a pile head displacement of less than 0.01 mm per minute. The test results showed that with an increase in the relative density of the cohesionless soil, the friction between the soil and pile increases as well as the effective stress. The factors affect and increase the uplift load-carrying capacity of the pile.

Faizi et al (2015) conducted a physical experiment to determine the ultimate pullout capacity of a pile in loose sand. Cylindrical piles with semicircular and circular cross sections with a constant diameter of 5 cm and different lengths of 5, 10, 15, and 20 cm were used in the test. The tests were conducted in a closed chamber that took the boundary effect on the pile into consideration. The experimental findings revealed that (i) the uplift capacity of the pile increases with the embedded length of the pile since it has a larger contact surface area with the soil, (ii) the deformation of the loose and dense sand due to the pile pullout depends on the relative density and dilatancy characteristics of the sand, and (iii) the test results were compared with the

modelling results by using PLAXIS® software with two and three dimensional models. The calculated deformations agree well with the laboratory measurements.

Another experimental study on the behavior of a single pile under combined uplift and lateral loadings was carried out by Reddy and Ayothiraman (2015). The response of the pile under individual uplift and lateral loadings was compared with that under the combined action of uplift and lateral loads. The test model pile had an outer diameter of 25.4 mm and an inner diameter of 19 mm. The pile was attached to a pile cap of 100 X 100 X 22 mm^3. The length-to-diameter ratios adopted for the test were 18, 28, and 38. The pile was embedded in a sand bed with a relative density of 70%. The test was conducted to study the behavior of a prototype pile in similar loading conditions. The results showed that the complex interaction of the soil and pile should be accounted for in the engineering design. The response to lateral loading for the long pile under individual and combined loadings is the same, whereas the uplift capacity of the pile under combined loads is decreased with an increase in the pile length.

Ayothiraman and Reddy (2014) conducted an experimental model study on the pile behavior in loose to medium dense sand under combined uplift and lateral loads. The test was conducted on an aluminum pile of 25.4 mm in diameter in a test tank with dimensions of 1.0 m ×1.0 m × 1.2 m^3. Static loads were applied onto the pile under uplift and lateral loading conditions by using a loading hanger. The pile head deflection was recorded by using a set of dial gauges. The measurements showed that the lateral capacity of the pile increases significantly under the combined loadings. This is due to the restraint provided by the vertical uplift load on the lateral movement of the pile. Similar behavior was observed for the uplift movement under combined loadings. The uplift pile movement is increased under combined loadings compared to the movement under individual loading.

2.7 Conclusion

Since pile foundations are a viable solution to many foundation problems of onshore and offshore structures, the performance of pile foundations under different combinations of loadings has become an interesting topic for researchers over the recent decades. Vertical piles for onshore structures can be subjected to lateral loads that are equal to 10% to 15% of the vertical loads. These laterals can be due to winds, earth pressure, traffic movement, etc., whereas for the offshore structures, the horizontal loads on the piles can go up to 30% of the vertical loads. Therefore, it is vital to understand the pile behavior under the combined action of axial and lateral loads. To study the pile performance, physical laboratory models have been used since full-scale prototype testing is much more expensive and time consuming to carry out. However, it should be noted that a number of factors are assumed in a laboratory scale model depending on the physical setup and testing conditions.

In this literature review, it is noted that there are more studies that focus on the performance of piles under individual and combined loadings by using numerical modelling rather than physical modelling. However, these studies do not consider the effect of ground freezing on the pile performance under combined loadings. The F-T of the ground is a common problem in cold regions. As no study is available on the effect of ground F-T on the pile performance under combined loadings (uplift and lateral), there is a need to study the response of piles subjected to combined loads in F-T ground. Furthermore, the pile–soil interaction may be altered due to F-T thereby affecting the pile strength to resist any deflections. Therefore, it is necessary to investigate the pile performance in freezing and thawing grounds subjected to combined loadings. Moreover, a better understanding of pile foundation will help in designing infrastructures and buildings to make them more adaptable in this ever-changing environment.

2.8 References

Adejumo, T. E., and Boiko, I. L. (2012). Pile Foundation and Installation Methods in Nigeria. *Electronic Journal of Geotechnical Engineering, EJGE, 17*(S).

Ahmad, T., and Khawaja, H. (2018). Review of Low-Temperature Crack (LTC) Developments in Asphalt Pavements. *The International Journal of Multiphysics, 12*(2), 169–187.

Aldaeef, A. A., and Rayhani, M. T. (2019). Interface shear strength characteristics of steel piles in frozen clay under varying exposure temperature. *The Japanese Geotechnical Society, 14*(6), 653–664.

Ayothiraman, R., and Reddy, K. M. (2014). Model experiments on pile behaviour in loose-medium dense sand under combined uplift and lateral loads. *Tunneling and Underground Construction*, (GSP-242), 633–643.

Basu, D., Salgado, R., and Prezzi, M. (2008). *Analysis of laterally loaded piles in Multilayered soil deposits* (Publication No. FHWA/IN/JTRP-2007/23, SPR-2630). Indiana, US: School of Civil Engineering Purdue University.

Brandl, H. (2008). Freezing-thawing behaviour of soils and unbound road layers. *Slovak Journal of Civil Engineering*, 4–12.

Briaud, J. L. (2013). *Geotechnical Engineering: Unsaturated and Saturated Soils* (1st ed.). New Jersey, US: Wiley.

Chang S., and Fall M (2022). *Strength, Microstructure and Deformation Behavior of Frozen Cemented Tailings Materials*. ASCE Journal of Cold Regions Engineering. 36(1): 04021017.

Chang, D., and Liu, J. K. (2013). Review of the influence of freeze-thaw cycles on the physical and mechanical properties of soil. *Sciences in Cold and Arid Regions*, *5*(4), 0457–0460.

Childress, A. (2020). *We Gave the Earth a Fever, Now It's Giving Us One: Predicting the Impact of Climate Change on HPAI H5N1 Outbreak Risk in Siberia*. Chadwick School, Palos Verdes, CA.

Crory, F. E. (1973). *Settlement Associated with Thawing of Permafrost*. Presented at the North America Contrib., 2nd Int. Conf. on Permafrost, Washington, D.C.: National Academy of Sciences.

Cruden, D. M. (2010). *More comprehensive characterization of landslides in permafrost*. Presented at the 63 Canadian Geotechnical Conference, Calgary.

Denchak, M. (2018). Permafrost: Everything You Need to Know. Retrieved November 19, 2021, from Natural Resources Defense Council website: https://www.nrdc.org/stories/permafrost-everything-you-need-know#:~:text=Just%20as%20a%20puddle%20of,consecutive%20years%2C%20it's%20called%20permafrost.

Desdemona, D. (2009, November 22). Permafrost thaw threatens Russia oil and gas complex: Study. Retrieved June 6, 2020, from https://desdemonadespair.net/2009/11/permafrost-thaw-threatens-russia-oi.html

Engineering Discoveries. (n.d.). Pile-foundation-classification-of-pile-foundations-pile-installation-methods. Retrieved January 15, 2022, from EngineeringDiscoveries.com website: https://civilengdis.com/pile-foundation-classification-of-pile-foundations-pile-installation-methods.

Faizi, K., Kalatehjari, R., Nazir, R., and Rashid, A. S. A. (2015). Determination of pile failure mechanism under pullout test in loose sand. *Central South University Press and Springer-Verlag Berlin Heidelberg*, *22*(4), 1490–1501.

Fall, M., Célestin, J.C., and Sen, H.F (2010). *Potential use of polymer-pastefill as waste containment barrier materials*. Journal of Waste Management 30: 2570-2578.

Fall, M., Célestin, J.C., Sen, H.F (2009). *Suitability of bentonite-paste tailings mixtures as engineer barrier materials for mine waste containment facilities*. Minerals Engineering 22 (9-10): 840-848.

Flerchinger, G. N., Lehrsch, G. A., and Mccool, D. K. (2005). Freezing and Thawing. In D. Hillel (Ed.), *Encyclopedia of Soils in the Environment* (Vol. 2). U.K.: Elsevier, Ltd., Oxford, U. K.

Gaaver, K. E. (2013). Uplift capacity of single piles and pile groups embedded in cohesionless soil. *AEJ - Alexandria Engineering Journal*, *52*(3), 365–372.

Government of Canada. (2019). *Canada's changing climate report, CCCR 2019* (Publication No. CCCR 2019; p. 444). Canada.

Government of Canada. (2021). Geoscience: Climate change. Retrieved April 7, 2021, from Https://www.nrcan.gc.ca/earth-sciences/earth-sciences-resources/geoscience-climate-change/10900 website: https://www.nrcan.gc.ca/earth-sciences/earth-sciences-resources/geoscience-climate-change/10900

Hanna, A., Forsyth, R., and Garvin, D. (1990). Thaw Settlement Around a Building on Warm Ice-Rich Permafrost. *Proceedings 5th Canadian Permafrost Conference*, 419–424. Quebec City, Canada.

He, W., Qi, G., and Jingbo, T. (2013). *Study on the shear strength parameters under different freezing and thawing cycles of soil slope in China*. *860–863*, 1280–1283.

Heydinger, A. G. (1987). Piles in permafrost. *J. Cold Reg. Eng*, *1*(2), 59–75.

JICA. (2019). *Quality control manual for bridge foundation* (First edition). Myanmar: Ministry of Construction, the Republic of the Union of Myanmar.

Kouretzis, G. (2018). *Fundamentals of Foundation Engineering and their Applications* (2018th ed.). Australia. Retrieved from https://www.researchgate.net/profile/George-Kouretzis/publication/323256947_Fundamentals_of_Foundation_Engineering_and_their_Applications/links/5a8a26a00f7e9b1a95542ec6/Fundamentals-of-Foundation-Engineering-and-their-Applications.pdf

Kozlowski, T. (2003). Soil freezing point as obtained on melting. *Cold Regions Science and Technology*, *38*(2), 93–101.

Ladanyi, B., and Theriault, A. (1990). A study of some factors affecting the adfreeze bond of piles in permafrost. *Proceedings of Geotechnical Engineering Congress GSP*, *27*, 213–224.

Lai, Y., Jin, L., and Chang, X. (2009). Yield criterion and elasto-plastic damage constitutive model for frozen sandy soil. *International Journal of Plasticity*, *25*(6), 1177–1205.

Lee, J., Kim, M., and Kyung, D. (2010). Estimation of Lateral Load Capacity of Rigid Short Piles in Sands Using CPT Results. *Journal of Geotechnical and Geoenvironmental Engineering*, *136*(1), 48–56.

Li, Z., Niu, F., Li, X., Li, A., Liu, M., Luo, J., and Shao, Z. (2018). Characteristics and controlling factors of frost heave in high-speed railway subgrade, Northwest China. *Cold Regions Science and Technology*, *153*, 33–44.

Loria, A. F. R., Frigo, B., and Chiaia, B. (2017). A non-linear constitutive model for describing the mechanical behaviour of frozen ground and permafrost. *Cold Regions Science and Technology*, *133*, 63–69.

Luthi, Z. L. (2010). *Thermal state of permafrost in central and western spitsbergen* (Phd. Thesis). University of Bern, Bern, Switzerland.

Oswell, J. M. (2011). Pipelines in permafrost: Geotechnical issues and lessons. *Can. Geotech Journal*, *48*(9), 1421–1431.

Neill, B. O. (2011). *The development of near-surface ground ice at Illisarvik, Richards Island, Northwest Territories* (Phd. Thesis, Carleton University). Carleton University, Ottawa, CA.

Peck, R. B., Hanson, W. E., and Thornburn, T. H. (1974). (Second Edition). New York, US: Wiley.

Penner, E., and Burn, K. N. (1970). Adfreezing and frost heaving of foundations. *Canadian Building Digest; No. CBD-128*.

Pewe, T. L., and Paige, R. A. (1963). *Frost heaving of piles with an example from Fairbanks, Alaska*. Alaska, United States.

Rahman, K. A., and Achmus, M. (2006). *Numerical modelling of the combined axial and lateral loading of vertical piles*. Presented at the 6th European Conference on Numerical Methods in Geotechnical Engineering, Graz, Austria.

Rayhani, M. T. (2018a). *Analysis and Design of Pile Foundations for Lateral Loads. CIVE 5501-Advanced Foundation Engineering.* Lecture Notes presented at the Carleton University, Ottawa, CA.

Rayhani, M. T. (2018). *Analysis and Design of Pile Foundations for Vertical Loads. CIVE 5501-Advanced Foundation Engineering*. Lecture Notes presented at the Carleton University, Ottawa, CA.

Reddy, K. M., and Ayothiraman, R. (2015). Experimental studies on behavior of single pile under combined uplift and lateral loading. *Journal of Geotechnical and Geo-Environmental Engineering, ASCE, 141*(7), 4015030.

Sawant, V. a., and Kumari, S. (2021). *Modeling in geotechnical engineering- Chapter 9—Analysis of laterally loaded pile*. India: Academic Press.

Schoeneich, P., and Fabre, D. (2019). The permafrost. Retrieved June 12, 2020, from Encyclopedia of the environment website: https://www.encyclopedie-environnement.org/en/soil/permafrost/#:~:text=Permafrost%20is%20a%20thermal%20and,bedrock%2C%20surface%20formations%2C%20soils.

Semnani, M. J. (2018). *Frost Heave as the Main Process Defining Natural Unforested Areas below a Temperature Treeline* (Masters Thesis). University of Calgary, Calgary.

Shakir, S., Mudassir, S., Abdullah, S., Najesh, Q., Pathan, M., Sufiyan, S., and Kharodia, O. (2020). Analysis of Raft & Pile Raft Foundation using Safe Software. *International Journal of Engineering and Technical Research*, *9*(07), 57–61.

Streletskiy, D. A., Shiklomanov, N., and Nelson, F. E. (2012). Permafrost, infrastructure, and climate change: A GIS based landscape approach to geotechnical modeling. *Arctic Antarctic and Alpine Research*, *44*(3), 368–380.

Taber, S. (1930). The mechanics of frost heaving. *The Journal of Geology*, *38*(4), 303–317.

Taha, A., and Fall, M., (2014). *Shear behaviour of the sensitive marine clay – steel interface*. Acta Geotechnique 9:969-980.

Taha, A., and Fall, M., (2013). *Shear behaviour of the sensitive marine clay – concrete interface*. ASCE Journal of Geotechnical and Geoenvironmental Engineering 139(4): 644-650.

Tang, L., Wang, X., Long, J., Deng, L., and Wu, D. (2018). *Frost heave and thawing settlement of frozen soils around concrete piles: A laboratory model test*. Presented at the Geo Edmonton, Alberta.

Tiedje, E. W. (2015). *The experimental characterization and numerical modelling of frost heave* (Phd. Thesis). McMaster University, Hamilton, Ontario.

Tomlinson, M., and Woodward, J. (2008). *Pile design and construction practice* (Fifth Edition). New York, US: Taylor & Francis.

Tsytovich, N. A. (1960). *Bases and Foundations on Frozen Soil* (No. 58; p. 93). Washington D.C United States: Highway Research Board.

Yu, S., Jianming, Z., Yongzhi, L., and Jigmin, W. (2002). Thermal regime in the embankment of Qinghai–Tibetan highway in permafrost regions. *Cold Regions Science and Technology*, *35*, 35–44.

Zhang, Y., White, D. J., Vennapusa, P. K. R., and Johnson, A. E. (2018). Investigating frost heave deterioration at pavement joint locations. *Journal of Performance of Constructed Facilities*, *32*(2), 4018001.

Chapter 3-
Physical Model Tests of Piles in Unfrozen and Freezing Soils Subjected to Combined Loads

Harshdeep Singh, Mamadou Fall

(submitted)

3.1 Abstract

Many civil engineering structures are subjected to significant lateral loads and overturning moments, in addition to vertical compressive load. Pile foundations for these structures in cold or permafrost regions should be adequately designed to resist a combination of the compressive, lateral, and uplift loads, and moments since they often act simultaneously. Passive soil resistance, which provides the lateral support to a pile, is a function of the soil thermal regime (freezing, thawing, and temperature). This manuscript presents and discusses the results of physical laboratory tests on model piles in freezing and unfrozen fine sand subjected to combined axial and lateral loads. The physical laboratory model in controlled condition simulates the actual pile behavior in the ground. The dimensions of the model pile are determined by using physical scaling principles. The setup is equipped with different sensors and instruments (e.g., LVDT, temperature sensors, and strain gauges) to monitor the pile and soil responses during static loading. The pile load capacities in frozen and unfrozen soil conditions are compared. The freezing of the sand layer has a significant effect on the capacities of the pile. Comparing the pile load capacities in the sand with a frozen layer with the unfrozen sand, it is noted that the lateral capacity is increased by 335% under individual loading and 648% under combined loadings in the sand with a frozen layer. On the other hand, the uplift capacity of the pile shows a decreasing trend under combined loadings compared to the uplift capacity under individual loading in the frozen soil. The results

from this study will be useful in designing pile foundations in cold regions under changing climatic conditions.

3.2 Introduction

Pile foundations are usually used in poor ground conditions with low bearing capacity at shallow depths, but shallow foundations cannot provide a viable solution economically, or where ground water is difficult to control during construction or for tall structures with massive loads. In addition, pile foundation is most suitable for frost susceptible soils in cold or permafrost regions since piles can be installed with the least disturbance to the ground.

The pile foundation can be subjected to a set of compressive, lateral, and uplift loads. Compressive load acts from the superstructure and the dead weight of the foundation itself. Many civil engineering structures, such as bridges, transmission towers, tall chimneys, and solar panels, are subjected to significant lateral loads and overturning moments in addition to vertical compressive load (Tomlinson and Woodward 2008). Potential sources of lateral loads (not including earthquakes) include wind, waves, water current, ice forces, vehicle acceleration and braking, debris loadings, and vessel impact. Consequently, pile foundations for these structures should be designed to resist not only compressive loads but also lateral and uplift loads and moments. In most cases, these loads (compressive, lateral, and uplift) and moments are simultaneously applied to the piles.

One of the important design considerations for foundation engineers is to determine the deflections and stresses in a soil-pile system in order to keep them within allowable limits (Allen 1984). Passive soil resistance can be very effective in providing lateral support for piles. However, this passive soil resistance is a function of the soil thermal regime (freezing, thawing, and temperature). Therefore, understanding and analyzing the effects of soil freezing or thawing on the load capacity of a pile subjected to combined vertical and lateral loads are absolutely

necessary in the design of pile foundations in cold or permafrost regions where the soil is susceptible to F-T actions particularly under the influence of global warming.

The thermal regimes of soils in Canada have shifted in the past decades due to global warming (Al-Umar et al. 2020, 2021; Nesralla and Fall, 2015, 2016). This shift may affect the geotechnical response or performance of pile foundations in these soils. The freezing or thawing of the ground alters the properties of the soil. According to Brandl (2008), the effect of freezing or thawing on the engineering properties of soils is not only dependent on the soil type and site conditions, but also the regional climate. Hence, more frequent temperature variations due to climate change have inspired researchers to investigate the effect of F-T on pile-soil interaction and its effect on pile foundation.

There have been several studies done to understand the behavior of piles under the influence of axial and lateral loads. For example, Fei et al. (2019) investigated laterally loaded piles in seasonal F-T ground and found that the pile capacity against horizontal loading increases by almost 70% in the frozen ground condition, and pile deflection is also reduced at the same percentage. Karthigeyan et al. (2006) examined a pile under axial and horizontal loadings. They concluded that the horizontal load carrying capacity is influenced by the axial loading on the pile and the length to diameter ratio (L/D) is a factor that affects the pile capacity under horizontal and combined loadings. Reddy and Ayothiraman (2015) analyzed piles under horizontal and uplift loadings and they the effects of the length to diameter ratio (L/D) on the pile capacity. They concluded that the pile capacity increases under the combined loadings, but cannot be considered for pile designs due to large pile head deflections. Gaaver (2013) examined a pile subjected to uplift loading, and observed that the uplift capacity of the pile is not only dependent on the embedded length of the pile, but also the soil properties. The uplift pile capacity increases with an increase in the embedded length and the relative density of the soil. Many more similar theories and numerical studies have been published (e.g., Xingyun et al. 2013, Azeez et al. 2019, Emirler et al. 2019, Sakr et al. 2019), but very few studies are supported by experimental results from

physical models. Moreover, no physical modeling studies have been conducted on the effects of the freezing and unfrozen states of the ground on the response of pile foundation subjected to combined axial and lateral loads.

The principal objective of this paper is to experimentally investigate the behavior of piles in freezing and unfrozen ground conditions under individual and combined effects of lateral and vertical (uplift) loadings through physical modeling. The experimental setup, program, outcomes, and observations are then presented and discussed.

3.3 Materials and experimental design

3.3.1 Material Used

3.3.1.1 Sand

In this study, locally available Ottawa sand was used. The geotechnical properties of the sand were determined in the laboratory as per ASTM standards D854-14 (specific gravity), D3080-04 (direct shear test), C136-01 (sieve analysis), and D7263-21 (density test). The results are summarized in Table 3.1, and the particle size distribution curve is presented in Figure 3.1. Based on USCS classification, the sand is considered to be SP (poorly graded with very little fines).

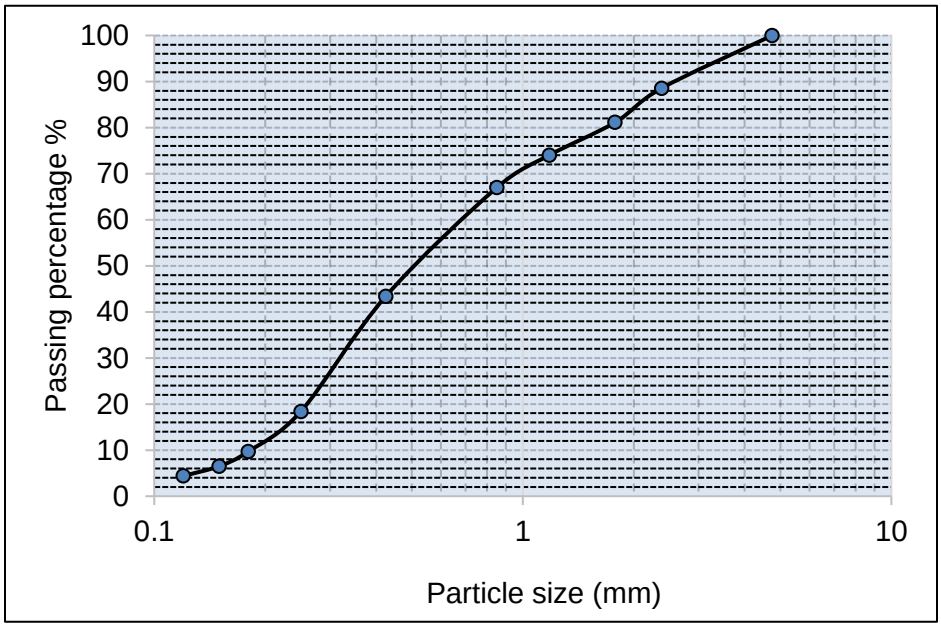

Figure 3.1 Sieve Analysis

Table 3-1 Mechanical properties of sand used in the experiment

Soils properties, unit	**Value**
Minimum dry density, kg/m^3	1480
Maximum dry density, kg/m^3	1644
Specific gravity	2.7
Friction angle at minimum dry density, °	37
Friction angle at maximum dry density, °	46

3.3.1.2 Model Test Piles

Two piles made from aluminum hollow tubes with a circular cross section that has an outer diameter (D) of 25 mm and inner diameter of 23 mm and different embedded lengths (L) were used in the experiment as shown in Figure 3.2. Pile A has an embedded length of 500 mm, while Pile B has 375 mm of embedded length. Both piles have an additional 50 mm of clear length between the pile cap and the top soil surface to avoid any influence of the latter on the pile-soil interaction. The pile was attached to an aluminum pile cap with dimensions of 100 x 100 x 22 mm. The tip of the pile was closed with the conical section to prevent any plugging of sand into the pile. In the laboratory model, different L/ D ratios affect the pile load capacities. Higher L/D values increase the pile load capacities (Sazzad et al. 2019). Therefore, two different L/D ratios of 20 and 15 are considered in this study.

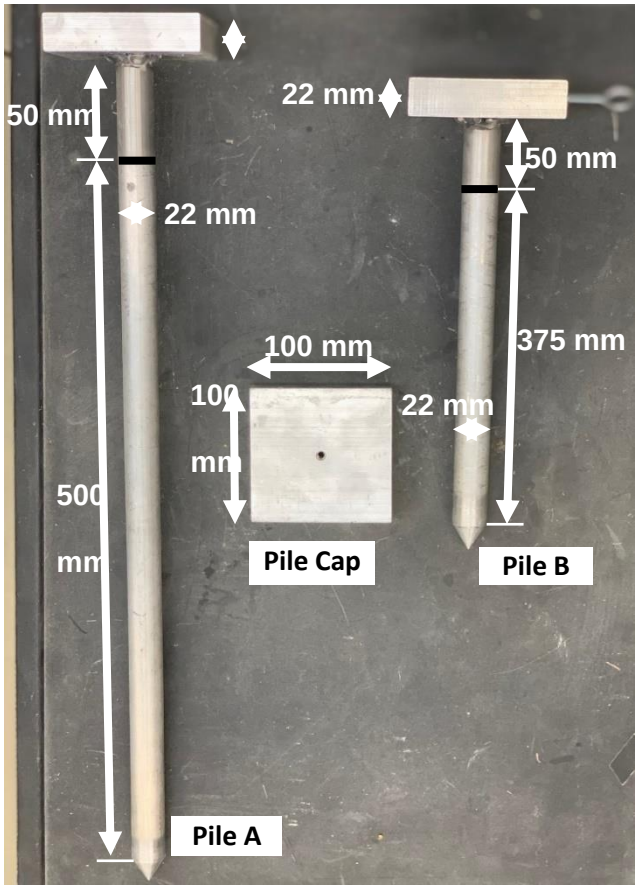

Figure 3.2 Image and dimensions of the model test piles

Physical model studies are usually carried out at a much smaller scale by scaling all aspects to determine the pattern or response of the prototype. Equation 1 is used to determine the scaling factor for the model pile to a full-scale prototype pile in the present experiment (Wood et al. 2002, Wood 2004). The scaling is based on the flexure rigidity of the model and prototype. The sand properties for the model and the prototype are considered to be the same in this study.

$$\left(EI_{(p)}\right)\Big/_{EI_{(m)}} = n^{4.5} \qquad 3.1$$

where,

n = scaling factor;

$EI_{(p)}$ = flexure rigidity of prototype pile; and

$EI_{(m)}$ = flexure rigidity of model pile.

3.4 Experimental setup

3.4.1 Main components of the setup

The experimental setup consisted of a steel tank with dimensions of 1300 x 725 x 725 mm, see Figures 3.3 and 3.4. The tank was filled with 1200 mm of sand and a 100 mm layer of gravel at the bottom. The tank was designed to accommodate a vertical and lateral load application mechanism to apply vertical and horizontal forces on the pile and pile cap, see Figure 3.2. Various sensors (5TE, MPS6, and LVDTs) were buried in the soil bed with a cooling system, see Figures 3.5 and 3.6.

The tank had an inlet at the bottom for the water supply to saturate the sand and an outlet to drain the water after the experiment. The dimensions of the experiment tank are based on previous studies (Bolton and Gui 1993, Teymur and Madabhushi 2003, Srivastava et al. 2016) to eliminate the boundary effects on the pile. According to Bolton et al. (1999) and Ullah et al. (2014), the distance between the pile periphery and the boundary should be a minimum of 10 times the diameter of the pile Dp. The boundary effect on the pile beyond 10 Dp is negligible. Different studies (e.g., Dong et al. 2017, Kong and Zhang 2017) have explained the relationship between the vertical boundary and the embedded length of the pile (L). They suggested that the effect of the vertical boundary ranges from 1 L to 4 L from the surface. However, the differences in the effects of the vertical boundary in this range are insignificant. Therefore, the vertical boundary was chosen at 2 L in this study. The entire tank was insulated by using fiberglass insulation to reduce the loss of heat during freezing.

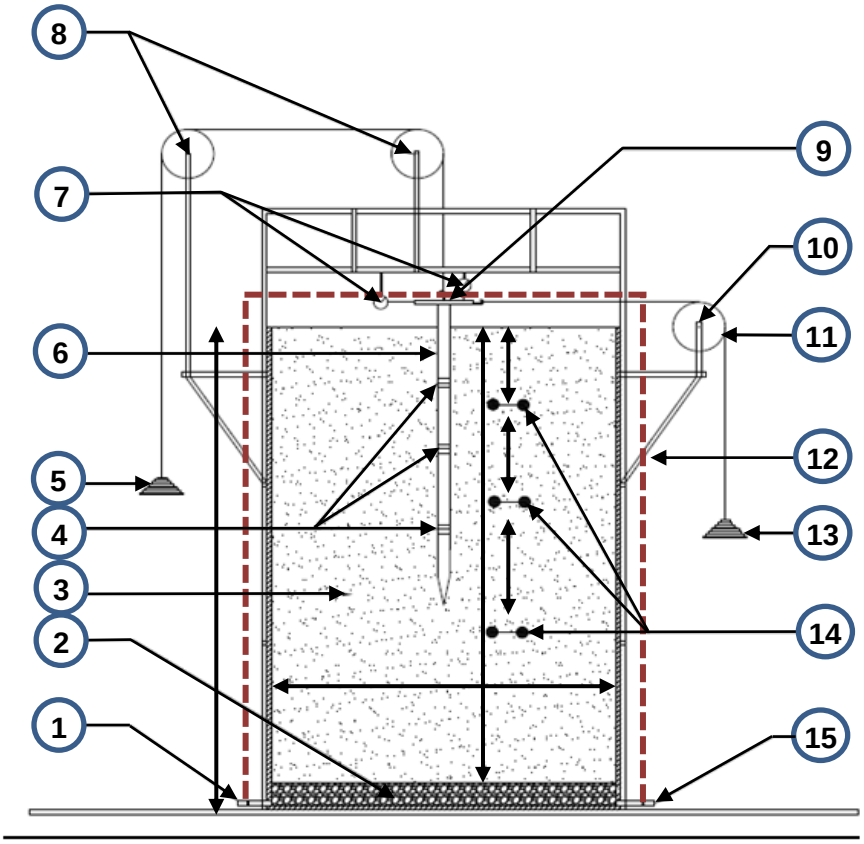

1. **Water Inlet**
2. **Gravel Bed**
3. **Sand Bed**
4. **Strain Gauge**
5. **Static loads**
6. **Pile**
7. **LVDT**
8. **Pulley**
9. **Pile Cap**
10. **Pulley**
11. **Metal Wire**
12. **Insulation**
13. **Static loads**
14. **Sensor sets**
15. **Water Outlet**

Figure 3.3 Schematic diagram of the experimental tank setup

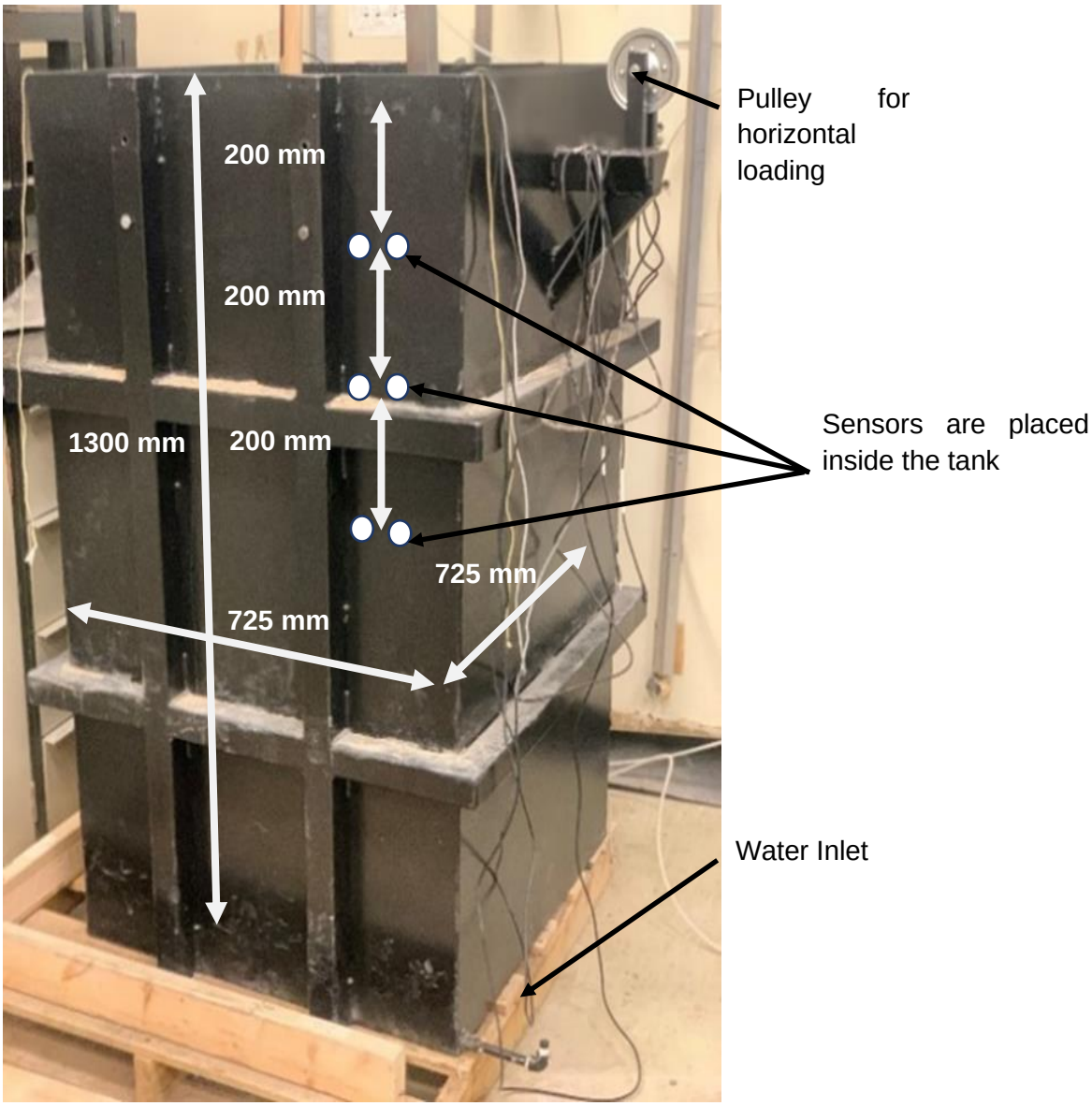

Figure 3.4 Experimental tank for testing piles

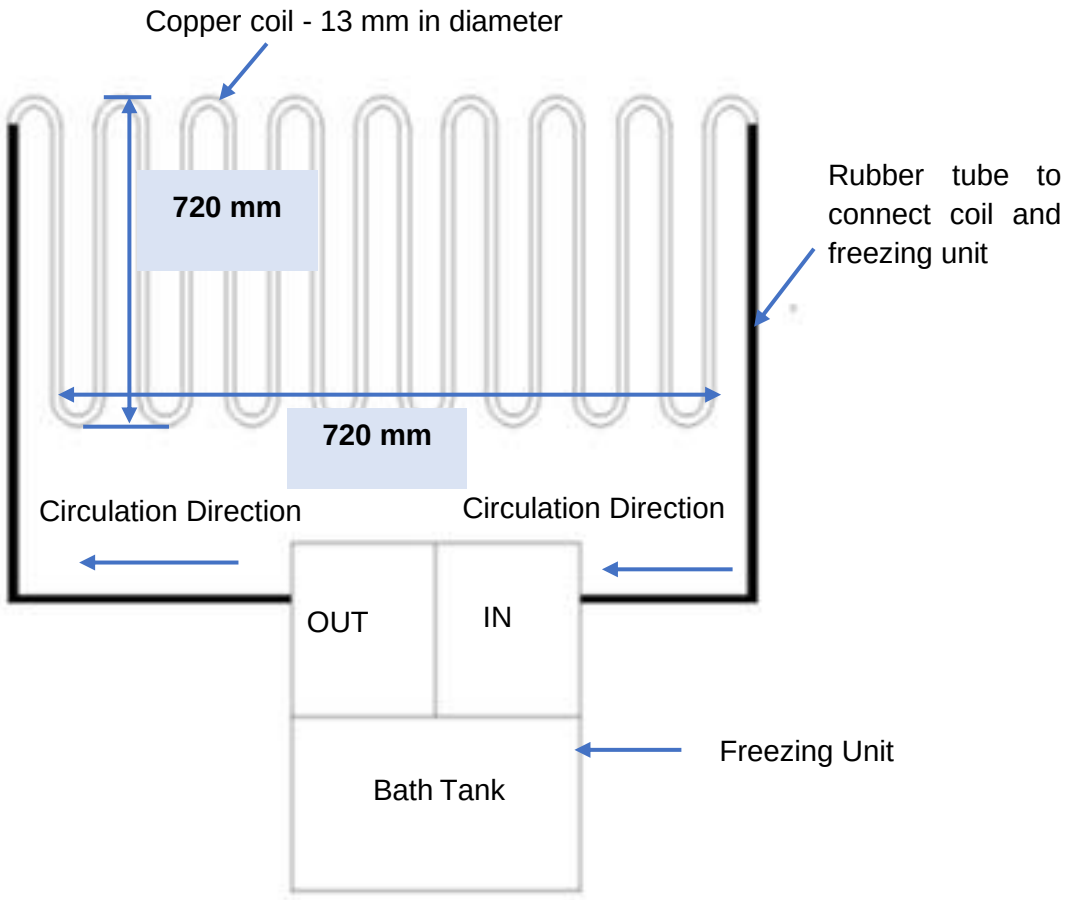

Figure 3.5 Schematic diagram of the experimental cooling system

To simulate natural ground freezing conditions in the laboratory, a cooling system, a DYNEO DD-1000F refrigerated/heating circulator, with an operating temperature range of -50°C to 200°C was used. The cooling system is shown in Figures 3.5 and 3.6. The cooling system has an integrated program that allows controlled one-dimensional cooling to achieve the targeted temperature. The copper coil is rested on the top of the soil bed and freezes the soil from top to the bottom up to the desired frost depth. The cooling machine circulated the liquid through the coil at -40°C. The frozen state of water in the soil was measured with sensors buried at different depths in the soil. The 5TE sensor used in the experiment has an operating temperature range between -40°C and +50°C with an accuracy of ±1°C and ±3 % for the volumetric water content. Similarly, the MPS-6 sensor has an operating temperature range of -40°C to +60°C with an accuracy of ±1°C and ±10%

for a pressure range of -9 kPa to -100 kPa. LVDTs can measure a maximum of 50 mm of movement with an accuracy of ±0.1%. The operating temperature range of the LVDT is 0° to +70°C.

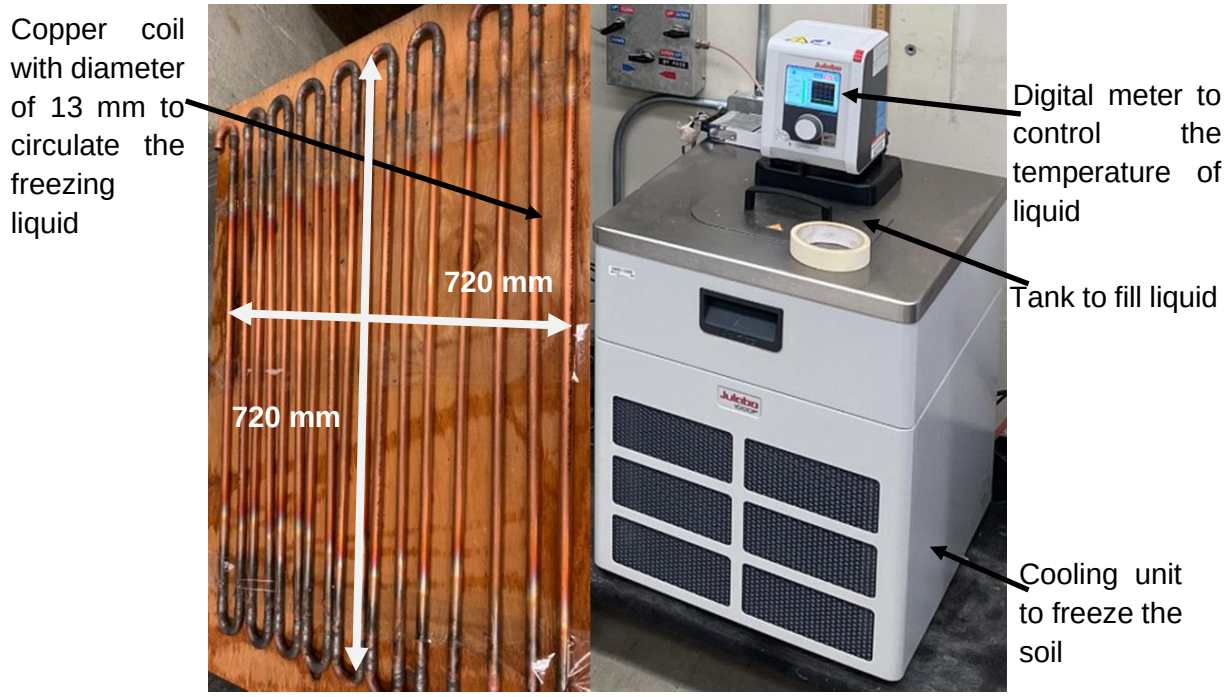

Figure 3.6 Cooling system

3.4.1.1 Loading arrangement

The experimental setup had a loading mechanism to apply static uplift and static horizontal forces on the pile (Figure 3.3). The loading was applied by using a combination of pulleys, dead weight, hangers, and steel cable as shown in the figure. The lateral loading has the flexibility to change the load eccentricity but, an eccentricity of 50 mm was maintained throughout in the experiment. Both vertical and horizontal loadings were applied on the pile head. The setup used 2 LVDTs to record the vertical displacement and the horizontal deflection of the pile head.

3.4.1.2 Sand bed preparation

The sand bed was divided into five layers. Each layer was compacted to a relative density of 65% by using a hammer to achieve a dense state (Roy and Bhalla 2017). The compaction of each layer was tested by taking a sample from each layer and measuring its density. The density of every sand layer was maintained constant to have a homogeneous soil bed for the experiment. The sand was removed after each experiment.

3.4.1.3 Pile installation

In order for the pile to remain vertical, a specially manufactured guide was used during compaction of the sand. When the sand bed had reached the bottom tip of the pile, the pile was held in position with a guide assembly. The sand was added in layers of 200 mm in thickness and each layer was compacted to achieved the desired density. The process continued until the soil reached the required embedded depth of the pile.

3.5 Experimental Procedure

3.5.1 Lateral loading

In the experiment, lateral loading on the pile was applied in accordance with the procedure recommended in the Bureau of Indian Standards (BIS; 1985). The initial reading of the LVDT was recorded before applying the load. The static lateral load on the pile was increased in steps. This was done by adding dead weights across the loading arrangement as illustrated in Figure 3.3. After each step of load increment, the load on the pile was allowed to stabilize, while the horizontal deviation or displacement of the pile head was measured by using the LVDT. The next step of load increment was applied only after the pile deflection had stabilized. This procedure was repeated until the ultimate pile capacity was reached.

There are well-established codes of practice to determine the lateral pile capacity of piles. The first most widely used method is the double tangent method. The load-deflection curve reaches a peak value at a certain load followed by a decrease in the load with increase in deflection (Patra

and Pise 2001). The second most common method is a load beyond which the load-deflection curve becomes linear i.e., the lateral deflection continues to increase with no further increase in load (Meyerhof et al. 1981). However, for this study, the ultimate pile capacity is considered when the pile fails or the maximum deflection of 12 mm is reached in accordance with the BIS (1985).

3.5.2 Uplift loading

The vertical loading on the pile was applied as per BIS (1985). An initial reading of the LVDT sensors was done before applying the load. The uplift load on the pile was increased in steps. After each load increment, the load on the pile was allowed to stabilize and the LVDT readings were continuously recorded. This was done by adding static weights as illustrated in Figure 3.3. This procedure was repeated until the pile reached the maximum deflection in accordance with the BIS (1985) or the pile failed. Pile failure was considered when the pile deflection continued to increase without increase in the applied load.

3.5.3 Combined loadings

Combined loadings on the pile were applied in two different scenarios. It is reasonable to assume that full-scale working piles will be subjected to safe/permissible loads only. Therefore, it is more appropriate to study a pile under combined loadings at a safe/allowable load. Consequently, the prototype pile was subjected to a safe/allowable load, and not the ultimate load. A FOS of 2 was adopted to obtain a safe load. In the first scenario, a constant uplift force was applied while lateral force was applied in steps. Once the lateral movement of the pile head ceased, the next increment of lateral load was added. The process continued until the displacement failure criteria were reached. The displacement was considered to have ceased when the displacement rate reached 0.1 mm/30 minutes as recommended in the BIS (1985). This rate of deflection is considered a stable state of the pile for the deflection failure test. In the second scenario, a constant lateral load was applied while a vertical uplift load increase was applied until failure. Loadings in both scenarios follow the procedure outlined in the BIS (1985) with an FOS of 2.

3.5.4 Freezing of soil and unfrozen soil

Once the tank was filled with sand, water was allowed to flow upward into the tank from the water inlet at the bottom of the tank (Figure 3.4). Then a copper coil (Figure 3.5) was placed on the saturated soil surface. The top of the tank and the tank walls were covered with insulating material to minimize heat loss during the cooling process. The liquid flowed through the coil at -40°C to initiate the freezing process. It took almost 3 days to freeze the sand to a depth of 5 cm for the laboratory model. This freezing depth of the model was scaled down for the frozen depth or depth of frost penetration in Ottawa. The frost depth in the Ottawa region ranges between 0.8 meters to 1.2 meters below the ground surface (Aldaeef and Rayhani 2020). However, reports (DST Consulting Engineering 2015) have suggested a frost penetration depth of 1.8 meters for safe construction practices. In addition to understanding the pile behavior in the freezing soil layer subjected to combined loads, the behavior of a pile in unfrozen soil is also investigated in this study. This unfrozen soil serves as a control layer as well as simulating approximately the thawed soil condition. Indeed, global warming has resulted in the loss of the frozen ground layers in many regions in Canada. Therefore, it is very crucial to understand the behavior of piles in the thawed ground.

3.6 Results and Discussion

3.6.1 Pile behaviour under single loading in unfrozen and frozen soil conditions

Two piles of different pile lengths (Pile A 500 mm and Pile B 375 mm) were tested in unfrozen soil conditions and Pile B was tested under freezing ground conditions to understand the behavior of a pile in frozen ground as well as compare the behavior of the pile with that in unfrozen soil conditions. The failure loads of the piles in unfrozen soil under individual and combined loads are listed in Table 3.2. Figures 3.7 and 3.8 compare the lateral and the uplift capacities of the piles in the unfrozen soil condition. It can be observed that the pile lateral and uplift capacities are

dependent on the embedded length of the pile. As shown in Figure 3.7, the lateral load capacity of the pile under individual loading is increased by almost 16% when the embedded length of the pile is increased from 375 mm to 500 mm; i.e., by 33%. The uplift capacity of the pile follows a similar trend (see Figure 3.8). Under individual load, the uplift capacity shows an increase of 28%. The increase in the pile capacities can be attributed to the fact that more pile resistance is available with longer embedded length (Azeez et al. 2019). With an increase in the embedded length, higher passive lateral resistance is developed from the surrounding soil and more soil will be displaced by the pile when it is loaded laterally. In the case of the pile subjected to uplift force, a longer embedded pile has a larger surface area which increases the skin frictional resistance (Levy 2010)

Figure 3.9 shows the vertical and lateral load deflection curves from the tests in the sand with a frozen layer and compares the results without the unfrozen layer. The measurements are summarized in Table 3.3. The lateral pile capacity under individual load is increased by many times, i.e., 435%, in the soil with a frozen layer, as shown in Figure 3.9. Note that the slope of the load-deflection curve from the experimental results does not change with increase in load. Even at higher deflection, the curve continues to be a straight line. In other words, the load-deflection response continues to be linear. According to Meyerhof et al. (1981) and Patra and Pise (2001), the ultimate lateral resistance can be considered as the peak load in the load-deflection curve or when the load-deflection curve becomes linear. However, in the present experiment, neither of the two conditions were achieved. Therefore, the ultimate load criterion is based on 12 mm deflection as discussed in the BIS (1985). The increase in the lateral capacity of the pile can be attributed to the ice developed due to freezing of the soil. The presence of the frozen layer in the soil provides additional strength to resist lateral movement of the pile when loaded laterally. The results indicate an increase in the pile-soil system stiffness in the frozen layer. Similar observations have been made by Fei et al. (2019), who observed an increase in the Young's modulus and the cohesion in the frost layer during seasonal freezing.

The influence of the presence and absence of the frozen soil layer on the uplift capacity of the pile under the action of singular loading is shown in Figure 3.9. Theoretically, the pile uplift capacity or the capacity of the pile in tension under static loading can be calculated by using the same equations as those for shaft resistance offered for the pile in compression under static loading (Tomlinson and Woodward 2008). There are numerous studies that can be referenced to understand the behavior of piles against uplift loading that take into consideration different scenarios and conditions (Mhaidib 137AD, Radhakrishna and Adams 1973, Gaaver 2013, Reddy and Ayothiraman 2015). In the present experiment, the pile uplift capacity under freezing conditions is found to be twice the pile capacity in the unfrozen state. This is expected because when the soil freezes, an adfreeze bond is developed between the soil and the pile at the interface, which resists the upward pile movement. On the other hand, the development of the forces due to freezing tends to push objects (pile) with different stiffnesses and freezing characteristics outwards (Pewe and Paige 1963). In this case, it is evident experimentally that the tangential adfreeze bond provides much more resistance against the uplift movement than the frost heave uplift force offered by the frozen soil layer. Hence, an increase in the uplift capacity of the pile can be seen with the frozen soil layer. Since the pile is not subjected to any compressive vertical loading, the pile is only restrained by the shaft friction against uplift forces. As the uplift loading is increased, the interface bond between the pile and soil weakens, and a sudden failure occurs. The friction between the sand particles is decreased in the frozen state (Aldaeef and Rayhani 2021).

Table 3-2 Failure loads of piles in unfrozen soils

			Failure load Individual (N)		Failure load combined loadings (N)	
Pile	**Length (mm)**	**L/D**	**Vertical P_u**	**Lateral H_u**	**Lateral load under constant vertical load (0.5 P_u)**	**Vertical load under constant lateral load (0.5 H_u)**
A	500	20	421	400	320	660
B	375	15	328	343	225	355

Table 3-3 Failure loads of pile (B) in unfrozen and frozen soil

			Failure load Individual (N)		Failure load combined loadings (N)	
Pile	**Length (mm)**	**L/D**	**Vertical P_u**	**Lateral H_u**	**Lateral load under constant vertical load (0.5 P_u)**	**Vertical load under constant lateral load (0.5 H_u)**
Unfrozen Soil	375	15	328	343	225	355
Frozen Layer			550	1495	1685	460

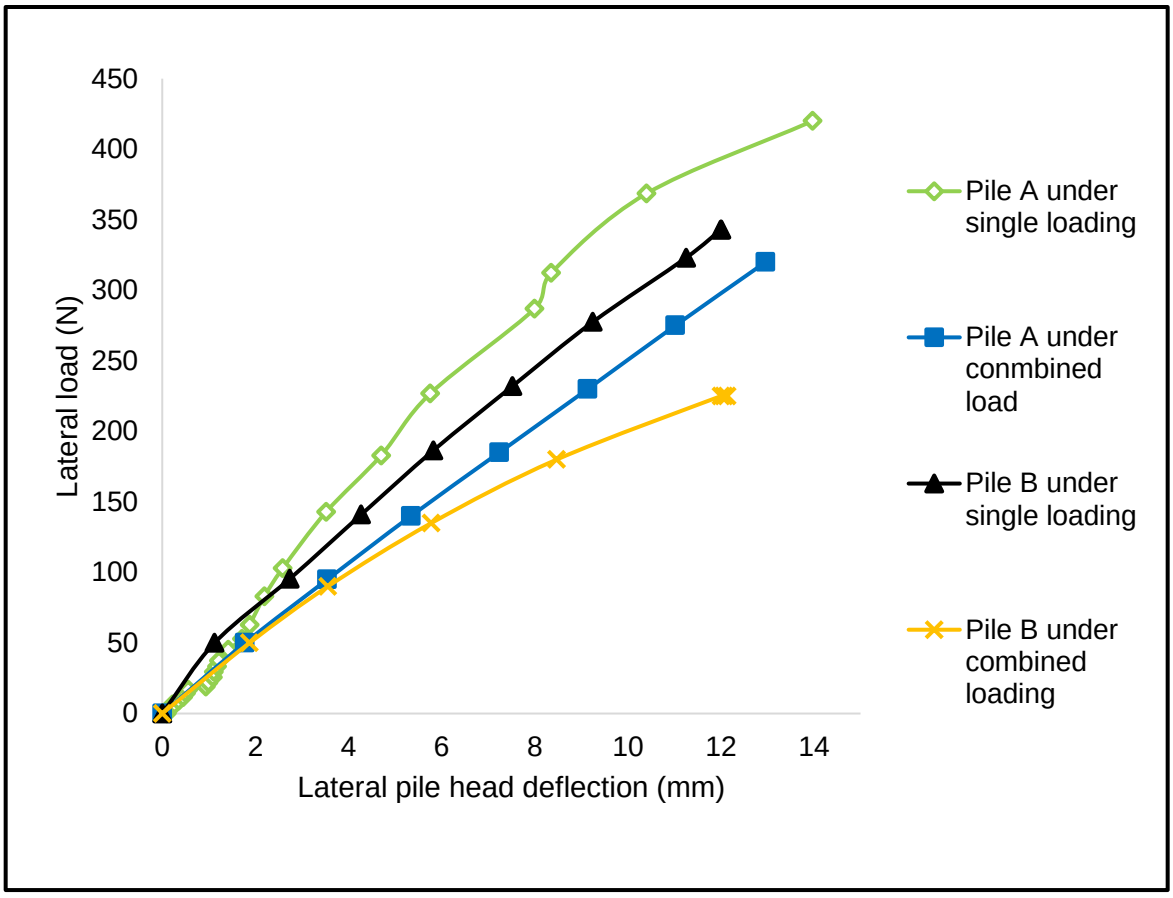

Figure 3.7 Lateral movement of pile head in unfrozen soil (length of Pile A: 500 mm; length of Pile B: 375 mm)

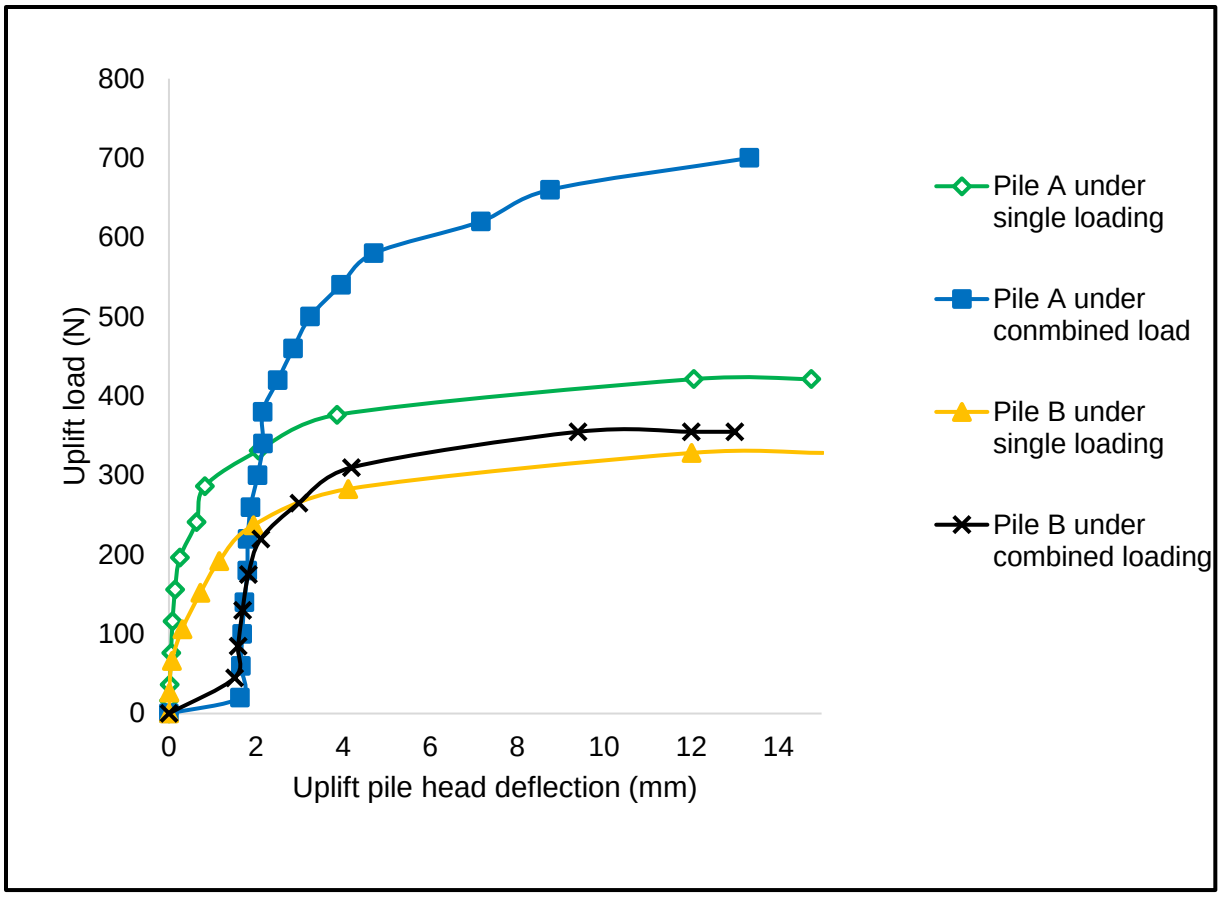

Figure 3.8 Uplift movement of pile head in unfrozen soil (length of Pile A: 500 mm; length of Pile B: 375 mm)

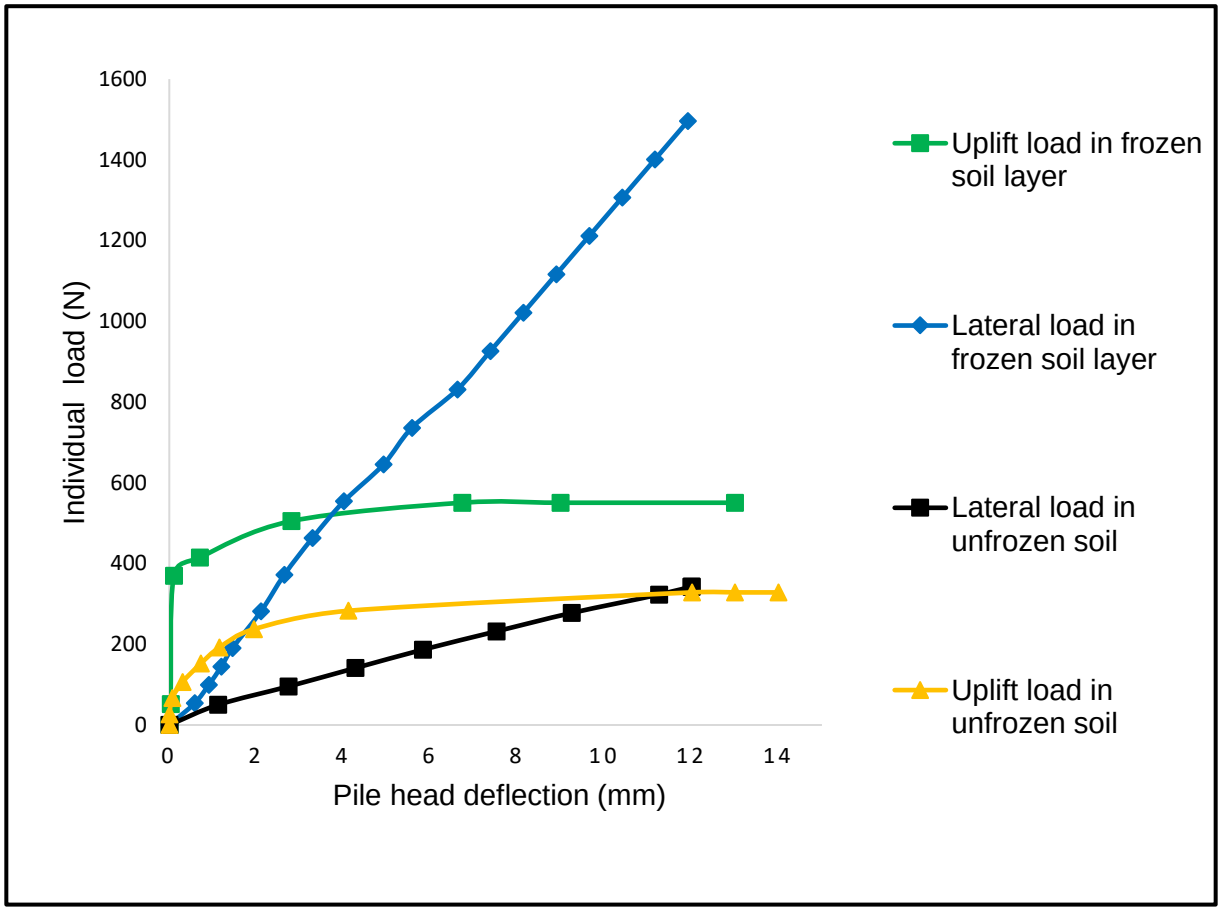

Figure 3.9 Individual failure load of pile (B) embedded in unfrozen soil and soil with a frozen top layer

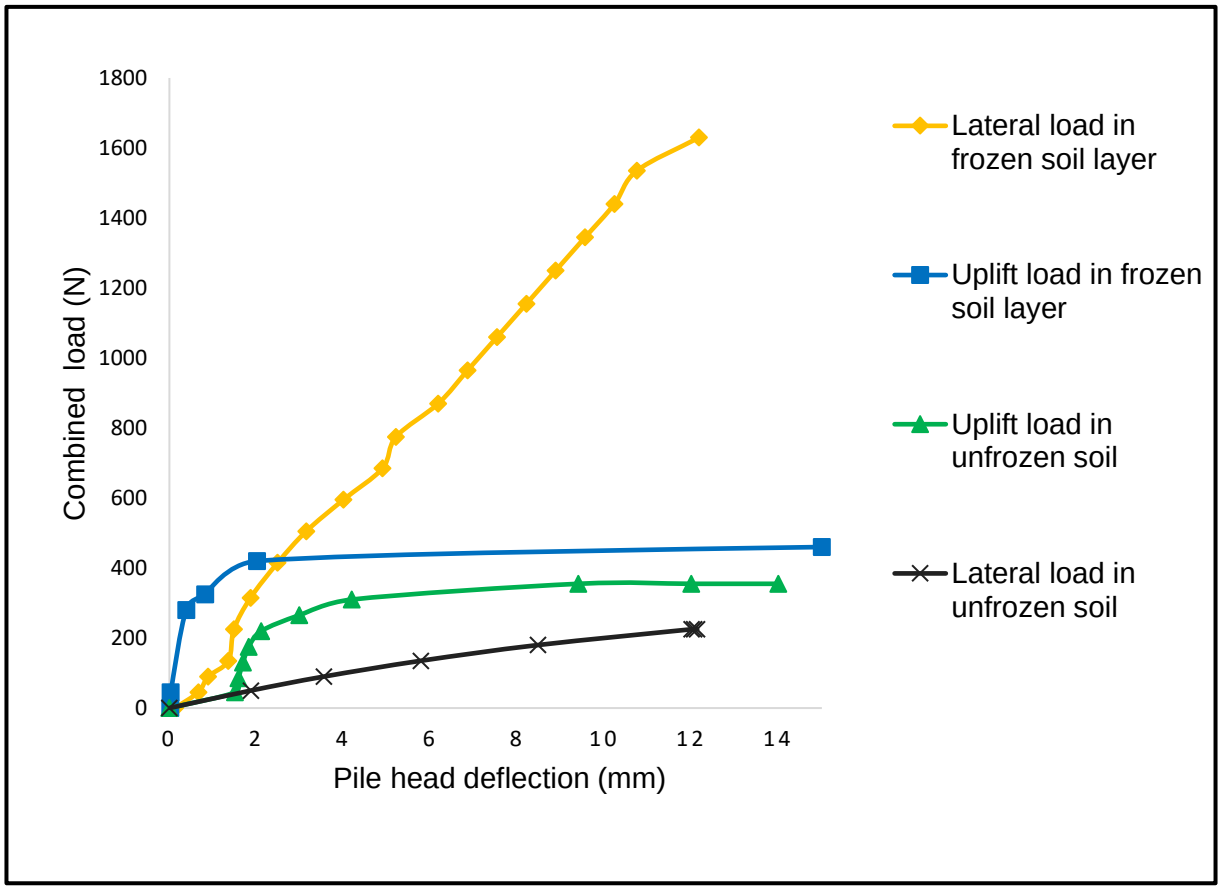

Figure 3.10 Combined failure load of pile (B) embedded in unfrozen soil and in soil with a frozen top layer

3.6.2 Pile behavior under combined loading in unfrozen and frozen soil conditions

A series of tests were conducted to understand the effect of the combined loadings (constant uplift load with increasing lateral load and the effect of constant lateral load with increasing uplift load) on a pile embedded in unfrozen soil and in soil with a frozen top layer. The results of the test are shown in Tables 3.2 and 3.3. Figures 3.7, 3.8 and 3.10 show the effects of the embedded pile length and frozen soil layer on the pile behavior under combined static loading. In many previous studies, the lateral and axial pile capacities of the pile have been mainly determined

separately. The coupling effect is mostly ignored due to a lack of sufficient knowledge of piles under combined loads (Karasev et al. 1977). Later, more research has been done to predict the pile behavior under the combined action of lateral and axial loadings (Liyang et al. 2012, Hussien et al. 2014, Chatterjee and Choudhury 2016, Ling et al. 2021). However, the results have always been inconclusive. Note from Figures 3.7 and 3.8 that both the lateral and uplift pile capacities under combined loadings in unfrozen ground are affected by the embedded length and the effect is similar to that of the pile under single loading. The lateral pile capacity with constant uplift load is increased by 42% (Figure 3.7), whereas the uplift capacity with constant lateral load shows an increase of 86% (Figure 3.8). The results show that even under combined loadings, the resistance provided by the pile shaft against uplift and the lateral support by the surrounding soil against pile deflection are higher for the pile with L/D = 20 compared to that with L/D = 15. Therefore, it is concluded that the pile capacities are significantly affected by the embedded length as discussed above. The mechanisms responsible for this behaviour have already been explained earlier.

Figure 3.10 shows the influence of the combined loadings on the behavior of Pile B in unfrozen soil and soil with a frozen top layer. The lateral and the uplift capacities of Pile B in soil with and without a frozen layer under combined loadings are listed in Table 3.3. The pile load carrying capacities and the pile head deflection are affected by the coupled effect of the uplift and lateral loads that are acting on the pile (Darr et al. 1990, Ayothiraman and Reddy 2014, Reddy and Ayothiraman 2015). Note that in Figure 3.1, the constant vertical load on the laterally loaded pile tends to increase the lateral pile head deflection by almost 35% in the unfrozen soil. The increase in the lateral deflection can be attributed to the fact that the presence of uplift load weakens the pile-soil interaction along the contact length of the pile (Ghosh et al. 2020). In contrast, it can be seen in Figure 3.8 that the presence of a constant lateral load on the pile under an increasing uplift force increases the uplift resistance by 10%. It can be observed that the resistance against the uplift deflection of the pile head is increased. The pile could be subjected to more load at any specific deflection compared to the pile under individual load in unfrozen soil. This increase in the

uplift capacity under combined loads is due to the coupled effect of the shaft friction of the pile and the passive resistance provided by the soil due to the acting of the lateral load. The constant lateral load that is acting on the pile provides extra resistance to the uplift movement of the pile under uplift loading (Reddy and Ayothiraman 2015). It is evident from the test results that the lateral and the uplift capacities of the pile are significantly affected by the combined loadings (lateral and uplift) when compared to the pile capacities under individual loading with the same soil conditions.

Figure 3.10 shows that the lateral and uplift pile capacities under combined loadings in soil with a frozen layer are much higher when compared to the pile capacities in unfrozen soil (i.e., in unfrozen or thawed soil conditions). Table 3.3 shows that the pile lateral capacity with constant uplift load in unfrozen and frozen ground is increased from 225 N to 1685 N, i.e. almost by 750%, and the uplift pile capacity under a constant horizontal load is increased almost by 1.5 times from 355 N to 460 N. Although a small portion of the pile length is embedded in the frozen soil layer, the effect of the frozen layer on the pile capacities is significant. The soil with a frozen layer provides much higher stability to the pile foundation against deflections. In frozen ground, the stiffness of the top soil layer subjected to seasonal freezing is increased by 2 orders of magnitude (Fei et al. 2019). It can also be noted from Figure 3.10 that for the pile in frozen soil, the uplift load does not have much influence on the lateral pile capacity. However, the effect of the constant lateral load on the uplift capacity reduces the vertical capacity by almost 20%. This can be attributed to the fact that the lateral load on the pile in the soil with a frozen layer weakens the adfreeze bond at the pile-soil interface and reduces the contact area of the pile with the soil. This results in the reduction of the skin friction offered by the pile surface and the adfreeze strength developed at the pile-soil interface in the frozen layer to resist against uplift deflection of the pile. Ultimately, this reduces the uplift pile capacity of the pile under combined loadings in comparison to the uplift capacity of the pile under individual loading in the soil with a frozen layer.

3.7 Summary and Conclusion

A physical laboratory model has been developed to study the behavior of prototype piles in unfrozen soil and in soil with a frozen layer under both individual and combined static loadings. Soil freezing is created in the laboratory by using a cooling system. The effects of a frozen soil layer on a pile is investigated and the results are compared with the pile behavior in unfrozen soil. The outcomes and conclusions of the experiments are summarized below.

- The individual lateral and uplift pile capacities are increased in the soil with a frozen layer when compared to the individual pile capacities in the unfrozen soil.
- In the soil with a frozen top layer, the lateral capacity of the pile under combined loads (increasing lateral and constant uplift loads) is increased compared to the lateral capacity of the pile in the unfrozen soil.
- In comparing the pile behavior in soil with a frozen layer and soil without a frozen layer, it is observed that with the combined action of the lateral and vertical loads on the pile under freezing conditions, the uplift capacity of the pile is slightly reduced when a constant lateral load is applied on the pile with increasing uplift load.
- The lateral and uplift pile capacities under individual and combined loads are increased with an increase in the embedded length of the pile under unfrozen ground conditions.

The author believes that the findings of this study enable a deeper understanding of the effects of the freezing and unfrozen states of the soil on the geotechnical response and stability of pile foundations subjected to combined axial and lateral loads, thereby contributing to a better design of piles in cold or permafrost regions under the influence of global warming.

3.8 References

Aldaeef, A. A., and Rayhani, M. T. (2020). Load transfer of pile foundations in frozen and unfrozen soft clay. *International Journal of Geotechnical Engineering*, *59*(6), 2110–2124.

Aldaeef, A. A., and Rayhani, M. T. (2021). Pile-soil interface characteristics in ice-poor frozen ground under varying exposure temperature. *Cold Regions Science and Technology*, *191*, 103377.

Allen, D. L. (1984). *A review and analysis of pile design* (Interim No. UKTRP-84-33; p. 38). Kentucky: Transportation Center Research.

Al-Umar, M., Fall, M., and Daneshfar B. (2021). *GIS based modeling of rainfall-induced landslide susceptibility of sensitive marine clays*. Geomechanics and Geoengineeing: An International Journal: 1-27

Al-Umar, M., Fall, M., Daneshfar B. (2020). GIS based modeling of snowmelt-induced landslide susceptibility of sensitive marine clays. Geoenvironmental Disasters 7:

Ayothiraman, R., and Reddy, K. M. (2014). Model experiments on pile behaviour in loose-medium dense sand under combined uplift and lateral loads. *Tunneling and Underground Construction*, (GSP-242), 633–643.

Azeez, O., Hummadi, R., and Hasan, A. (2019). Effect of embedded length on laterally loaded capacity of pile foundation. *American Scientific Research Journal for Engineering*, *56*(1), 182–192.

Bolton, M. D., and Gui, M. W. (1993). *The Study of Relative Density and Boundary Effects for Cone Penetration Tests in Centrifuge* (No. CUED/D-SOILS/TR256). University of Cambridge, UK.

Bolton, M. D., Gui, M. W., Garnier, J., Corte, J., F., Bagge, G., and Renzik, R. (1999). *Centrifuge cone penetration tests in sand*. *49*(4), 543–552.

Brandl, H. (2008). Freezing-thawing behaviour of soils and unbound road layers. *Slovak Journal of Civil Engineering*, 4–12.

Bureau of Indian Standards. (1985). *Code of practice for design and construction of pile foundations, BIS 1985 Part-4 Load test on Piles.* Bureau of Indian Standards.

Chatterjee, K., and Choudhury, D. (2016). Analytical and numerical approaches to compute the influence of vertical load on lateral response of single pile. *Japanese Geotechnical Society Special Publication*, *2*(36), 1319–1322.

Darr, K. A., Reese, L. C., and Wang, S., T. (1990, May). *Coupling Effects of Uplift Loading and Lateral Loading on Capacity of Piles*. Presented at the 22nd Annual Offshore Technology Conference, Huston, Texas.

Dong, J., Chen, F., Zhou, M., and Zhou, X. (2017). Numerical analysis of the boundary effect in model tests for single pile under lateral load. *Bulletin of Engineering Geology and the Environment*, *77*(3), 1057–1068.

DST Consulting Engineering. (2015). *Geotechnical investigation report 301 Palladium Drive Ottawa, Ontario* (No. IN-SO-021872). Ottawa,CA: DST Consulting Engineering.

Emirler, B., Tolun, M., and Yildiz, A. (2019). 3D Numerical Response of a Single Pile under Uplift Loading Embedded in Sand. *Geotechnical and Geological Engineering*, *37*(5), 4351–4363.

Fei, W., Yang, W. F., Zhaohui Joey Yang, Tiecheng Sund, and Sund, T. (2019). Ground freezing impact on laterally loaded pile foundations considering strain rate effect. *Cold Regions Science and Technology*, *157*, 53–63.

Gaaver, K. E. (2013). Uplift capacity of single piles and pile groups embedded in cohesionless soil. *AEJ - Alexandria Engineering Journal*, *52*(3), 365–372.

Ghosh, P., Mukherjee, S., Roy, N., and Banerjee, S. (2020). Response of single pile to lateral load with constant uplift. *Advances in Computer Methods and Geomechanics*, 283–298.

Hussien, M. N., Tobita, T., Lai, S., and Karray, M. (2014). On the influence of vertical loads on the lateral response of pile foundation. *Computers and Geotechnics*, *55*, 392–403.

Karasev, O. V., Talanov, G. P., and Benda, S. F. (1977). *Investigation of the work of single situ-cast piles under different load combinations*. *14*(3), 173–177.

Karthigeyan, S., Ramakrishna, V. V. G. S. T., and Rajagopal, K. (2006). Influence of vertical load on the lateral response of piles in sand. *Computers and Geotechnics , Indian Institute of Technology Madras, Chennai 600 036*, *33*(2), 121–131.

Kong, L. G., and Zhang, L. M. (2017). Centrifuge Modeling of Torsionally Loaded Pile Groups. *Journal of Geotechnical and Geoenvironmental Engineering*, *133*(11), 1374–1384.

Levy, S. M. (2010). Basic construction components. In *Construction Process Planning and Management-An owner's guide to successful projects* (pp. 277–305). United States.

Ling, Z. X., Yuan, X. J., Yan, H., and Shong-Loong, C. (2021). Model test study on horizontal bearing behavior of pile under existing vertical load. *Soil Dynamics and Earthquake Engineering*, *147*, 106820.

Liyang, F., Chen, H., and Chen, S. (2012). Influences of axial load on the lateral response of single pile with integral equation method. *International Journal for Numerical and Analytical Methods in Geomechanics*, *36*(16), 1831–1845.

Meyerhof, G. G., Mathur, S. K., and Valsangkar, A. J. (1981). Lateral resistance and deflection of rigid walls and piles in layered soils. *Can. Geotech. J*, *18*(2), 159–170.

Mhaidib, A. I. A. (137 C.E.). Experimental study on the effect of compressive loads on uplift capacity of model piles in sand. *International Journal of Geotechnical Engineering*, *6*(1), 133.

Nesralla C., and Fall M (2016). Highway structure stabilizing through heat drain. GeoVancouver 2016 – the 69th Canadian Geotechnical Conference (CGC), Oct. 2-5, 2016, Vancouver, Canada CD Rom.

Nesralla C., and Fall M (2015). Highway structure stabilization through convection pipe cooling (CPC). Geoquebec 2015 – the 68th Canadian Geotechnical Conference (CGC) and 7th Canadian Permafrost Conference, Sep. 20-23 2015, Quebec, Canada CD Rom.

Patra, N. R., and Pise, P. J. (2001). Ultimate Lateral resistance of pile group in sand. *Journal of Geotechnical and Geoenvironmental Engineering*, *127*(6), 481–487.

Pewe, T. L., and Paige, R. A. (1963). *Frost heaving of piles with an example from Fairbanks, Alaska*. Alaska, United States.

Radhakrishna, H. S., and Adams, J. I. (1973). Long-term uplift capacity of augered footings in fissured clay. *Canadian Geotechnical Journal*, *10*(4), 647–652.

Reddy, K. M., and Ayothiraman, R. (2015). Experimental studies on behavior of single pile under combined uplift and lateral loading. *Journal of Geotechnical and Geo-Environmental Engineering, ASCE*, *141*(7), 4015030.

Roy, S., and Bhalla, S. K. (2017). Role of geotechnical properties of soil on civil engineering structures. *Resources and Enviroment*, *7*(4), 103–109.

Sakr, M., Nazir, A., Azzam, W., and Sallam, A. (2019, March). *Uplift capacity of single pile with wing in sand-numerical study*. Presented at the International Conference on Advances in Structural and Geotechnical Engineering, Hurghada, Egypt.

Sazzad, M. M., Ashikuzzaman, M., Roni, M. A. U., and Ahmed, M. (2019, February). *Effect of length to diameter ratio on the load-deflection characteristics of laterally loaded driven piles in sand*. Presented at the 2nd International Conference on Planning, Architecture and Civil Engineering (ICPACE 2019), Rajshahi-6204, Bangladesh.

Srivastava, V., Chore, H. S., and Dode, P. A. (2016). Interaction of building frame with pile foundation. *Open Journal of Civil Engineering*, *06*(02), 195–202.

Teymur, B., and Madabhushi, S. P. G. (2003). Experimental study of boundary effects in dynamic centrifuge modelling. *Géotechnique*, *53*(7), 655–663.

Tomlinson, M., and Woodward, J. (2008). *Pile design and construction practice* (Fifth Edition). New York, US: Taylor & Francis.

Ullah, S. N., Hu, Y. X., White, D., and Stanier, S. (2014). Lateral boundary effect in centrifuge tests for spudcan penetration in uniform clay. *Applied Mechanics and Materials*, *553*, 458–463.

Wood, D. M. (2004). *Geotechnical Modelling* (1st Edition). London, UK: Taylor & Francis group.

Wood, D. M., Crewe, A., and Taylor, C. (2002). Shaking table testing of geotechnical models. *IJPMG- International Journal of Physical Modelling in Geotechnics*, *2*(1), 01–13.

Xingyun, W., Xiaochao, T., and Lian, F. (2013). Numerical simulation for uplift bearing capacity and affecting factors of the digging piles in slope ground. *Applied Mechanics and Materials*, *423–426*, 1292–1295.

Chapter 4- Physical Model Tests of Piles Under Freeze-thaw Cycles Subjected to Individual and Combined Loads

Harshdeep Singh, Mamadou Fall

(submitted)

4.1 Abstract

Seasonal freeze-thaw (F-T) cycles have a significant effect on the mechanical properties of soils and the behavior of pile foundations in soils subjected to F-T cycles under different loading conditions. Foundation soil exposed to F-T cycles will affect the performance of the pile foundation. Therefore, the effects of the F-T cycles should be accounted for in designing piles in the cold regions like Canada. In recent years, the climatic conditions are changing in Canada due to global warming which increases the number of F-T cycles in many regions annually. The objective of the study is to investigate the influence of different number of F-T cycles on the behaviour of piles in sandy soils. Laboratory experiments are conducted on physical model piles under individual and combined axial and lateral loadings subjected to F-T cycles. The model is scaled by using standard scaling principles and the testing apparatus is equipped with different sensors (LVDTs, strain gauges, and temperature sensors) to measure the temperatures, forces and displacements. The results show that with increased number of F-T cycles, the lateral pile capacities under individual and combined loads show a steady increase. The lateral load capacity is increased from 350 N with no F-T cycle to 430 N with 5 F-T cycles under individual loading and from 225 N with no F-T cycle to 455 N with 5 F-T cycles under combined loadings. However, the uplift load capacity of the pile remains constant under individual and combined loadings and there is no change due to the F-T cycles. The findings from this experimental study will be helpful to understand the behavior of piles subjected to seasonal F-T cycles and improve the design of pile foundations in cold regions.

4.2 Introduction

Pile foundations have been widely used in engineering structures such as bridges, high rise buildings, transmission towers, etc., to transfer loads to deeper ground or bedrocks with higher strength. The pile may be subjected to a combination of axial and lateral loads (but not earthquake loads). Axial loads are developed due to ground freezing or from the superstructure, whereas lateral loads come from wind, waves, passive earth pressure, etc. Frozen ground accounts for almost 23% of world's land area (Zhou et al. 2018), which is often populated with infrastructures and buildings. When the ground surface temperature drops below 0°C, water in the soil starts to freeze. Not all the water in the soil changes its state to ice at 0°C. The ground is said to be in a frozen state when water in the soil pores freezes and changes its state from liquid to solid (ice; Penner 1962; Pewe and Paige 1963). Frozen ground exhibits higher mechanical strength and is considered suitable to support buildings (Lai et al. 2009; He et al. 2014; Loria et al. 2017; Tang et al. 2018) The ice acts as a bonding agent that binds soil particles together (Andersland and Ladanyi 2004). In frozen ground, pile foundations are usually preferred because of their stability with higher load capacity compared to footing foundations (Tang et al. 2018).

In frozen ground, when a pile is subjected to combined loads (lateral and uplift), complex interactions occur between the pile and the soil at the pile-soil interface. The adfreeze bond developed along the pile surface considerably increases the pile load capacities (Aldaeef and Rayhani 2020a). There have been many studies on piles under combined loadings (e.g. Meyerhof et al. 1981; Das and Rozendal 1983; Darr et al. 1990; Patra and Pise 2001; Liyang et al. 2012; Gaaver 2013; Ayothiraman and Reddy 2014; Crowther 2015; Reddy and Ayothiraman 2015; Azeez et al. 2019) and on frozen grounds (Pewe and Paige 1963, Poulos and Davis 1980, Crowther 2015, Awwad et al. 2018, Tang et al. 2018, Fei et al. 2019, Aldaeef and Rayhani 2020a, 2020b, 2021). However, there is no physical model study available to investigate the influence of F-T cycles on pile behavior under the combined action of lateral and uplift loads.

More than two-thirds of bridges in the United States are subjected to seasonal freezing (Yang et al. 2017). These bridges and many other structures are constructed on pile foundations. The pile-soil interaction is dependent on the thermal regime of the soil. Due to increases in global warming, soils that have been frozen for years are thawing and not permanently frozen. Consequently, more and more soils are subjected to F-T cycles annually. The F-T cycle of soil is a phenomenon based on the thawing of ice in frozen soil during warm weather and freezing of water during the winter season. Studies have shown that thermal cycles severely alter the mechanical and physical properties of the soil such as the internal friction angle, density, thermal and hydraulic conductivities, infiltration, shear strength, and penetrability. For instance, Bo et al. (2015) observed that increases in the number of F-T cycles reduce the cohesion of soil. Other studies have linked the changes in soil properties such as mechanical strength, porosity and elastic modulus to F-T cycles (Alkire and Morrison 1984, Li et al. 2012, Ma et al. 2019). Climatic conditions vary depending on the geographical locations and cold regions, and high alpine environments are more prone to more F-T cycles. Therefore, the F-T cycles of soils should be an important consideration in designing pile foundations in cold regions that are subjected to combined loadings. There are very limited studies available on pile-soil interactions subjected to F-T cycles with combined loadings (Aldaeef and Rayhani 2015, 2020a, Tang et al. 2018). The paucity of available information on pile behavior subjected to F-T cycles and combined loadings with increasing environmental changes makes this study of great importance.

This physical model experiment in this study focuses on the investigation of the behavior of piles under individual and combined loadings subjected to various F-T cycles (0,1,3, and 5) in sand for a better understanding of piles in unfrozen and frozen soils. This physical model experiment will be very useful in pile design in cold regions.

4.3 Test Material and Experimental Setup

4.3.1 Test Material

4.3.1.1 Sand

In this experiment, locally available Ottawa sand was used. The basic geotechnical properties of the sand were determined in the laboratory in accordance with the ASTM standards D854-14 (specific gravity), D3080-04 (direct shear test), C136-01 (sieve analysis), and D7263-21 (density test). The soil properties are summarized in Table 4.1. The particle size distribution curve is shown in Figure 4.1. Based on USCS classification, the sand is classified as SP (poorly graded soil with very little fines).

Table 4-1 Soil Properties

Soils properties, unit	**Values**
Minimum dry density, kg/m^3	1480
Maximum dry density, kg/m^3	1644
Specific gravity	2.7
Friction angle at minimum dry density, °	37
Friction angle at maximum dry density, °	46

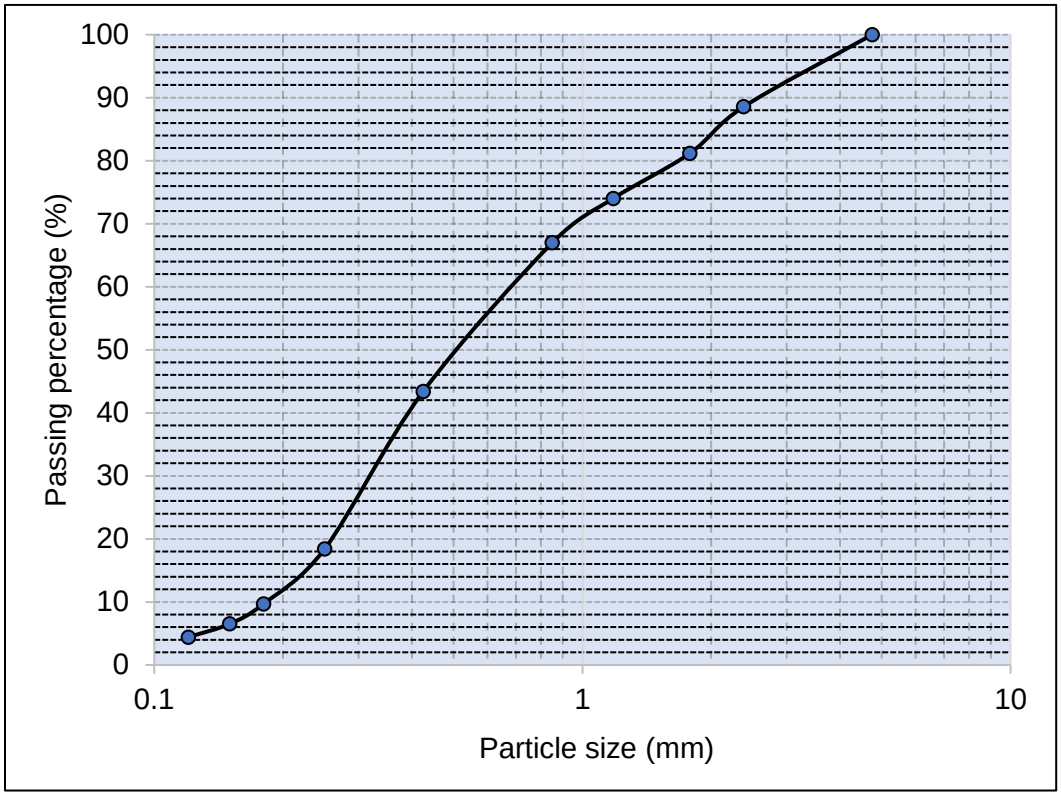

Figure 4.1 Grain size distribution curve of the sand used in the experiment

4.3.1.2 Model test pile

Figure 4.2. shows the pile used for the physical modeling. The model pile is made from an aluminum tube having an external diameter (D) of 25 mm, an internal diameter of 23 mm, and a length (L) of 375 mm. The top of the pile is welded to an aluminum block with dimensions of 100 x 100 x 22 mm to serve as a pile cap. To prevent the pile cap from interfering with the pile, the pile cap has a clearance of 50 mm above the soil surface. The tip of the pile is shaped into a cone to avoid plugging of the tube when it is inserted in the sand. Laboratory physical modeling is a simulation of a full-scale field experiment. The scaling factor for the model pile is based on Equation 4.1 given by Wood et al. (2002) and Wood (2004). The flexural rigidity is used to scale the model pile to the field assuming the same soil properties.

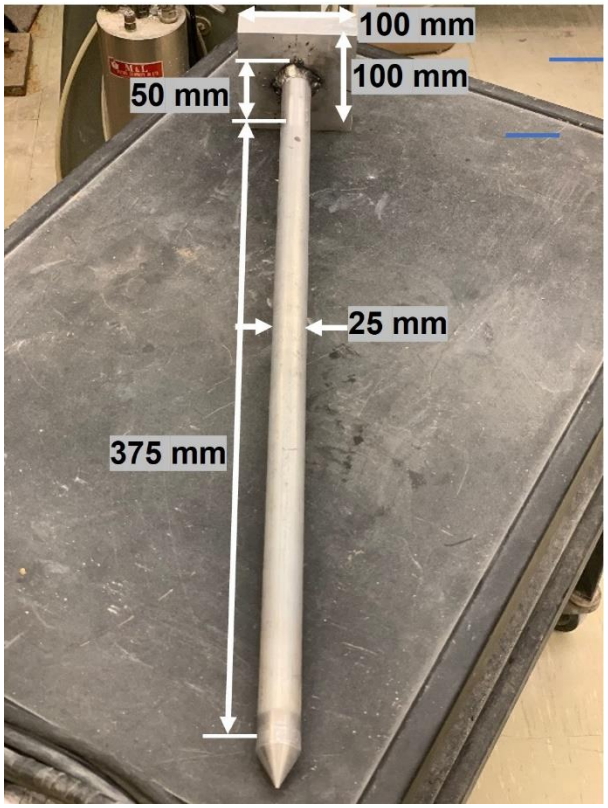

Figure 4.2 Model Pile

$$EI(p)\Big/_{EI(m)} = n^{4.5} \qquad 4.1$$

where

n = scaling factor

EI(p) = Flexure rigidity of prototype pile

EI(m) = Flexural rigidity of model pile

4.4 Experimental Setup

4.4.1 Main components of the setup

The experimental setup consists of a steel tank of 1300 x 725 x 725 mm in size with clean Ottawa sand, modeled pile and pile cap, see Figure 4.3. Loadings are applied using ae vertical and horizontal loading hanger and pully system with a variety of monitoring sensors (5TE, MPS6, LVDT), and a cooling system, see Figures 4.4 and 4.5.

The dimensions of the tank are determined to minimize boundary effects on the pile based on previous studies (e.g., Kishida 1963; Bolton and Gui 1993; Bolton et al. 1999; Teymur and Madabhushi 2003; Ullah et al. 2014; Reddy and Ayothiraman 2015; Dong et al. 2017; Sharafkhah and Shooshpasha 2018). Hence, the distance from the pile to the sides of the tank is equal to a minimum of 10 times the pile diameter D. The vertical zone of influence is considered to be equal to twice the length of the pile from the pile tip to the bottom of the tank. Based on these criteria, the dimensions of the experiment tank is shown in Figure 4.3.

4.4.2 Freezing setup and sensors

Figure 4.4 shows the schematic of the freezing apparatus used in the experiment. Freezing was accomplished using the DYNEO DD-1000F refrigerated/heating circulator with a temperature range of -50°C to 200°C. The cooling system allows one-dimensional cooling. The copper coil was placed on the top of the soil for freezing from top to bottom. The entire tank was insulated using fiberglass insulation. see Figure 4.5, to minimize heat loss. The cooling system circulated liquid coolant at -40°C to freeze the water in the soil. Sensors were installed in the soil layers to record different parameters at different depths and also monitor the frozen state of water in the soil. The 5TE sensor were used in the experiment to determine the soil freezing temperature and changes in water contents. The 5TE sensor operates in a temperature range between -40° to +50° C with an accuracy of ±1°C for the temperature and ±3% for the volumetric water content. Similarly, the MPS-6 is used to monitor the soil temperature and changes in water potential during

freezing and thawing of the soil. This sensor has an operating temperature range between -40°C and +60°C with an accuracy of ±1°C and an operating matric suction range between -9 kPa and -100 kPa with an accuracy of ±10%. A linear variable differential transformer (LVDT's) was used to measure displacement of the pile cap. The LVDTs used in the experiment can record a maximum displacement of 50 mm with an accuracy of ±0.1% and an operating temperature between 0° and +70° C.

4.4.3 Loading arrangement

The setup was equipped with a cable and pully system to apply static pullout and static lateral forces on the pile. Load was applied on the pile using an arrangement of pulleys, dead weight, hangers, and steel cable, as illustrated in Figure 4.3. The loading arrangement was equipped with two LVDTs to record vertical and horizontal movements of the pile cap.

4.4.4 Sand bed preparation

The tank was filled with sand up to 1,200 mm in height with a 100 mm thick layer of gravel at the bottom. The sand was evenly compacted in five layers. Every layer of sand was compacted with a hammer to achieve a relative density of 65%. A relative density in the range of 60% to 80% is considered as a dense state (Ganju et al. 2017; Roy and Bhalla 2017; Choo 2018). The density of every layer was verified by taking a core sample and measuring the density before proceeding to the next layer.

4.4.5 Pile installation

A steel guide, as shown in Figure 4.6, is used to hold the pile in position while filling the tank with sand. This guide assembly used in the experiment ensured the pile remained vertical during placement of the sand. Once the sand bed reached the tip of the pile, the pile was firmly held by the steel assembly in position to avoid any pile movement during the compaction.

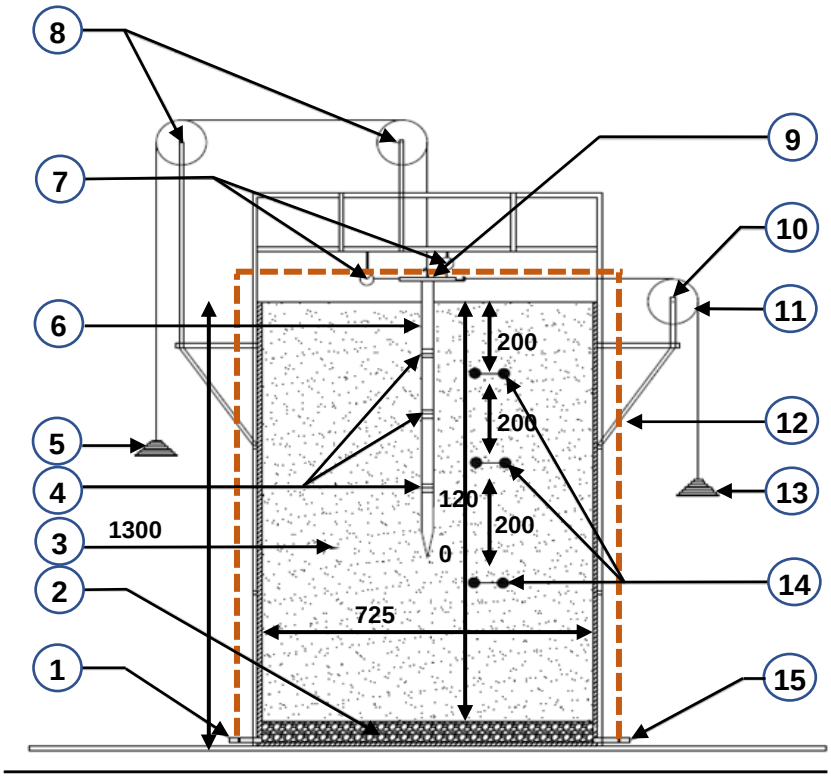

8. Water Inlet
9. Gravel Bed
10. Sand Bed
11. Strain Gauge
12. Static loads
13. Pile
14. LVDT
16. Pulley
17. Pile Cap
18. Pulley
19. Metal Wire
20. Insulation
21. Static loads
22. Sensor sets
23. Water Outlet

Figure 4.3 Schematic diagram of the experimental tank setup

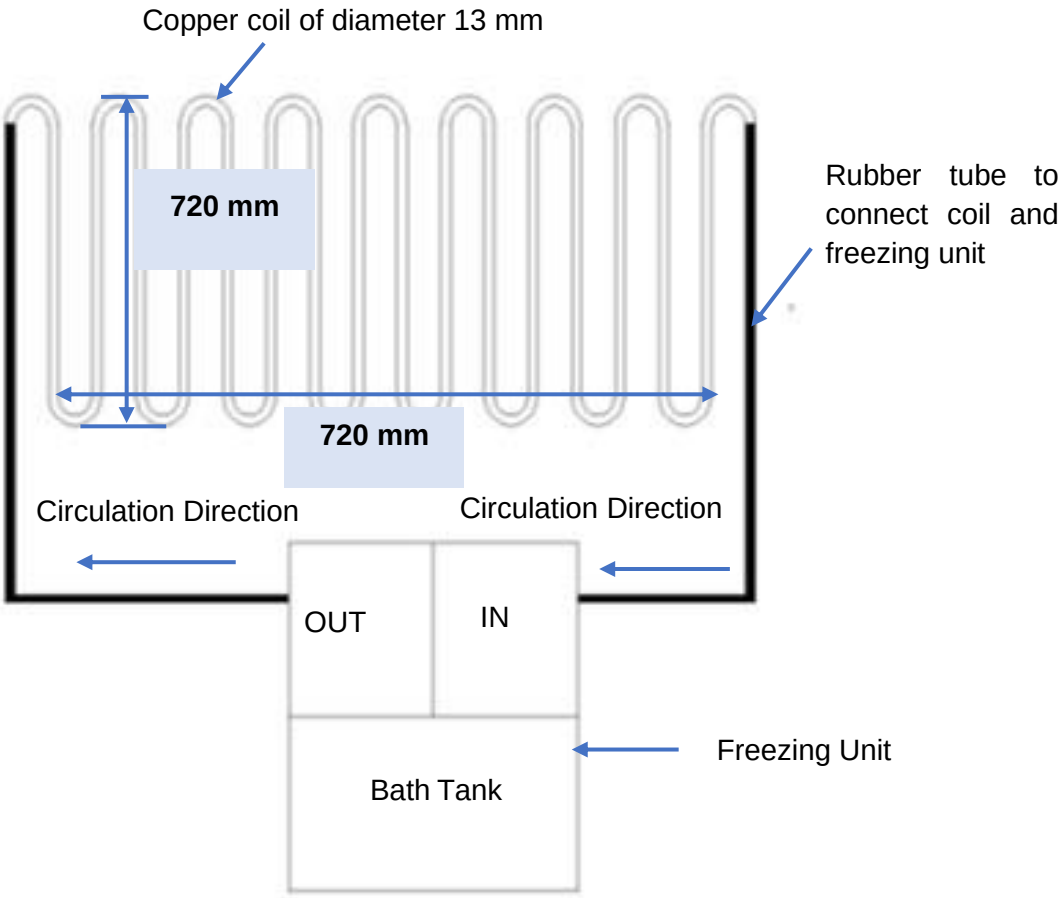

Figure 4.4 Schematic diagram of the experimental cooling system

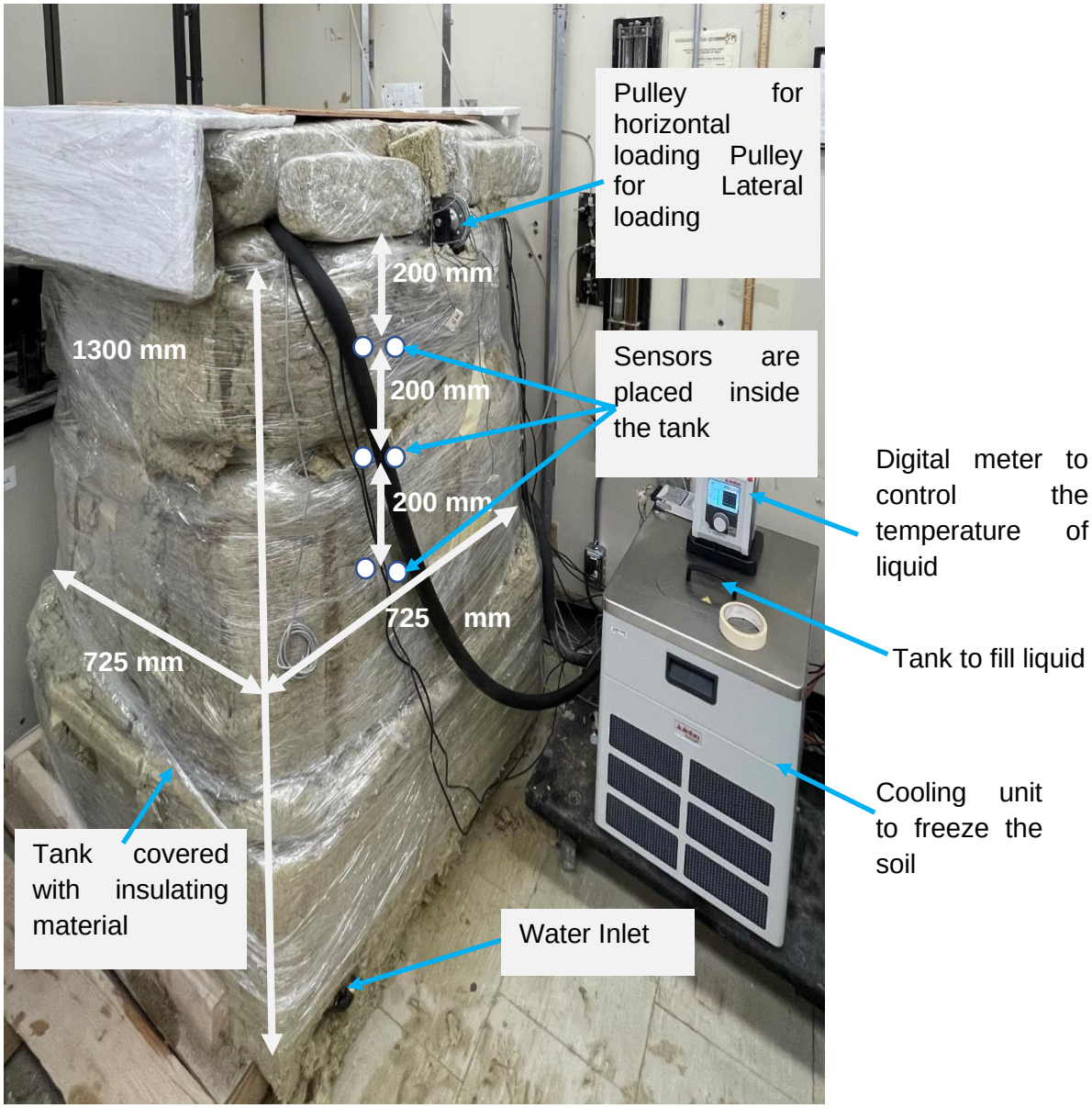

Figure 4.5 Experimental tank

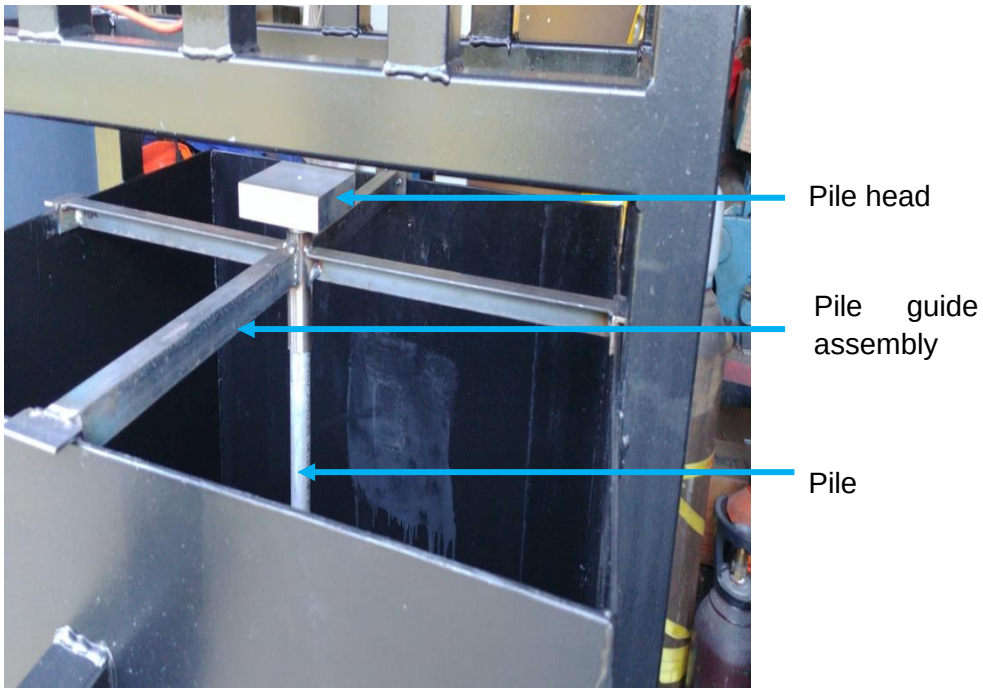

Figure 4.6 Experimental tank for model pile test

4.5 Experiment Procedure

4.5.1 Freeze-thaw cycles

The actual frozen ground conditions in the Ottawa region are simulated in the laboratory. The soil in the experiment was frozen to the frost depth of 5 cm. The frozen condition was checked by monitoring the temperature with the sensors embedded in the soil bed as explained in Section 4.4.1.1. Once the soil freeze to the required depth, the cooling copper coil was removed from the soil bed and the soil was allowed to thaw naturally at room temperature without any surcharge load on the soil's surface. During the experiment, a series of tests were conducted with multiple number of freeze-thaw cycles (1, 3 and 5 cycles). The freezing process took almost 2 to 3 days to freeze the soil up to the required depth and 1 day to thaw naturally to complete one freeze-thaw cycle. All data was collected continuously with a computer.

4.5.2 Lateral loading

The pile was statically loaded horizontally as per BIS (1985). The initial readings of the LVDT were taken to identify the unloaded condition before the lateral load is applied to the pile in small increments. Each increment was added after the horizontal displacement of the pile had ceased. The pile cap deflection was continuously recorded with the LVDTs. This process continued until the failure criterion in terms of deflection of 12 mm has reached as defined in BIS (1985).

The ultimate lateral load capacity of the pile can be determined using different methods, The double tangent method and the load-deflection curve analysis are the most commonly used Methods. According to Patra and Pise (2001), in the double tangent method, the load-deflection curve reaches a peak deflection at failure. The failure load is the ultimate load beyond which there is no further lateral resistance provided by the pile against lateral loading. Meyerhof et al. (1981) and Chari and Meyerhof (1983) considered the ultimate lateral capacity of a pile as the load beyond which the load-displacement curve becomes linear or almost linear. Broms (1964) proposed a subgrade pressure method for determining the ultimate lateral capacity of a pile. In this experimental, the ultimate lateral pile capacity of the pile is considered when either the pile fails at a certain load or a maximum displacement of 12 mm.

4.5.3 Uplift loading

The uplift load was applied on the pile as per BIS (1985). The initial reading of the LVDT was recorded to identify the unloaded condition. The pile was then loaded in increments. Dead weights were used to load the pile, as shown in Figure 4.3. After loading the pile at each step, the deflection of the pile was allowed to stabilize. This process was repeated until the pile had reached the maximum deflection criteria. It is assumed that a full-scale pile in an actual structure will only be subjected to a safe/permissible load only.

4.5.4 Combined loading

Under combined loading, the pile was loaded under two different scenarios: Firstly, a constant uplift force was applied with increasing lateral force; secondly, a constant lateral force was applied with increasing uplift force. In both scenarios, the load was increased in small increments and the pile deflection was allowed to stabilize before the application of the next load increment. The deflection was considered to stabilize when the pile deflection rate is less than 1 mm per 30 minutes according to BIS (1985). Since the prototype pile is subjected to the working loads, an FOS of 2 is considered for the safe working condition in the experiment.

4.6 Results and Discussion

4.6.1 Pile behavior under individual load and freeze-thaw cycles

The changes in the uplift capacity and lateral capacity of the pile for different number of freeze-thaw cycles (0, 1, 3 and 5 cycles) are summarized in Table 4.2 and the results are plotted in Figures 4.7 and 4.8. It is seen that the uplift capacity remains almost the same under different number of freeze-thaw cycles with small increase in the capacity. Ma et al. (2019) stated that a dense soil loses its strength due to freezing and thawing and explained that when a dense sand freezes, water in the pores tends to expand due to phase change from liquid to solid, affecting the density of the soil. Li et al. (2019) studied the effect freeze-thaw cycles on soil properties and explained that the angle of internal friction increases with increase in the number of F-T cycles and the shear strength of the sand varies according to the applied confining pressures. During freezing, the pores in the sand expand whereas during thawing, the pores in the soil contract, realigning the soil particles and changing the soil mechanical behavior (Chang and Liu 2013). The results from the present model test show that freezing and thawing of sand layer up to the model depth of 5 cm (downscaled the depth frost penetration in the Ottawa region) does not affect the soil pile interaction against uplift loading. The uplift resistance of the pile depends mainly on the

mobilized skin friction between the pile and the soil (Tomlinson and Woodward 2008), while the soil pressure (K) is an influential factor affecting the shaft resistance. The pile axial capacity increases with an increase in the soil confining pressure (Naggar and Wei 1999). In the case of determining the lateral pile capacity, there are many studies on the analysis of lateral load capacity of a pile (Poulos and Davis 1980, Meyerhof et al. 1981, Patra and Pise 2001, Lee et al. 2010) but none of these studies considered a physical model to estimate lateral pile capacity considering the effects of freeze-thaw cycles in sand. The results from this experiment on lateral capacity follow a similar trend as the uplift capacity. Lateral pile capacity did not show significant changes due to the freezing and thawing of the sand layer. The ultimate capacity remains between the range of 350 N to 450 N and pile rotation is observed when approaching the ultimate lateral pile capacity. The support provided by the surrounding soil is unchanged even after applying a number of thermal cycles. Overall, the individual pile capacities (uplift and lateral) remain unaffected due to freeze and thaw cycles. This may be affected by the pile dimension and the sand conditions in this experiment. It is evident from the results that a L/D ratio of 15 in dense sand eliminates any effect of freeze-thaw cycles on the individual pile capacities. Also, the passive resistance provided by the soil to support the pile remains constant throughout the loading phase and remains unaffected by freeze-thaw cycles of the top sand layer.

Table 4-2 Failure loads of the piles under individual loads

Number of the freeze-thaw cycle	L/D	Failure individual loading (N)	
		Vertical Load P_u (N)	Lateral Load H_u (N)
0	15	328	350
1		330	360
3		360	400
5		340	430

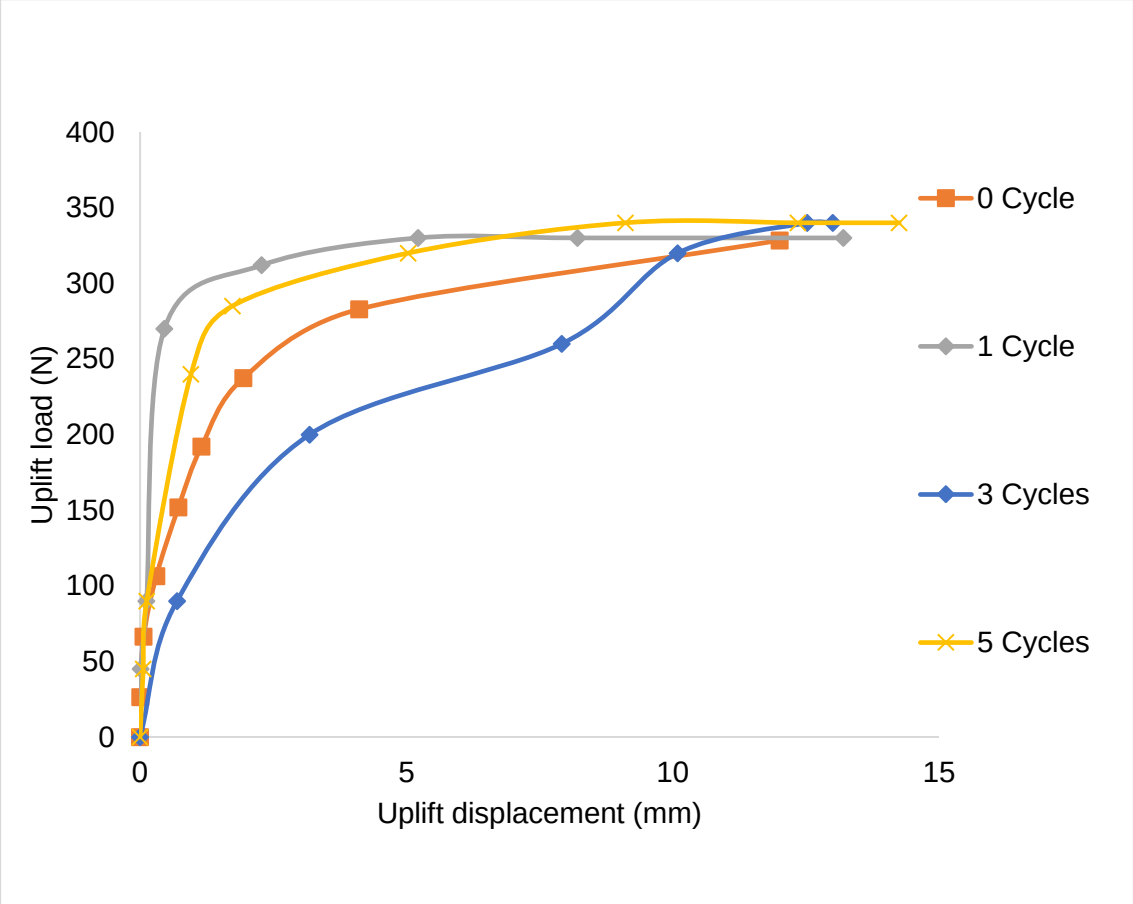

Figure 4.7 Uplift load-deflection curve under individual load

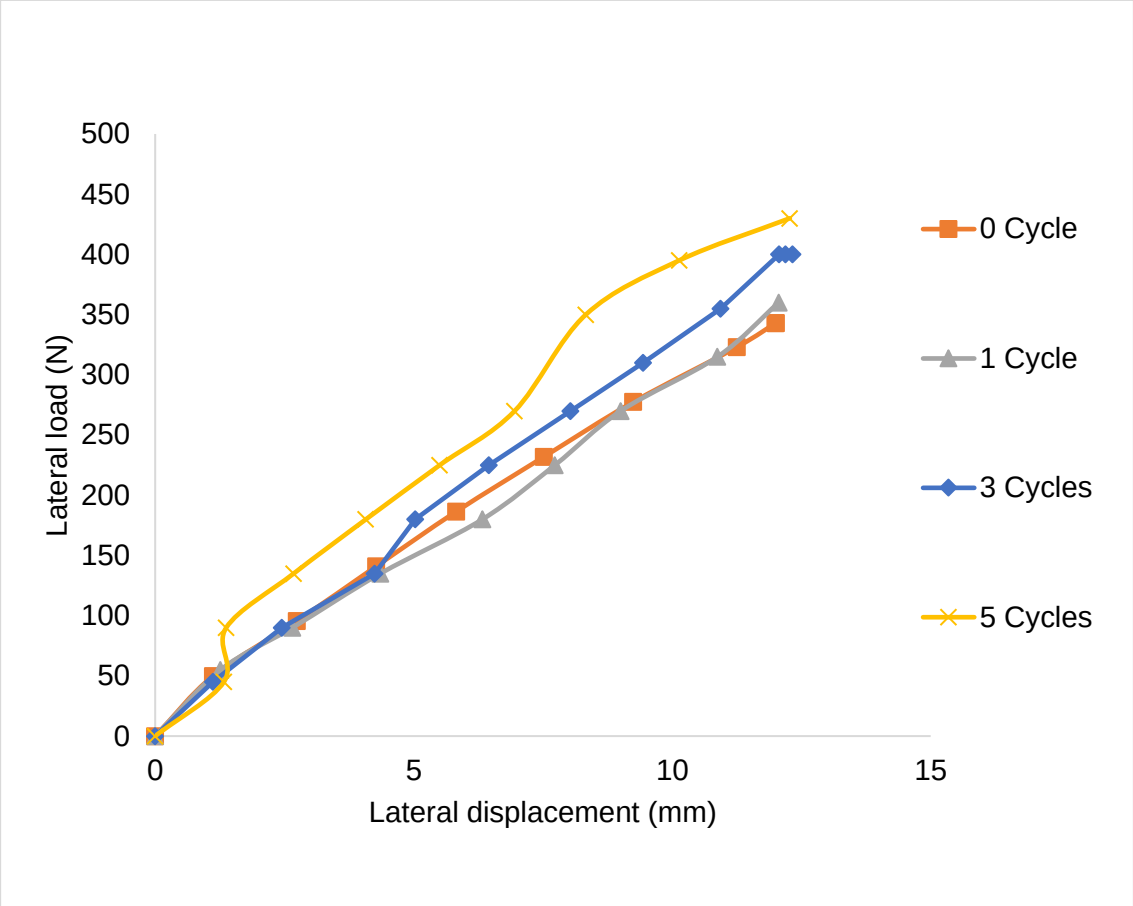

Figure 4.8 Lateral load-deflection curve under Individual load

4.6.2 Pile behavior under combined loading and freeze-thaw cycles

The effects of F-T cycles on the ultimate pile capacities (uplift and Lateral) under combined loading is discussed in this section. The results are summarized in Table 4.3, and Figures 4.9 and 4.10 show the pile capacities under different number of thermal cycles (0, 1, 3, and 5). Figure 4.9 shows a nonlinear behavior under uplift load with deflection. The results show no change in the uplift capacity under a constant lateral load for different number of F-T cycles. The pile-soil interaction remains unaffected by the F-T cycles against uplift load under combined loadings and

the failure loads are within the same range of values. However, when the uplift capacities under combined loads are compared with those under individual load, it is evident that the pile uplift capacity is increased by a factor of 1.5. The increase in the pile capacity is evident at small uplift deflection. Only a 1.1 mm uplift deflection is recorded at 435 N load under combined loadings after 5 F-T cycles. The same deflection is recorded at 195 N under individual load with no F-T cycle. This shows that even after a number of F-T cycles have occurred, a constant static lateral load applied on the pile provides resistance against the pullout force that is acting on the pile similar to the unfrozen soil. Rahman and Achmus (2006), Ayothiraman and Reddy (2014), Reddy and Ayothiraman (2015) observed similar uplift pile capacity behavior under combined loadings in unfrozen soils. This means that a part of the uplift load on the pile is transferred to the soil that surrounds the pile. The pile-soil interaction becomes more complex under combined loading. The pile under an incremental lateral load subjected to constant uplift force with different F-T cycles shows linear behavior (Figure 4.10). The response of the pile is constant throughout the tests with different F-T cycles. The ultimate lateral capacity with a constant uplift load steadily increases from 225 N with no F-T cycle to 455 N with 5 F-T cycles. The failure criterion of 12 mm deflection as per the BIS (1985) is reached at higher loadings with increase in the number of thermal cycles. In other words, higher passive resistance of the soil is mobilized with increase in the number of F-T cycles. Achmus and Thieken (2010) suggested that the mobilized passive earth pressure is reduced with an increase in the tensile force on the laterally loaded pile which agrees with the current observations. The lateral pile capacity under the combined action of lateral and uplift loads is decreased when compared to the lateral pile capacity under individual loading. It can be concluded from the experimental results that the F-T cycles affect the pile behavior under combined loadings.

Table 4-3 Failure loads of the piles under individual loads

Number of the freeze-thaw cycles	L/D	Failure combined loading (N)	
		Lateral load under constant vertical load (N)	Vertical load under constant lateral load (N)
0	15	225	580
1		326	550
3		430	565
5		455	580

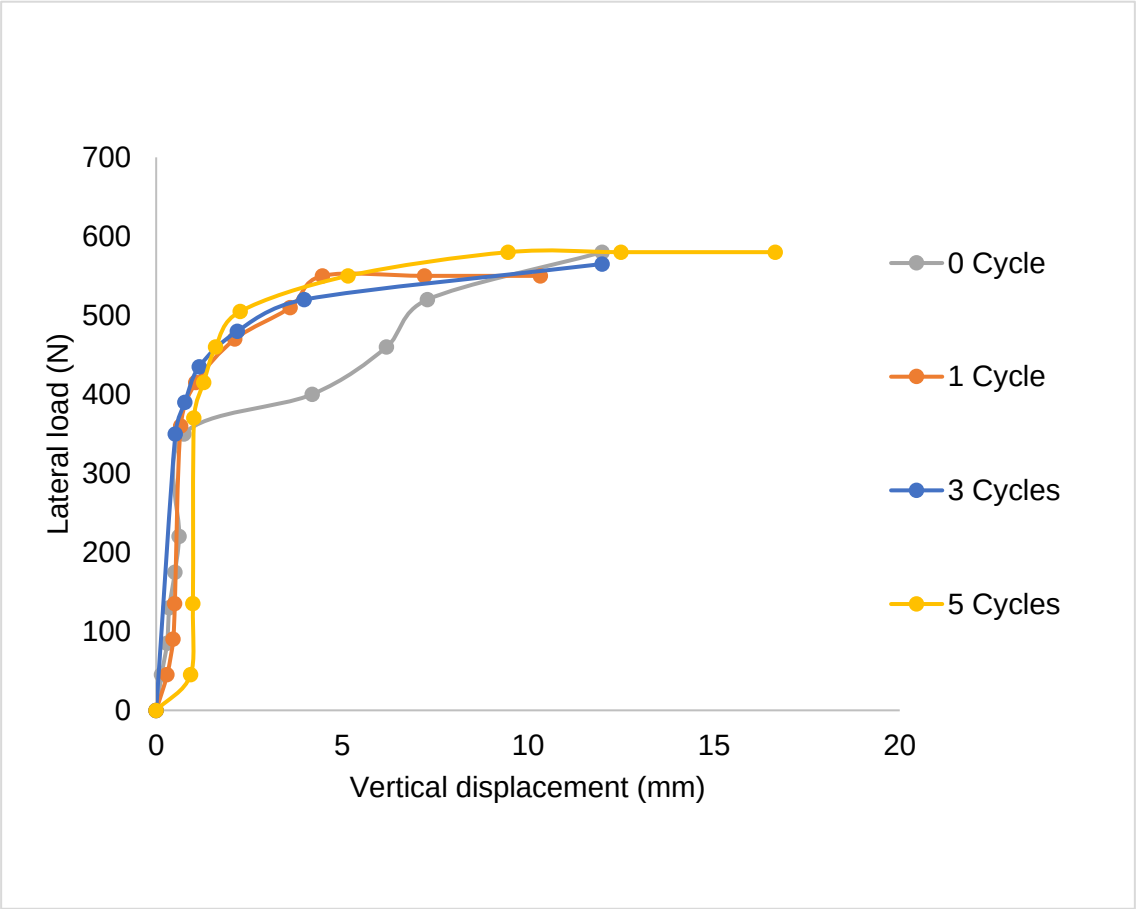

Figure 4.9 Uplift load-deflection curve under combined load

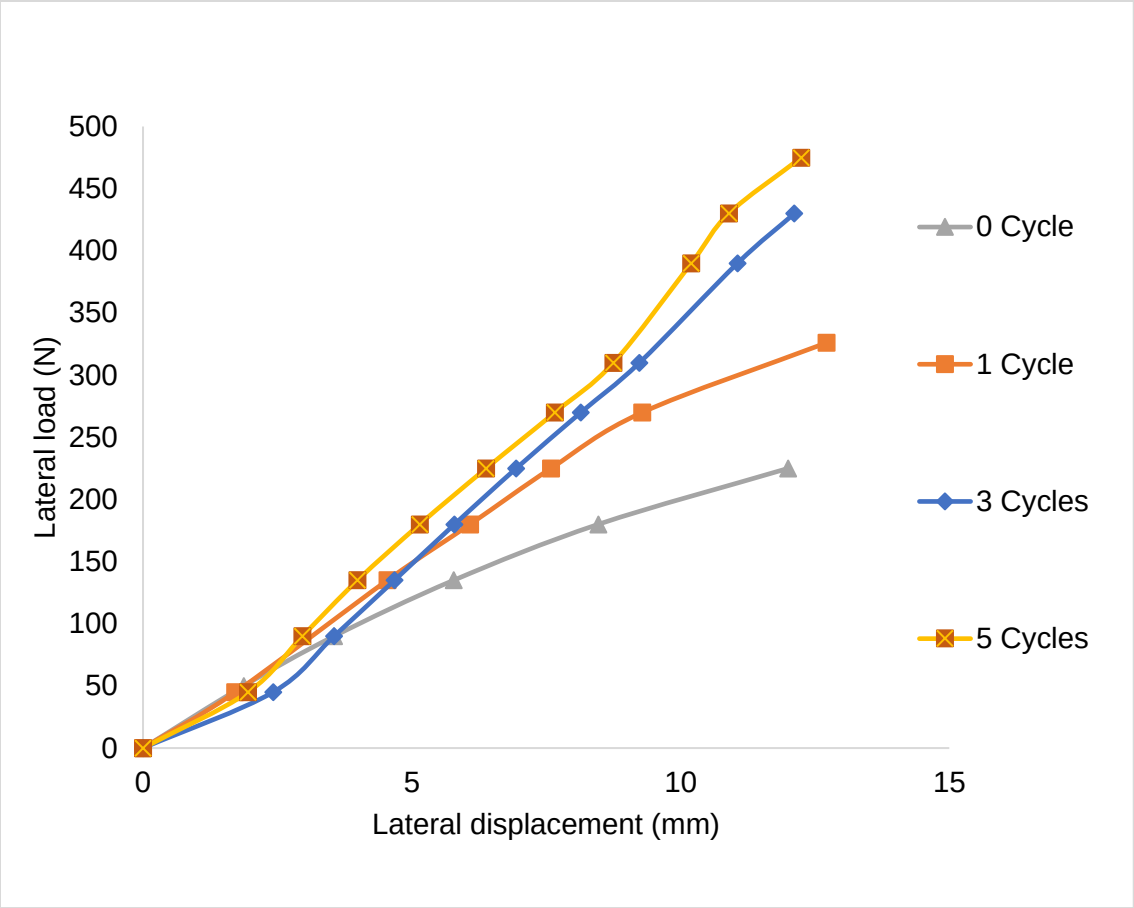

Figure 4.10 Lateral load-deflection curve under combined loads

4.7 Summary and Conclusion

A physical laboratory model has been developed to study the effect of freezing and thawing of a top soil layer on the pile response under individual and combined static loadings. The ultimate pile capacities were measured under different number of F-T cycles. The outcomes and conclusions of the experiments are summarized below.

- Freezing and thawing of the top layer affects the lateral pile capacity under individual and combined loadings (uplift and lateral). Different combinations of these factors may lead to different results.

- The lateral load capacity of the pile under individual loading increases with an increase in the number of F-T cycles.
- The individual uplift capacity of the pile remains almost unaffected by the freezing and thawing of the soil layer.
- The F-T cycles do not show any effect on the uplift pile capacity under combined loadings. However, the uplift pile capacity under combined loads is increased substantially by almost 50%, when compared with the uplift capacity under individual load.
- A steady increase in the lateral capacity of the pile under combined loads with an increase in the F-T cycles is observed.
- At 0 and 1 F-T cycles, the lateral pile capacity under individual loading is more than the lateral pile capacity under the combined loadings with even higher lateral pile capacity under combined loadings at 3 and 5 F-T cycles.

4.8 References

Achmus, M., and Thieken, K. (2010). On the behavior of piles in non-cohesive soil under combined horizontal and vertical loading. *Acta Geotechnical*, *5*(3), 199–210.

Aldaeef, A. A., and Rayhani, M. T. (2015). *Load transfer of pile foundations in warming frozen ground*. Presented at the 68th Canadian Geotechnical Conf, Canada.

Aldaeef, A. A., and Rayhani, M. T. (2020a). Load transfer of pile foundations in frozen and unfrozen soft clay. *International Journal of Geotechnical Engineering*, *59*(6), 2110–2124.

Aldaeef, A. A., and Rayhani, M. T. (2020b). Pull-Out Capacity and Creep Behavior of Helical Piles in Frozen Ground. *Journal of Geotechnical and Geoenvironmental Engineering*, *146*(12), 04020140.

Aldaeef, A. A., and Rayhani, M. T. (2021). Pile-soil interface characteristics in ice-poor frozen ground under varying exposure temperature. *Cold Regions Science and Technology*, *191*, 103377.

Alkire, B. D., and Morrison, J. M. (1984). *Change in Soil Structure Due to Freeze-Thaw and Repeated Loading* (Publication No. 918). Washington District of Columbia, United States: Transportation Research Board.

Andersland, O. B., and Ladanyi, B. (2004). *Frozen Ground Engineering* (Second Edition). Hoboken, New Jersey, US: John Wiley & Sons, Inc.

Awwad, T., Shakhmov, Z. A., Lukpanov, R. E., and Yenkebayev, S. B. (2018). Experimental Study on the Behavior of Pile and Soil at the Frost Condition. In *Sustainability Issues for the Deep Foundations*. Cairo, Egypt.

Ayothiraman, R., and Reddy, K. M. (2014). Model experiments on pile behaviour in loose-medium dense sand under combined uplift and lateral loads. *Tunneling and Underground Construction*, (GSP-242), 633–643.

Azeez, O., Hummadi, R., and Hasan, A. (2019). Effect of embedded length on laterally loaded capacity of pile foundation. *American Scientific Research Journal for Engineering*, *56*(1), 182–192.

Bo, X. S., Jun, Q. J., Ming, L. yuan, Wei, Z. Z., and Tian, X. X. (2015). Effects of freeze-thaw cycles on soil mechanical and physical properties in Quinghai- Tibet plateau. *Journal of Mountain Science*, *12*(4), 999–1009.

Bolton, M. D., and Gui, M. W. (1993). *The Study of Relative Density and Boundary Effects for Cone Penetration Tests in Centrifuge* (No. CUED/D-SOILS/TR256). University of Cambridge, UK.

Bolton, M. D., Gui, M. W., Garnier, J., Corte, J., F., Bagge, G., and Renzik, R. (1999). *Centrifuge cone penetration tests in sand*. *49*(4), 543–552.

Broms, B. (1964). Lateral resistance of piles in cohesionless soils. *Japanese Society of Soil Mechanics and Foundation Division*, 123–156.

Bureau of Indian Standards. (1985). *Code of practice for design and construction of pile foundations, BIS 1985 Part-4 Load test on Piles.* Bureau of Indian Standards.

Chang, D., and Liu, J. K. (2013). Review of the influence of freeze-thaw cycles on the physical and mechanical properties of soil. *Sciences in Cold and Arid Regions*, *5*(4), 0457–0460.

Chari, T., and Meyerhof, G. G. (1983). Ultimate capacity of rigid single piles under inclined loads in sand. *Can. Geotech Journal*, *20*(4), 849–854.

Choo, J. (2018). Mohr–Coulomb plasticity for sands incorporating density effects without parameter calibration. *Int J Numer Anal Methods Geomech*, *42*(18), 2193–2206.

Crowther, G. S. (2015). Lateral Pile Analysis Frozen Soil Strength Criteria. *Journal of Cold Regions Engineering*, *29*(2), 4014011.

Darr, K. A., Reese, L. C., and Wang, S., T. (1990, May). *Coupling Effects of Uplift Loading and Lateral Loading on Capacity of Piles*. Presented at the 22nd Annual Offshore Technology Conference, Huston, Texas.

Das, B. M., and Rozendal, D. B. (1983). *Ultimate Uplift Capacity of Piles in Sand*. Transportation Research Record 945.

Dong, J., Chen, F., Zhou, M., and Zhou, X. (2017). Numerical analysis of the boundary effect in model tests for single pile under lateral load. *Bulletin of Engineering Geology and the Environment*, *77*(3), 1057–1068.

Fei, W., Yang, W. F., Zhaohui Joey Yang, Tiecheng Sund, and Sund, T. (2019). Ground freezing impact on laterally loaded pile foundations considering strain rate effect. *Cold Regions Science and Technology*, *157*, 53–63.

Gaaver, K. E. (2013). Uplift capacity of single piles and pile groups embedded in cohesionless soil. *AEJ - Alexandria Engineering Journal*, *52*(3), 365–372.

Ganju, E., Prezzi, M., and Salgado, R. (2017). Algorithm for generation of stratigraphic profiles using cone penetration test data. *Computers and Geotechnics*, *90*, 73–84.

He, W., Qi, G., and Jingbo, T. (2013). *Study on the shear strength parameters under different freezing and thawing cycles of soil slope in China*. *860–863*, 1280–1283.

Kishida, H. (1963). Stress distribution by model pile in sand. *Building Research Institute*, *4*(1), 1–23.

Lai, Y., Jin, L., and Chang, X. (2009). Yield criterion and elasto-plastic damage constitutive model for frozen sandy soil. *International Journal of Plasticity*, *25*(6), 1177–1205.

Lee, J., Kim, M., and Kyung, D. (2010). Estimation of Lateral Load Capacity of Rigid Short Piles in Sands Using CPT Results. *Journal of Geotechnical and Geoenvironmental Engineering*, *136*(1), 48–56.

Li, G., Ma, W., Zhao, S., Mao, Y., and Mu, Y. (2012). Effect of Freeze-Thaw Cycles on Mechanical Behavior of Compacted Fine-Grained Soil. In *Cold Regions Engineering 2012: Sustainable Infrastructure Development 72 in a Changing Cold Environment, ASCE* (72–81). Quebec City, Canada.

Li, J., Wang, F., Yi, F., Wu, F., Liu, J., and Lin, Z. (2019). Effect of Freeze-Thaw Cycles on Triaxial Strength Property Damage to Cement Improved Aeolian Sand (CIAS). *Materials (Basel)*, *12*(17), 2801.

Liyang, F., Chen, H., and Chen, S. (2012). Influences of axial load on the lateral response of single pile with integral equation method. *International Journal for Numerical and Analytical Methods in Geomechanics*, *36*(16), 1831–1845.

Loria, A. F. R., Frigo, B., and Chiaia, B. (2017). A non-linear constitutive model for describing the mechanical behaviour of frozen ground and permafrost. *Cold Regions Science and Technology*, *133*, 63–69.

Ma, Q., Zhang, K., Jabro, J. D., Ren, L., and Liu, H. (2019). Freeze–thaw cycles effects on soil physical properties under different degraded conditions in Northeast China. *Environmental Earth Sciences*, *78*(10), 1–12.

Meyerhof, G. G., Mathur, S. K., and Valsangkar, A. J. (1981). Lateral resistance and deflection of rigid walls and piles in layered soils. *Can. Geotech. J*, *18*(2), 159–170.

Naggar, M. H. E. I., and Wei, Ji. Q. (1999). Axial capacity of tapered piles established from model tests. *Canadian Geotechnical Journal*, *36*(6), 1185–1194.

Patra, N. R., and Pise, P. J. (2001). Ultimate Lateral resistance of pile group in sand. *Journal of Geotechnical and Geoenvironmental Engineering*, *127*(6), 481–487.

Penner, E. (1962). *Ground freezing and frost heaving*. National Research Council Canada.

Pewe, T. L., and Paige, R. A. (1963). *Frost heaving of piles with an example from Fairbanks, Alaska*. Alaska, United States.

Poulos, H. G., and Davis, E. H. (1980). *Pile foundation analysis and design*. New York, US: Wiley.

Rahman, K. A., and Achmus, M. (2006). *Numerical modelling of the combined axial and lateral loading of vertical piles*. 575–581. Graz, Austria.

Reddy, K. M., and Ayothiraman, R. (2015). Experimental studies on behavior of single pile under combined uplift and lateral loading. *Journal of Geotechnical and Geo-Environmental Engineering, ASCE*, *141*(7), 4015030.

Roy, S., and Bhalla, S. K. (2017). Role of geotechnical properties of soil on civil engineering structures. *Resources and Enviroment*, *7*(4), 103–109.

Sharaf Khah, M., and Shooshpasha*, I. (2018). Physical modeling of behaviors of cast-in-place concrete piled raft compared to free-standing pile group in sand. *Journal of Rock Mechanics and Geotechnical Engineering*, *10*(4), 703–716.

Tang, L., Wang, X., Long, J., Deng, L., and Wu, D. (2018). *Frost heave and thawing settlement of frozen soils around concrete piles: A laboratory model test*. Presented at the Geo Edmonton, Alberta.

Teymur, B., and Madabhushi, S. P. G. (2003). Experimental study of boundary effects in dynamic centrifuge modelling. *Géotechnique*, *53*(7), 655–663.

Tomlinson, M., and Woodward, J. (2008). *Pile design and construction practice* (Fifth Edition). New York, US: Taylor & Francis.

Ullah, S. N., Hu, Y. X., White, D., and Stanier, S. (2014). Lateral boundary effect in centrifuge tests for spudcan penetration in uniform clay. *Applied Mechanics and Materials*, *553*, 458–463.

Wood, D. M. (2004). *Geotechnical Modelling* (1st Edition). London, UK: Taylor & Francis group.

Wood, D. M., Crewe, A., and Taylor, C. (2002). Shaking table testing of geotechnical models. *IJPMG- International Journal of Physical Modelling in Geotechnics*, *2*(1), 01–13.

Yang, Z. J., Li, Q., Horazdovsky, J., Hulsey, J. L., and Elmer E., M. (2017). Performance and Design of Laterally Loaded Piles in Frozen Ground. *Journal of Geotechnical and Geoenvironmental Engineering*, *143*(5), 6016031.

Zhou, Z., Ma, W., Zhang, S., Yanhu, M., and Guoyu, L. (2018). Effect of freeze-thaw cycles in mechanical behaviors of frozen loess. *Cold Regions Science and Technology*, *146*, 9–18.

Chapter 5- Conclusions and recommendations

5.1 Conclusions

The main observations from this experimental investigation are as follows:

1. Pile behavior under individual and combined loadings is significantly affected by soil with a frozen layer. F-T cycles also have considerable influence on the pile performance under individual and combined loadings.
2. The lateral capacity of the pile under individual and combined loadings in soil with a frozen layer is higher than the pile capacities in unfrozen ground.
3. The individual and combined uplift capacities of the pile in the soil with a frozen layer are increased in comparison to those in the soil without a frozen layer.
4. The uplift capacity of the pile under combined loadings is observed to be less than that under individual load in the soil with a frozen layer.
5. The lateral and uplift capacities of the pile under individual and combined loadings are increased with increase in the pile's embedded length.
6. There is a constant increase in the lateral capacity of the pile under individual and combined loadings with an increase in the number of freeze-thaw cycles (0,1,3 and 5)
7. The uplift capacity of the pile remains stable under individual and combined loading throughout the freeze-thaw (0,1,3 and 5) cycles.
8. Under the influence of freeze-thaw cycles (0,1,3 and 5), the pile capacity for combined loading are higher than the values of uplift pile capacity under individual loading.

5.2 Recommendations for further studies

This study focuses on pile behavior under individual and combined loads in clean sand. Taking into consideration the scope of the study, experimental limitations, time and cost, the following recommendations are proposed for future work.

- Pile behavior in different soils with varying depths of the frozen layer should be analysed to investigate the pile performance in thawing soils subjected to single and combined loadings.
- Different types of piles and pile dimensions can be tested under individual and combined loadings subjected to a higher number of F-T cycles.
- Coupled numerical models should be developed and validated in future studies to numerically investigate the behavior and performance of piles in thawing soils subjected to single and combined loadings.
- Coupled numerical models should be established and validated in future studies to numerically assess the behavior and performance of piles in soils exposed to freeze-thaw cycles subjected to single and combined loading.

APPENDIX A - Thaw Consolidation Model

The assessment of the settlements associated with the thawing of soil is paramount in designing any engineering structure in permafrost and frozen ground. Therefore, developing a model to understand the interactions of the settlement rate of the soil and the pore water pressure is important. A model that captures the thermo hydro-mechanical process can be a complex one that involves heat transfer in soil coupled with thaw consolidation.

In the past, various studies have set out to determine the small strain consolidation in soils. However, their theories are not applicable in ice-rich soils, which have the potential to have large consolidation strains. To determine one-dimensional large strain consolidation, Figure A.1 shows a frozen soil sample at temperature T = 0 which is subjected to load P. Thawing is initiated at T >0 when the frozen surface of the soil begins to melt and water is released from the frozen material. Water released at the thaw front and contained in the ground is subjected to a pore water pressure gradient. The gradient is generated from both thawed soil self-weight and applied load. The model is divided into two regions: the frozen and the thawing regions. Heat transfer occurs through the entire soil mass whereas consolidation is confined to the thawing region. The upper boundary for the thawing ground surface is located at a = 0, and the lower boundary is located at an arbitrary depth of a = H_i.

At T = 0, the temperature of the soil T_f is below the freezing point. The thermal boundary condition is changed by increasing the surface temperature of the soil. The lower boundary condition at a = H_0 is defined as the geothermal flux boundary. At T > 0, heat transfer occurs between the thawed and frozen regions at the interface depth a = z(T), which is defined as a moving boundary. The consolidation domain extends from the ground surface at a = 0 where the load P is applied

to the moving interface boundary at a = z(T). The thaw consolidation settlement is a function of depth and temperature. The surface settlement at a = 0 is denoted by s(0, T).

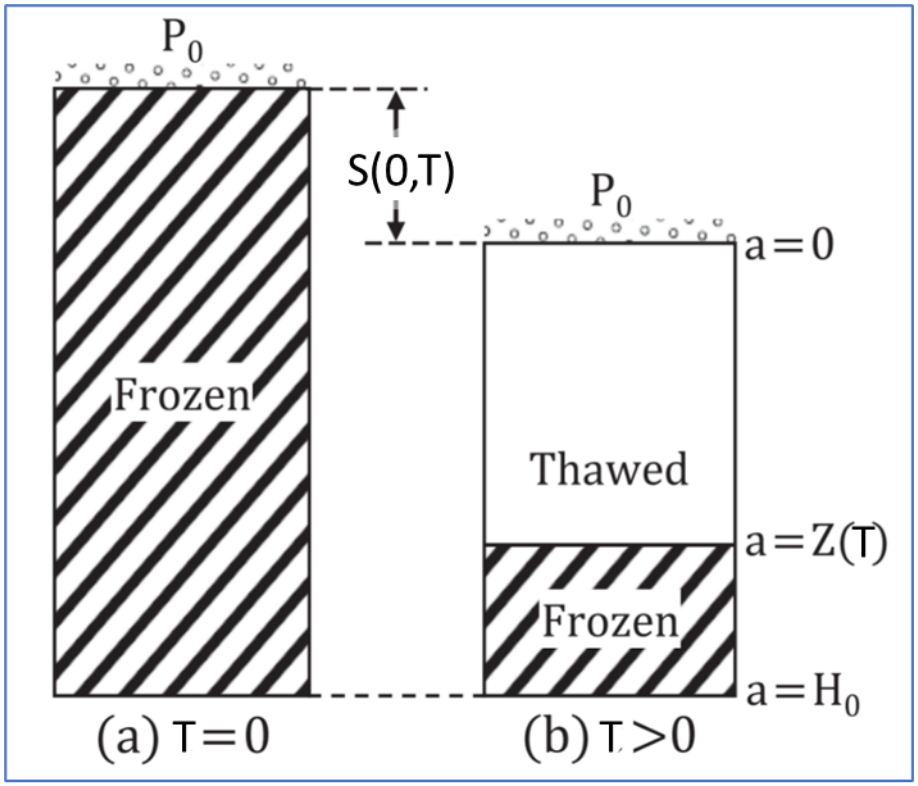

Figure A1 Consolidation settlement of thawing soil (Dumais and Konard 2017)

For the one-dimensional consolidation model, the Lagrangian convective coordinates with the consolidation theory proposed in Gibson et al. (1981) is used. Figure A.2 (a) represents the frozen state, and Figure A.2 (b) represents the thawing state of the soil. The lower datum boundary is taken as a = Z(t), whereas the upper boundary remains at a = 0. The soil element $A_0B_0C_0D_0$ with thickness ∂a is located at the Lagrangian coordinate position height “a” from the datum.

At t > 0, the thaw consolidation states of the soil with the use of the convective theory is shown in Figure A 2b. The soil element is denoted by ABCD, and the datum boundary is at $\xi = Z(t)$.

The soil element of thickness $\partial\xi$ is located at the coordinate position ξ from the datum. At t > 0, the thaw depth is given by Equation A4.

$$\boldsymbol{H(t) = Z(t) - s(0,t)} \qquad (\boldsymbol{A1})$$

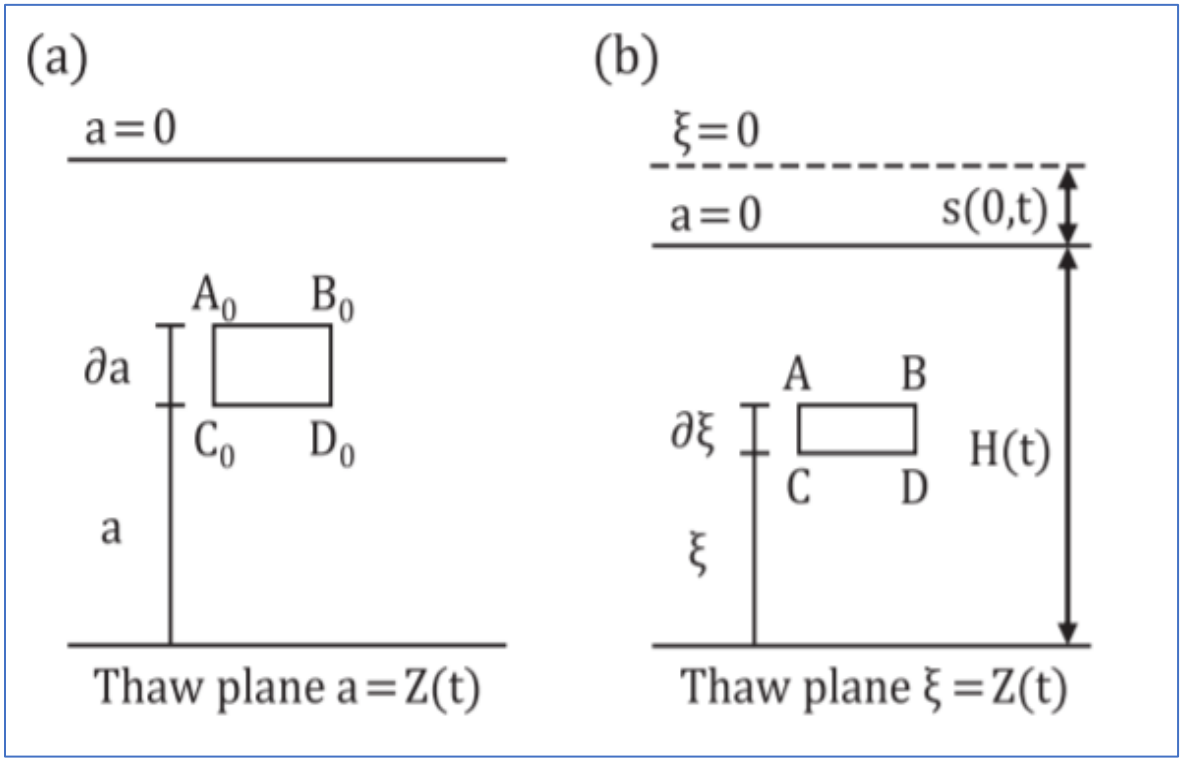

Figure A2 Consolidation settlement of thawing soil element (Dumais and Konard 2017)

During surface settlement, the upper boundary moves by s(0, t). The convective coordinate position of the top boundary located at the surface of soils at a = 0 is given by Equation A5.

$$\boldsymbol{\xi(0,t) = s(0,t)} \qquad (\boldsymbol{A2})$$

The general equation at any depth related to the convective coordinates (ξ), Lagrangian coordinates (a) and to settlement s(a, t) can be expressed as:

$$\boldsymbol{\xi = a + s(a,t)} \qquad (\boldsymbol{A3})$$

The change between the Lagrangian and the convective coordinates is given by Equation A4.

$$\boldsymbol{\frac{\partial \xi}{\partial a} = \frac{1+e}{1+e_f}} \qquad (\boldsymbol{A4})$$

where

e_f = e(a,0), initial void ratio of frozen soil, and

e = e (a, t), void ratio at time t

In derived equations using the Lagrangian coordinates, the basic assumption considered for the modeling is the soil particle and the pore water is assumed to be incompressible.

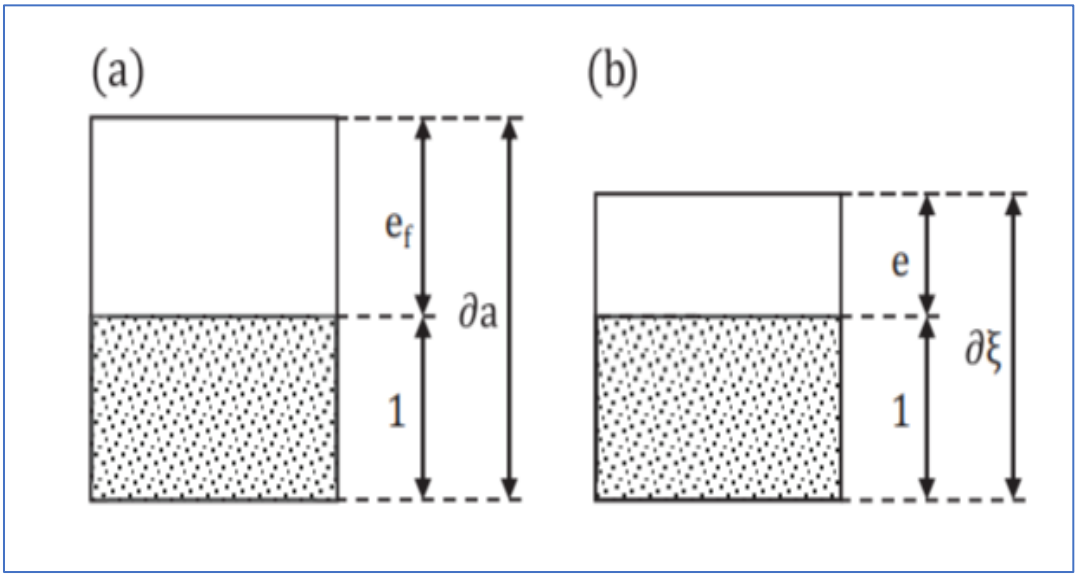

Figure A3 Void change ratio during thaw consolidation ((Dumais and Konard 2017)

$$\frac{\partial \sigma_v}{\partial a} = \frac{(G_s + e)\,\Upsilon_w}{(1 + e_f)} \qquad (A5)$$

where σ_v is the total vertical stress, G_e is the specific gravity of the soil, and Υ_w is the unit weight of the water.

$$\frac{\partial u}{\partial a} = \frac{\partial u_e}{\partial a} + \frac{(1 + e)\Upsilon_w}{(1 + e_f)} \qquad (A6)$$

where u is the total pore-water pressure, and u_e is the excess pore-water pressure.

$$v_w - v_s = -\frac{k_v(e)(1 + e_f)}{\Upsilon_w^e}\frac{\partial u_e}{\partial a} \qquad (A7)$$

where v_w and v_s are the velocity of the pore water and soil particles respectively relative to the datum and k_v(e) is the vertical hydraulic conductivity which is a function of the void ratio.

References

Dumais, S., and Konard, J. M. (2017). One-dimensional large-strain thaw consolidation using nonlinear effective stress – void ratio – hydraulic conductivity relationships. *Canadian Geotechnical Journal*.

Gibson, R. E., Schiffm, R. L., and Cargill, K. (1981). The theory of one-dimensional consolidation of saturated clays. Finite nonlinear consolidation of thick homogeneous layers. *Canadian Geotechnical Journal*.

APPENDIX B - Experiment Photographs

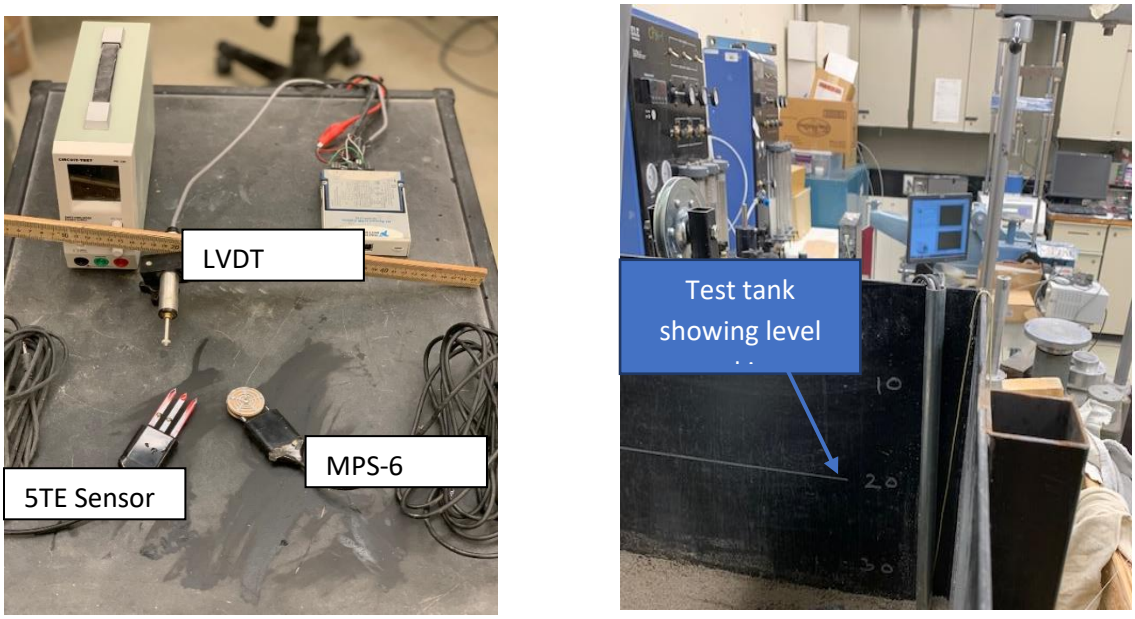

Figure B1 (a) Sensors used in experiment, and (b) Setup tank with soil level markings

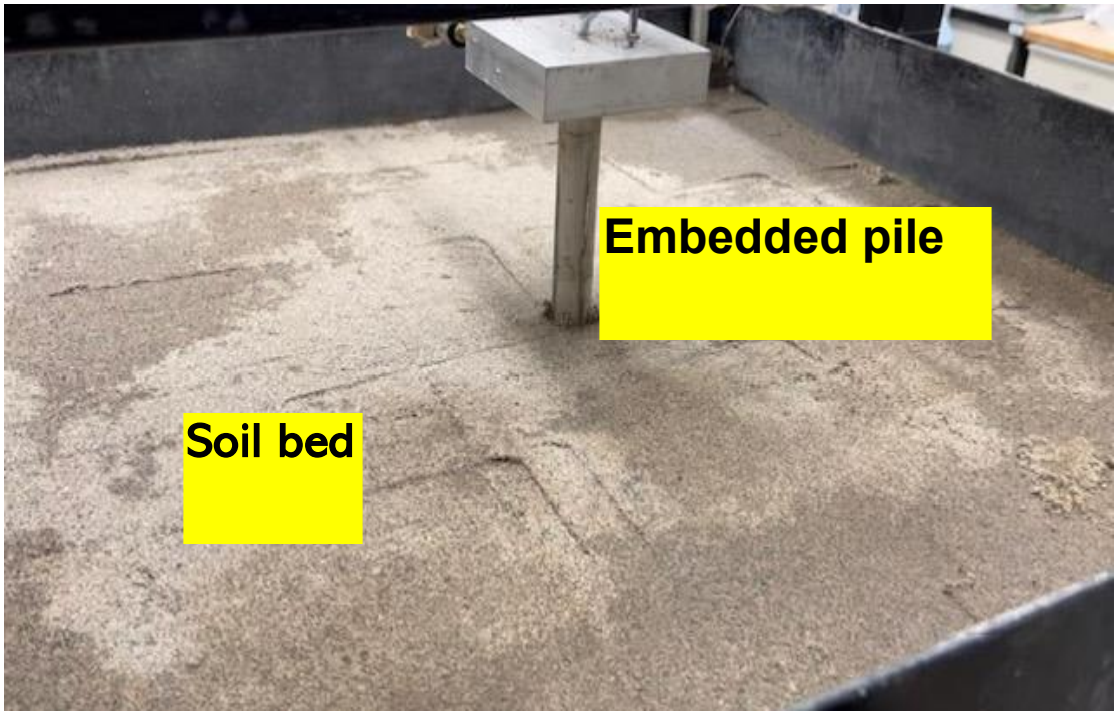

Figure B2 Sand bed prepared for saturation

Figure B3 Soil freezing coils

Figure B4 Freezing machine display showing the temperature profile

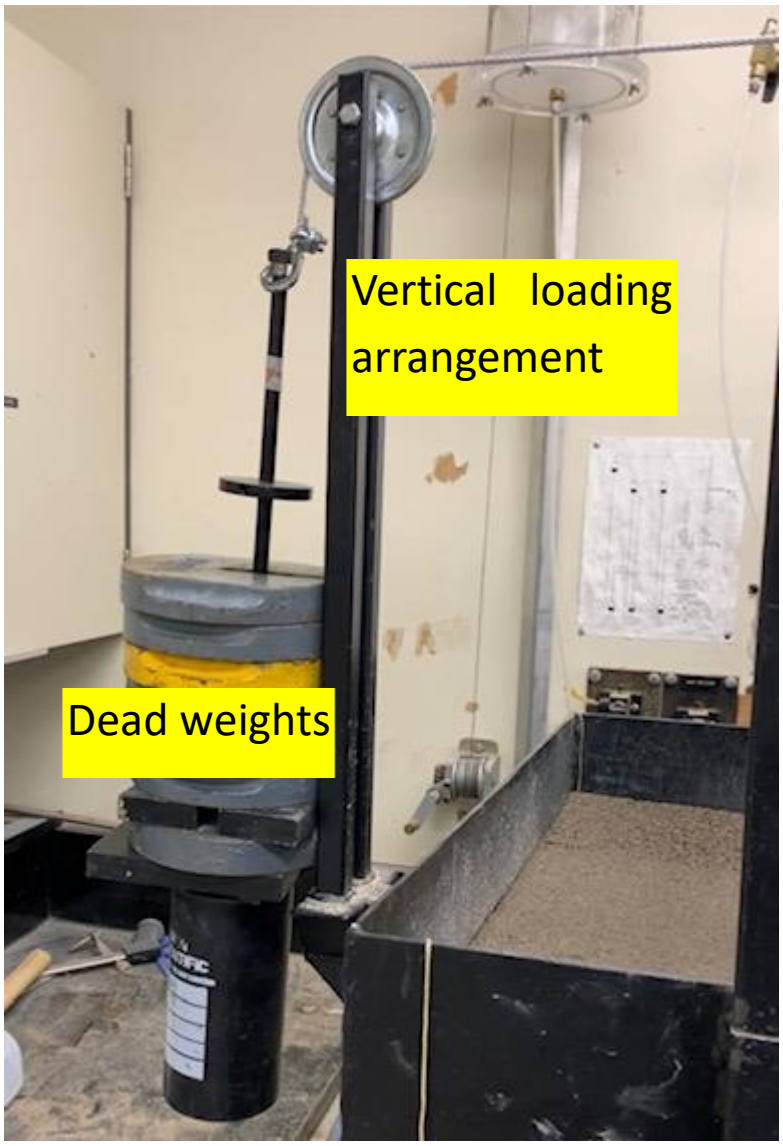

Figure B5 Static vertical loading on pile